GDAHA representations with Teichmüller, Stokes, and Painlevé

by

Davide Dal Martello

A thesis submitted to
the University of Birmingham
for the degree of
Doctor of Philosophy

School of Mathematics
University of Birmingham
5 February 2024

Abstract

The Painlevé VI equation governs the isomonodromic deformation problem of both 2-dimensional Fuchsian and 3-dimensional irregular types of linear systems of ODEs. Through Harnad duality, this feature turns into a map between the two systems, which translates to monodromy as a middle convolution operation.

This thesis studies the quantum algebraic manifestation of the systems' monodromy data by introducing a noncommutative analogue of the middle convolution functor. The Fuchsian data are known to quantize as the $CC_1^\vee$ DAHA; we construct a quantization of the irregular ones that match the $\tilde{E}_6$-type GDAHA, provided a specialization of the algebra parameters.

Both quantum data are then shown to exhibit an alternative realization in higher Teichmüller terms. In particular, this framework advances the GDAHA representation theory by providing the first explicit representation of the universal GDAHA of type $\tilde{E}_6$, which can be reduced to the quantum irregular monodromy data by a new quiver-theoretical operation.

Acknowledgements

If I have seen further,

it is by standing on the shoulders of giants.

— Isaac Newton

Heartfelt thanks to my advisory team:
Marta, whose passion, guidance, and support were the constant inspiration that helped me get this far; and Ana, whose kindness always restores my faith in this profession.

And a special thank-you to my coach Mairi: it is your training that maintained my mind-body balance during this exhilarating yet testing journey.

Finally, thanks to mamma, papà, and my fratellone Andrea, who warmly tolerated my bad moods during the hardest times; vi voglio bene!

Funding My PhD studies were supported by the EPSRC Studentship #2438494.

Publication Chapters 2 and 3 are adapted from the arXiv preprint 2307.06803 [9] that has been accepted for publication in *Advances in Mathematics*. Chapter 1 and Appendix B are adapted from the MRes thesis I submitted in my second year of PhD.

Contents

Introduction

This thesis explores the quantum algebraic manifestation of two sets of monodromy data connected with the Painlevé theory, through the lens of both a new quantum middle convolution and the higher Teichmüller toolkit.

The two sets of monodromy data, each consisting in a tuple of matrices, come from two linear systems of ordinary differential equations (ODE), one 2-dimensional Fuchsian and the other 3-dimensional irregular, that are intimately related to the Painlevé theory. Indeed, the sixth Painlevé (PVI) equation gives the isomonodromic deformation condition for both cases [20, 24, 32]. Moreover, for a specialization of the irregular system, the isomonodromic problem is known to connect with the theory of Frobenius manifolds [11].

The link between monodromy matrices and quantum algebra in this Painlevé-based differential framework was first explored in [33], for the Fuchsian case. Quantum algebras are noncommutative and 'quantum' in the deformation sense: they depend on a parameter whose so-called classical limit recovers the underlying algebra meant as the undeformed object. They often play the role of coordinate rings for noncommutative spaces, providing a quantization framework for classical algebraic geometry. Influential examples include quantum groups, Temperley-Lieb algebras, and double affine Hecke algebras (DAHA). In particular, using classical Teichmüller theory, the Fuchsian monodromy matrices quantize to recover the DAHA controlling Askey-Wilson polynomials. Introducing a quantum version of the middle convolution functor, this thesis completes the picture by extending the link to

the irregular case: the quantum algebra emerging from the irregular monodromy data is a specialization of the generalized double affine Hecke algebra (GDAHA) of type $\tilde{E}_6$.

With both Fuchsian and irregular data promoted to the quantum algebraic realm, a new connection with higher Teichmüller geometry [15, 19] emerges. Higher Teichmüller theory extends the classical one beyond PSL_2, with remarkable applications in representation theory, quantum moduli spaces, topological quantum field theories (TQFT) and more [19]. This geometric framework provides an alternative realization of both quantum monodromy data, with the bonus of advancing the GDAHA representation theory in the process.

After this preamble, we dedicate the Introduction to the setup and structure of the thesis, including an overview of the main open problems the theory we develop fits in.

For pairwise distinct numbers $u_1, u_2, u_3, \theta_1, \theta_2, \theta_3, \theta_\infty \in \mathbb{C}$, we start by defining the two types of linear systems of ODEs on the complex plane under consideration:

- Fuchsian 2-dimensional systems in the form

$$\frac{\mathrm{d}}{\mathrm{d}\lambda}\Phi = \left(\sum_{k=1}^{3} \frac{A_k}{\lambda - u_k}\right)\Phi, \tag{I.1}$$

  where each matrix $A_k \in \mathfrak{sl}_2(\mathbb{C})$ has spectrum $\{\pm\frac{\theta_k}{2}\}$, and

$$-(A_1 + A_2 + A_3) =: A_\infty = \frac{1}{2}\begin{pmatrix} \theta_\infty & 0 \\ 0 & -\theta_\infty \end{pmatrix}; \tag{I.2}$$

- irregular 3-dimensional systems in the form

$$\frac{\mathrm{d}}{\mathrm{d}z}\Psi = \left(D + \frac{\Theta - \mathbb{1}}{z}\right)\Psi, \tag{I.3}$$

  where $D = \mathrm{diag}(u_1, u_2, u_3)$, Θ has diagonal part $\{-\theta_1, -\theta_2, -\theta_3\}$ and the eigenvalues $\mu_1 = \frac{1}{2}(\mathrm{Tr}(\Theta) + \theta_\infty)$, $\mu_2 = \frac{1}{2}(\mathrm{Tr}(\Theta) - \theta_\infty)$, $\mu_3 = 0$.

The former is Fuchsian in that all four poles u_1, u_2, u_3, ∞ are simple, while the irregular nature of the latter stems from the pole of order two at ∞.

Their relationship is twofold. On the one hand, setting $(u_1, u_2, u_3) = (0, t, 1)$ both isomonodromic deformation problems reduce to the celebrated sixth Painlevé (PVI) equation

$$y_{tt} = \frac{1}{2}\left(\frac{1}{y} + \frac{1}{y-1} + \frac{1}{y-t}\right) y_t^2 - \left(\frac{1}{t} + \frac{1}{t-1} + \frac{1}{y-t}\right) y_t + \frac{y(y-1)(y-t)}{t^2(t-1)^2}\left[\alpha + \beta\frac{t}{y^2} + \gamma\frac{t-1}{(y-1)^2} + \delta\frac{t(t-1)}{(y-t)^2}\right], \quad \text{(I.4)}$$

for complex parameters $\alpha, \beta, \gamma, \delta$ whose correspondence is given by $\alpha = \frac{(\theta_\infty - 1)^2}{2}, \beta = -\frac{\theta_1^2}{2}$, $\gamma = \frac{\theta_3^2}{2}, \delta = \frac{1-\theta_2^2}{2}$. In fact, this is an instance of Harnad duality [20]. On the other hand, their conjugation classes are in bijection:

Theorem I.1 ([32], Theorem 24) *There exists a bijection between equivalence classes of* 2×2 *systems* (I.1) *and equivalence classes of* 3×3 *systems* (I.3)*, explicitly realized by the following formulae:*

$$A_k = \frac{1}{2}\begin{pmatrix} a_k b_k & -a_k^2 \\ b_k^2 - \frac{\theta_k^2}{a_k^2} & -a_k b_k \end{pmatrix}, \quad \text{(I.5)}$$

$$\Theta = \begin{pmatrix} -\theta_1 & \frac{1}{2}\left(a_1 b_2 - a_2 b_1 - \theta_1\frac{a_2}{a_1} - \theta_2\frac{a_1}{a_2}\right) & \frac{1}{2}\left(a_1 b_3 - a_3 b_1 + \theta_1\frac{a_3}{a_1} - \theta_3\frac{a_1}{a_3}\right) \\ \frac{1}{2}\left(a_2 b_1 - a_1 b_2 - \theta_1\frac{a_2}{a_1} - \theta_2\frac{a_1}{a_2}\right) & -\theta_2 & \frac{1}{2}\left(a_2 b_3 - a_2 b_2 - \theta_2\frac{a_3}{a_2} - \theta_3\frac{a_2}{a_3}\right) \\ \frac{1}{2}\left(a_3 b_1 - a_1 b_3 - \theta_1\frac{a_3}{a_1} - \theta_3\frac{a_1}{a_3}\right) & \frac{1}{2}\left(a_3 b_2 - a_2 b_3 - \theta_2\frac{a_3}{a_2} - \theta_3\frac{a_2}{a_3}\right) & -\theta_3 \end{pmatrix}, \quad \text{(I.6)}$$

where a_k *and* b_k*,* $k = 1, 2, 3$*, are constants such that*

$$\sum_{k=1}^{3} a_k b_k = -\theta_\infty, \quad \sum_{k=1}^{3} a_k^2 = 0, \quad \sum_{k=1}^{3} \frac{\theta_k^2}{a_k^2} - b_k^2 = 0. \quad \text{(I.7)}$$

Remark I.2 *Setting* $\theta_1 = \theta_2 = \theta_3 = 0$*,* Θ *turns skew-symmetric and recovers the Dubrovin*

differential operator [11], whose space of isomonodromic deformations coincide with that of semisimple Frobenius manifolds.

Multi-valuedness for each of the solutions $\Phi(\lambda)$ and $\Psi(z)$ can be encapsulated in a set of constant invertible matrices:

- four matrices $M_1, M_2, M_3, M_\infty \in \mathsf{SL}_2(\mathbb{C})$ for the Fuchsian system, generating a group with relation
$$M_1 M_2 M_3 M_\infty = \mathbb{1}; \tag{I.8}$$
- three matrices $M_0^L, S_1, S_2 \in \mathsf{GL}_3(\mathbb{C})$ for the irregular system, subject to
$$M_0^L S_1 S_2 = \mathbb{1}. \tag{I.9}$$

The quadruple is made of genuine monodromy data while the triple, involving the pair of Stokes matrices S_i, goes by 'generalized' monodromy data.

In the Fuchsian case, the quantum algebraic manifestation of such matrix data is understood [33], for the canonical quantization of the monodromy group delivers a quantum algebra isomorphic to the double affine Hecke algebra of type $CC_1^\vee$:

Definition I.3 *The $CC_1^\vee$ DAHA is generated over $\mathbb{C}$ by four elements $V_0, \check{V}_0, V_1, \check{V}_1$, subject to the relations*

$$\begin{aligned}
(V_0 - k_0)(V_0 + k_0^{-1}) &= 0,\\
(\check{V}_0 - \check{k}_0)(\check{V}_0 + \check{k}_0^{-1}) &= 0,\\
(V_1 - k_1)(V_1 + k_1^{-1}) &= 0,\\
(\check{V}_1 - \check{k}_1)(\check{V}_1 + \check{k}_1^{-1}) &= 0,\\
\check{V}_1 V_1 V_0 \check{V}_0 &= q^{-\frac{1}{2}},
\end{aligned}$$

where $k_0, k_1, \check{k}_0, \check{k}_1, q \in \mathbb{C}^*$ *and* $q^m \neq 1, m \in \mathbb{Z}_{>0}$.

Explicitly, Theorem 3 [33] gives quantum matrices $M_i^\hbar$, $i = 1, 2, 3, \infty$, whose classical limit $q \to 1$ recovers a special coordinatization of the monodromy group coming from classical Teichmüller theory:

$$M_1^\hbar = \begin{pmatrix} 0 & -e^{S_1+\frac{p_1}{2}} \\ e^{-S_1-\frac{p_1}{2}} & -e^{\frac{p_1}{2}} - e^{-\frac{p_1}{2}} \end{pmatrix}, \quad M_2^\hbar = \begin{pmatrix} -e^{\frac{p_2}{2}} - e^{-\frac{p_2}{2}} - e^{S_2+\frac{p_2}{2}} & -e^{\frac{p_2}{2}} - e^{-\frac{p_2}{2}} - e^{S_2+\frac{p_2}{2}} - e^{-S_2-\frac{p_2}{2}} \\ e^{S_2+\frac{p_2}{2}} & e^{S_2+\frac{p_2}{2}} \end{pmatrix},$$
$$M_3^\hbar = \begin{pmatrix} -e^{\frac{p_3}{2}} - e^{-\frac{p_3}{2}} - e^{-S_3-\frac{p_3}{2}} & -e^{-S_3-\frac{p_3}{2}} \\ e^{\frac{p_3}{2}} + e^{-\frac{p_3}{2}} + e^{S_3+\frac{p_3}{2}} + e^{-S_3-\frac{p_3}{2}} & e^{-S_3-\frac{p_3}{2}} \end{pmatrix}, \quad M_\infty^\hbar := q^{-\frac{1}{2}} \left(M_1^\hbar M_2^\hbar M_3^\hbar\right)^{-1}. \tag{I.10}$$

Remark I.4 *Matrices* (I.10) *come from the canonical quantization of the Poisson bracket*

$$\{s_i, s_{i+1}\} = 1, \quad i = 1, 2, 3;\ i + 3 \equiv i, \tag{I.11}$$

where each variable p_i *is a Casimir element. Namely, we promote all the variables* s_i *to operators (done visually by capitalization) under the commutators*

$$[S_i, S_j] = i\hbar\{s_i, s_j\}. \tag{I.12}$$

By the Baker–Campbell–Hausdorff formula with $q = e^{-i\hbar}$*, one obtains the q-commutations*

$$e^{S_{i+1}} e^{S_i} = q e^{S_i} e^{S_{i+1}}, \quad i = 1, 2, 3;\ i + 3 \equiv i. \tag{I.13}$$

The resulting quantum algebra

$$\mathbb{T}_q^3 := \mathbb{C}\langle e^{\pm S_1}, e^{\pm S_2}, e^{\pm S_3}\rangle \Big/ (e^{S_2} e^{S_1} - q e^{S_1} e^{S_2}, e^{S_3} e^{S_2} - q e^{S_2} e^{S_3}, e^{S_1} e^{S_3} - q e^{S_3} e^{S_1}) \tag{I.14}$$

is an algebraic quantization of the 3*-torus* $\mathbb{T}^3$*: its classical limit recovers the coordinate ring* $\mathbb{C}[\mathbb{T}^3] = \mathbb{C}[x^{\pm 1}, y^{\pm 1}, z^{\pm 1}]$.

In order to unravel the quantum algebra corresponding to the irregular case, we enhance to the noncommutative realm a factorization result of Killing and a monodromy-compatible map known as the middle convolution. Indeed, the irregular and Fuchsian systems come together with their monodromy data to form the following commutative diagram:

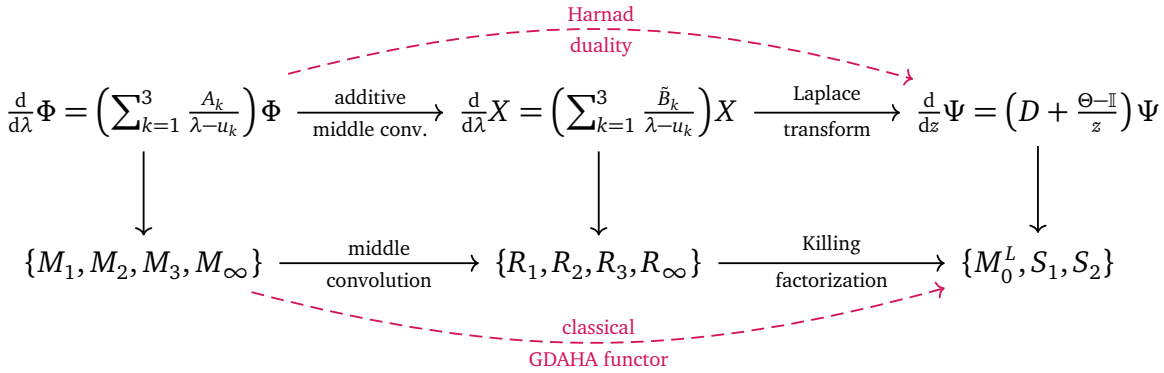

(I.15)

The upper row lives in the realm of systems; taking (generalized) monodromy through the vertical arrows, we obtain its monodromic counterpart. Thus, the lower row prescribes the recipe to send the Fuchsian monodromy data to the irregular ones by precisely composing an action of the middle convolution with the Killing factorization. In particular, the middle convolution can only map between Fuchsian monodromy matrices and the factorization is needed to extract the irregular ones.

In light of this classical framework, our winning strategy consists in a full quantization of the lower row: by composing quantum analogues of the two arrows, we construct a map sending the known quantum Fuchsian data to a quantum realization of the irregular ones. Namely, the image of the quantum matrices (I.10) is a quantum algebra whose generators recover in the $q \to 1$ limit genuine generalized monodromy data for (I.3). As such, we succeed in promoting the irregular data to the quantum algebraic world.

Mirroring the Fuchsian picture, the resulting quantum irregular data themselves recover

a known quantum algebra: it is H_{E_6}, the generalized double affine Hecke algebra (GDAHA) of type $\tilde{E}_6$, provided a specialization of its parameters.

In total, there are four GDAHAs: one for each of the affine Dynkin diagrams $\tilde{D}_4, \tilde{E}_6, \tilde{E}_7$ or $\tilde{E}_8$. Adding that $CC_1^\vee$ is isomorphic to H_{D_4}, the GDAHA of type $\tilde{D}_4$, our composition realizes in the quantum realm a (functorial) map that sends the representation theory of H_{D_4} into that of H_{E_6}, hence the name of *GDAHA functor* (Figure I.1).

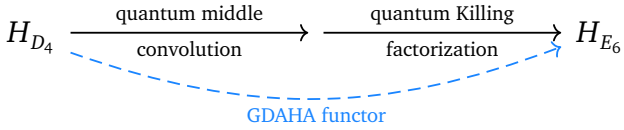

Figure I.1: The quantum counterpart of the lower row in diagram (I.15).

Considering both the intrinsic quantum nature and representation-theoretic breadth, this new functor is defined in purely quantum algebraic terms, with its monodromic role recast as just one of the possible applications.

A natural yet ambitious open program is a full quantization of diagram (I.15), completing the lower row given by the GDAHA functor. In a recent paper [41], a proposed quantization of the irregular system (I.3) is given by the dynamical Knizhnik-Zamolodchikov (DKZ) equation

$$\mathrm{d} - \left(\hbar \frac{\Omega}{z} + \mathrm{ad}(\mu \otimes 1)\right) \mathrm{d}z,$$

where $\Omega \in \mathfrak{g} \otimes \mathfrak{g}$ is the Casimir element of $\mathfrak{g} = \mathfrak{sl}_3(\mathbb{C})$, $\mu \in \mathfrak{h}$ belongs to the Cartan subalgebra $\mathfrak{h}$ of $\mathfrak{g}$, and $\hbar$ is a formal parameter. The isomonodromic deformation equations of DKZ match the Casimir equation, which is dual to the standard Knizhnik-Zamolodchikov (KZ) equation [40]. The latter is the quantization of the isomonodromic deformation equations of the 2×2 linear system (I.1) [37]. As observed by Harnad [39], this duality "is essentially the 'quantum' version" of the duality between the isomonodromic deformation equations of the linear systems (I.1) and (I.3). As of yet, a complete proof of this statement, including

the quantization of the Fuchsian system (I.1), is still unknown.

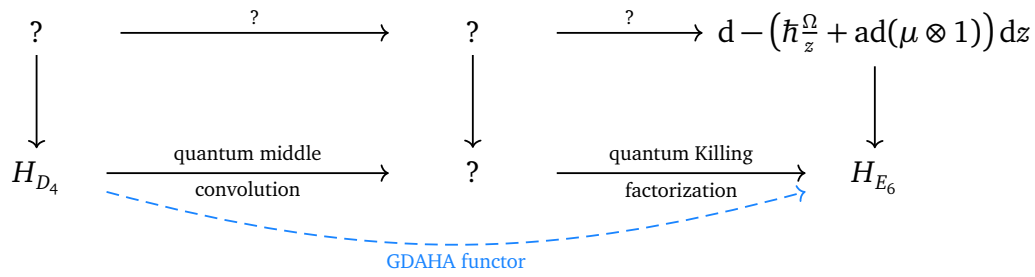

Figure I.2: The state of the art of a quantum analogue of diagram (I.15).

If the first half of the thesis has a marked algebraic flavour, the second half brings in the geometric one. Indeed, both Fuchsian and irregular quantum data turn out to exhibit an alternative genesis via higher Teichmüller geometry.

Developed in a sequence of papers involving Fock, Goncharov and Shen [14, 15, 19], higher Teichmüller theory generalizes the classical one beyond PSL_2, allowing for higher rank groups. In particular, we recall both the recipes to coordinatize the underlying moduli space and turn it quantum. The former assigns a set of Fock-Goncharov coordinates $\{Z_\alpha\}$ on a triangle, prescribing gluing rules to extend the coordinatization to any triangulation, while the latter triggers noncommutativity via q-commuting relations $Z_\alpha Z_\beta = q^m Z_\beta Z_\alpha$, $m \in \mathbb{Z}$.

These coordinates can be combined into transport matrices T_i associated with directed flows between two sides of the triangle. These matrices serve as multiplicative building blocks: a single matrix can be assigned to any path running on a triangulation by reading off the way it flows through the triangles. More precisely, we get a map assigning an element of $\mathsf{Mat}_n(\mathcal{X})$, i.e., $n \times n$ matrices over the quantum algebra $\mathcal{X}$ of the rank n Teichmüller space, to paths on a Riemann surface Σ:

$$\Sigma \ni \gamma \longmapsto M \in \mathsf{Mat}_n(\mathcal{X}).$$

For the application to the GDAHA representation theory, the triangulation comes from

the dual of the surface's fat graph and the (closed) paths are taken as representatives in the fundamental group $\pi_1(\Sigma)$. By choosing $n = 2$ (classical Teichmüller theory) and the four-holed Riemann sphere, the resulting matrices match the representation of H_{D_4} given by the quantum Fuchsian monodromy matrices (I.10). More surprisingly, for $n = 3$ (true higher Teichmüller) and three holes, the machinery delivers an explicit representation of H_{E_6} under *no* restrictions on its parameters. Let us highlight this is the first such representation in the literature, a feature we stress by using the notion of universal GDAHA. Indeed, in contrast with the well-understood representation theory of H_{D_4} [28, 31, 34], for the other cases $\tilde{E}_{6,7,8}$ only representations requiring special values of the parameters are available [17].

As one would expect, the quantum irregular data from the GDAHA functor—whose algebra is isomorphic to a specialization of H_{E_6}—can be found inside our Teichmüller-based representation of the universal $\tilde{E}_6$-type GDAHA. This match happens through a new graph-theoretical operation we call quiver seizure, and completes the anticipated realization of both quantum monodromy data in higher Teichmüller terms.

A natural problem to attack next with this geometric machinery is the construction of analogous explicit representations for the two remaining GDAHAs of type $\tilde{E}_{7,8}$. In both cases, we expect an increase in the rank of the Teichmüller theory, and a consequent surge in computational complexity to be tackled with efficient computer-aided symbolic calculus.

The thesis is organized as follows:

Chapter 1 recalls the well-known notions involved with the classical picture, starting from the monodromy data;

Chapter 2 quantizes the diagram's lower row by constructing the GDAHA functor and computing its action on the quantum Fuchsian monodromy data;

Chapter 3 brings in the higher Teichmüller toolkit to construct the representation of the universal GDAHA, which is then reduced to the quantum irregular data via quiver seizures;

Appendix A describes the differential facet of the diagram's upper row, with the explicit formula (I.6) indeed obtained by Laplace transforming the action of an 'additive' middle convolution for systems;

Appendix B studies in detail the proof behind the middle convolution's Riemann-Hilbert correspondence;

Appendix C lightens the reading by collecting the most involved formulae.

One last note: each section is meant to be self-contained, and the reader can follow the overarching narrative via the introductory paragraphs at the beginning of each chapter.

Chapter 1

The monodromic facet

We start the chapter recalling the well-known genesis of the monodromy data for both systems (I.1-I.3). While the Fuchsian case provides the natural framework, the irregular one is more involved and requires the richer concept of generalized monodromy. We conclude the chapter describing the classical building blocks, namely the middle convolution and the Killing factorization, behind our main functorial construction of Chapter 2.

Both operations are deeply connected with monodromy theory: the former by design, the latter by chance.

1.1 Monodromy data

Monodromy theory studies the behaviour of complex functions around singularities. Monodromy phenomena are the by-product of the failure of certain functions to be single-valued as we perform analytic continuation along a loop encircling a singularity. Such failure can be characterized by a set of monodromy data that encode the transformations the function is subject to as we loop around its singularities.

Both the solutions $\Phi(\lambda)$ and $\Psi(z)$ are multi-valued in their respective punctured plane; we are going to define their monodromy data starting with the simpler Fuchsian case, closely following [32].

Remark 1.1.1 *Dealing with systems of ODEs, we look for a fundamental (matrix) solution: a square matrix whose linearly independent columns provide a basis in the vector space of all solutions. As a consequence, monodromy data themselves are given by a set of matrices.*

1.1.1 The Fuchsian case

The solution of the Fuchsian system (I.1) is multivalued analytic on the (genus zero) four-holed Riemann sphere with no boundaries, namely $\Sigma_{0,4,0} := \overline{\mathbb{C}} \setminus \{u_1, u_2, u_3, \infty\}$.
To define its monodromy matrices, we fix a basis $\gamma_1, \gamma_2, \gamma_3$ of loops in $\pi_1\left(\Sigma_{0,4,0}, \infty\right)$ as in Figure 1.1 and rely on the local theory at infinity:

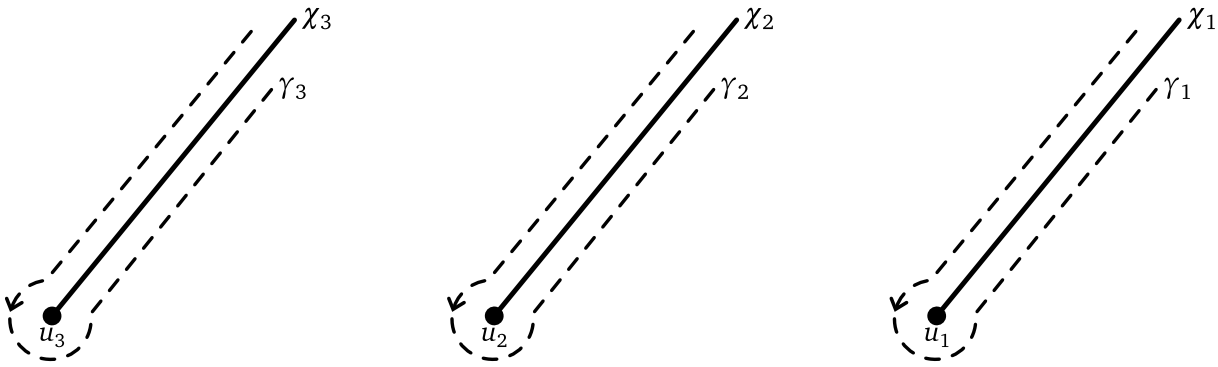

Figure 1.1: In the λ-plane, the branch-cuts χ_j connecting the finite singularities to ∞ together with the counterclockwise loops γ_j. The decreasing order has been chosen without loss of generality.

Proposition 1.1.2 ([32], Proposition 15) *For $\theta_\infty \notin \mathbb{Z}$, the Fuchsian system (I.1) admits a fundamental matrix solution in the form*[1]

$$\Phi_\infty(\lambda) \sim \left(\mathbb{1} + \mathcal{O}\left(\lambda^{-1}\right)\right) \lambda^{-A_\infty} \quad \text{as } \lambda \to \infty, \quad \lambda^{-A_\infty} := e^{-A_\infty \log \lambda}. \tag{1.1.1}$$

The solution Φ_∞ can be analytically continued on the whole universal covering of $\Sigma_{0,4,0}$. For any element $\gamma \in \pi_1\left(\Sigma_{0,4,0}, \infty\right)$, we denote the result of the analytic continuation of $\Phi_\infty(\lambda)$ along the loop γ by $\gamma[\Phi_\infty(\lambda)]$. Being $\gamma[\Phi_\infty(\lambda)]$ and $\Phi_\infty(\lambda)$ two fundamental matrices in

[1] Choosing the logarithm's branch-cut to be aligned with the common direction of the cuts χ_1, χ_2, χ_3.

the neighbourhood of ∞, they must satisfy

$$\gamma[\Phi_\infty(\lambda)] = \Phi_\infty(\lambda) M_\gamma, \tag{1.1.2}$$

for some constant invertible 2×2 matrix M_γ depending only on the homotopy class of γ. In particular, the matrix $M_\infty := M_{\gamma_\infty}$, for γ_∞ a simple loop encircling ∞ in the counterclockwise direction, is given by

$$M_\infty = \exp(2\pi i A_\infty). \tag{1.1.3}$$

For the product of two loops $\gamma, \tilde{\gamma} : [0,1] \to \Sigma_{0,4,0}$ defined as

$$\gamma\tilde{\gamma} : t \mapsto \begin{cases} \gamma(2t) & 0 \leqslant t \leqslant \frac{1}{2}, \\ \tilde{\gamma}(2t-1) & \frac{1}{2} \leqslant t \leqslant 1, \end{cases} \tag{1.1.4}$$

the resulting monodromy representation is the anti-homomorphism

$$\begin{array}{ccc} \pi_1\left(\Sigma_{0,4,0}, \infty\right) & \to & \mathsf{SL}_2(\mathbb{C}) \\ \gamma & \mapsto & M_\gamma \\ M_{\gamma\tilde{\gamma}} & \mapsto & M_{\tilde{\gamma}} M_\gamma. \end{array} \tag{1.1.5}$$

The images $M_j := M_{\gamma_j}$ of the (counterclockwise) generators γ_j, $j = 1,2,3$, are the monodromy matrices of the Fuchsian system. Since the loop $\gamma_3\gamma_2\gamma_1$ is homotopic to γ_∞^{-1}, the generators obey the cyclic relation

$$M_1 M_2 M_3 M_\infty = \mathbb{1}. \tag{1.1.6}$$

Fundamental solutions $\Phi_j(\lambda)$ are similarly defined near any of the poles u_j:

Proposition 1.1.3 ([32], Proposition 16) *For $\theta_j \notin \mathbb{Z}$, the Fuchsian system (I.1) admits a*

fundamental matrix solution in the form

$$\Phi_j(\lambda) \sim G_j\big(\mathbb{1} + \mathcal{O}(\lambda - u_j)\big)(\lambda - u_j)^{\Lambda_j} \quad \text{as } \lambda \to u_j, \tag{1.1.7}$$

where

$$\Lambda_j = \begin{pmatrix} \frac{\theta_j}{2} & 0 \\ 0 & -\frac{\theta_j}{2} \end{pmatrix} \tag{1.1.8}$$

and the invertible matrix G_j is defined by $A_j = G_j \Lambda_j G_j^{-1}$.

Each of the solutions provided by the two propositions represents a distinguished base near one of the punctures. They interact in the obvious way: continuing $\Phi_\infty(\lambda)$ to the neighbourhood of u_j yields the relation

$$\Phi_\infty(\lambda) = \Phi_j(\lambda) C_j, \tag{1.1.9}$$

for some invertible matrix C_j. The so-called connection matrices C_1, C_2, C_3 are such that

$$M_j = C_j^{-1} e^{2\pi i \Lambda_j} C_j, \qquad j = 1, 2, 3. \tag{1.1.10}$$

Thus, for non-integer θ_js, the spectra of the monodromy matrices read as

$$\text{eigen}(M_j) = \exp(\pm \pi i \theta_j). \tag{1.1.11}$$

We can finally give the following

Definition 1.1.4 *For non-integer parameters, the* Fuchsian monodromy data *are given by the set of constant matrices $\{M_1, M_2, M_3\}$.*

Remark 1.1.5 *M_∞ is omitted as not independent, being uniquely determined by the cyclic relation* (1.1.6)*. Similarly, for each connection matrix via* (1.1.10)*.*

For quantum algebraic purposes, we add M_∞ and match the Introduction's anticipated quadruple

$$\{M_1, M_2, M_3, M_\infty\}. \tag{1.1.12}$$

1.1.2 The irregular case

We move to the monodromy data of the irregular system (I.3). This system has two poles, a simple one at 0 and a double one at ∞. The solution $\Psi(z)$ is multi-valued analytic outside 0 and ∞: when analytically continued along paths encircling punctures, monodromy matrices appear.

We start with the simpler local theory at zero, assuming a branch-cut between zero and infinity has been defined along a fixed line χ and a branch of $\log z$ accordingly selected.

Proposition 1.1.6 ([32], Proposition 1) *There exists a gauge transformation*

$$\Psi = G(z)\tilde{\Psi} = \sum_{k=0}^{\infty} G_k z^k \tilde{\Psi}$$

convergent near 0*, with principal term* G_0 *defined by* $\Theta = G_0 \mu G_0^{-1}$*,* $\mu = \mathrm{diag}(\mu_1, \mu_2, \mu_3)$*, mapping the irregular system* (I.3) *to the Birkhoff Normal form*

$$\frac{\mathrm{d}}{\mathrm{d}z}\tilde{\Psi} = \left(\frac{\mu - \mathbb{1}}{z} + \sum_{k \geqslant 1} \mathfrak{R}_k z^{k-1} \right) \tilde{\Psi}, \tag{1.1.13}$$

where $(\mathfrak{R}_k)_{ij} \neq 0$ *if and only if* $\mu_i - \mu_j = k$*. As a consequence, for* $\mathfrak{R} := \sum_{k \geqslant 1} \mathfrak{R}_k$ *there exists a fundamental matrix solution in the form*

$$\Psi_0(z) \sim G(z) z^{\mu - \mathbb{1}} z^{\mathfrak{R}} \quad \text{as } z \to 0. \tag{1.1.14}$$

As the number of possible integral differences between the eigenvalues of Θ is finite, only a finite number of matrices $\mathfrak{R}_k$ is non-zero and they all vanish in the so-called non-resonant

case, i.e., $\mu_i - \mu_j \notin \mathbb{Z}$ for all $i, j = 1, 2, 3$.

Given the form of Ψ_0, the corresponding monodromy matrix for a counterclockwise loop around the origin simply reads

$$M_0 = \exp(2\pi i \mu) \exp(2\pi i \mathfrak{R}). \tag{1.1.15}$$

The local theory near infinity is rather different, due to the order two pole. In general, this leads to a twofold outcome: solutions around ∞ are only defined in sectors, instead of discs, and have exponential growth, instead of polynomial.

Proposition 1.1.7 ([32], Proposition 4) *There exists a unique formal power series*

$$P(z) = \sum_{k=0}^{\infty} P_k z^{-k}, \tag{1.1.16}$$

with $P_0 = \mathbb{1}$, whose formal gauge transformation $\Psi = P(z)\tilde{\Psi}$ brings the irregular system (I.3) to the normal form

$$\frac{\mathrm{d}}{\mathrm{d}z}\tilde{\Psi} = \left(D + \frac{\theta - \mathbb{1}}{z}\right)\tilde{\Psi}, \quad \theta := \mathrm{diag}(-\theta_1, -\theta_2, -\theta_3). \tag{1.1.17}$$

As a consequence, there is a unique formal *fundamental solution in the form*[2]

$$\Psi_\infty \sim P(z) z^{\theta - \mathbb{1}} e^{zD} \quad \text{as } z \to \infty. \tag{1.1.18}$$

This establishes only the existence of formal solutions: true ones require more machinery.

Definition 1.1.8 *The half-line*

$$\mathfrak{r}_{ij} = \left\{ z \;\middle|\; \mathrm{Re}\,[z(u_i - u_j)] = 0,\ \mathrm{Im}\,[z(u_i - u_j)] < 0 \right\} \tag{1.1.19}$$

[2] Fixing the logarithm's branch as in the previous section.

oriented from zero to infinity is called a Stokes ray.

Definition 1.1.9 *An oriented line χ in the complex plane is called* admissible *with respect to the points (u_1, u_2, u_3) if it is such that all the Stokes rays $\mathfrak{r}_{ij}$, $i > j$, lie to the left of χ.*

Lemma 1.1.10 ([32], Lemma 8) *Fixed an admissible oriented line χ, there exists $\varepsilon > 0$, two sectors Π_L and Π_R defined as*

$$\begin{aligned} \Pi_L &= \{z : \arg(\chi) - \varepsilon < \arg(z) < \arg(\chi) + \pi + \varepsilon\}, \\ \Pi_R &= \{z : \arg(\chi) - \pi - \varepsilon < \arg(z) < \arg(\chi) + \varepsilon\}, \end{aligned} \tag{1.1.20}$$

and two unique fundamental solutions $\Psi_L(z)$ in Π_L and $\Psi_R(z)$ in Π_R, such that

$$\Psi_{L,R} \sim \left(\mathbb{1} + \mathcal{O}\left(z^{-1}\right)\right) z^{\theta - \mathbb{1}} e^{zD} \quad as \quad \Pi_{L,R} \ni z \to \infty, \tag{1.1.21}$$

i.e., for all $n \in \mathbb{Z}_+$ and for $z \to \infty$ inside $\Pi_{L,R}$,

$$\lim_{z \to \infty} z^n \left(\Psi_{L,R} - \left(\mathbb{1} + \mathcal{O}\left(z^{-1}\right)\right) z^{\theta - \mathbb{1}} e^{zD}\right) = 0.$$

In both of the narrow sectors

$$\begin{aligned} \Pi_+ &:= \left\{z \;\middle|\; \arg(\chi) - \varepsilon < \arg(z) < \arg(\chi) + \varepsilon\right\}, \\ \Pi_- &:= \left\{z \;\middle|\; \arg(\chi) - \pi - \varepsilon < \arg(z) < \arg(\chi) - \pi + \varepsilon\right\}, \end{aligned}$$

obtained intersecting Π_L and Π_R, we have two fundamental matrices. Again, they must be related by a constant invertible matrix:

$$\Psi_L(z) = \Psi_R(z) S_+, \quad z \in \Pi_+, \tag{1.1.22}$$

$$\Psi_L(z) = \Psi_R(z) S_-, \quad z \in \Pi_-. \tag{1.1.23}$$

Definition 1.1.11 *S_+, S_- are called* Stokes matrices *(associated to the admissible line χ).*

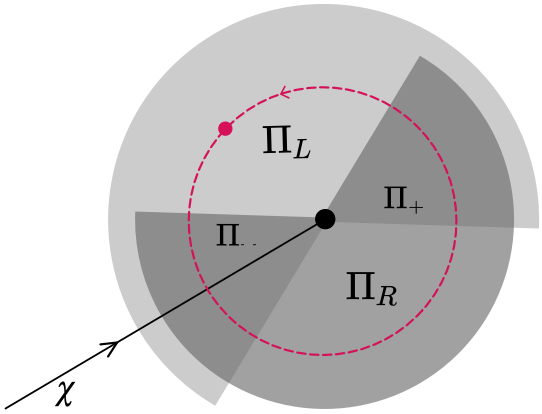

Figure 1.2: Sectors $\Pi_{L,R,+,-}$ and a counterclockwise loop around infinity starting from Π_L.

Technically, $S_\pm$ are not monodromy matrices as the information they encode is not purely topological: they cannot be singled out by looping a solution around the puncture at ∞. Passing to the richer concept of *generalized* monodromy allows to consider Stokes and standard monodromy matrices alike.

Summing up, we have built three distinguished bases in the space of solutions, $\Psi_0(z)$ near 0 and $\Psi_{L,R}(z)$ near ∞ depending on the choice of the admissible line χ, and generated three corresponding matrices M_0 and $S_{+,-}$, the first uniquely defined by μ and $\mathfrak{R}$.

To conclude, we define the connection matrices $C_{L,R}$ as in the Fuchsian case:

$$\Psi_0(z) = \Psi_{L,R}(z)C_{L,R}, \quad z \in \Pi_{L,R}.$$

We reduce the list of generalized monodromy data $(\mu, \mathfrak{R}, S_+, S_-, C_L, C_R)$ taking advantage of the cyclic relation

$$C_L^{-1}S_+^{-1}S_-C_L = M_0^{-1},$$

obtained performing the red loop in Figure 1.2 for Ψ_0:

$$\Psi_0 \to \Psi_L C_L \to \Psi_R S_- C_L \to \Psi_L S_+^{-1} S_- C_L \to \Psi_0 C_L^{-1} S_+^{-1} S_- C_L = \Psi_0 M_0^{-1}. \tag{1.1.24}$$

The last equality expresses a topological fact already used in (1.1.6), now adapted to $\mathbb{C}^*$: a counterclockwise loop around infinity is homotopic to a clockwise one around the origin. Similarly, $C_R = S_+ C_L$.

Definition 1.1.12 *The* (generalized) irregular monodromy data *are given by the set of constant matrices*

$$\{\mu, \mathfrak{R}, S_+, C_L\}. \tag{1.1.25}$$

In the non-resonant case we drop $\mathfrak{R}$ from the set and, expressing all monodromy data with respect to Ψ_L so that $M_0^L := C_L M_0 C_L^{-1}$, the independent ones reduce to $\{M_0^L, S_+^{-1}, S_-\}$ subject to the cyclic relation $M_0^L S_+^{-1} S_- = \mathbb{1}$. Simply define $S_1 := S_+^{-1}$ and $S_2 := S_-$ to match the Introduction's anticipated triple

$$\left\{M_0^L, S_1, S_2\right\}. \tag{1.1.26}$$

Moreover[3], using the asymptotic behaviour (1.1.21), S_+ must be upper unitriangular while S_- must be lower triangular with $e^{-2\pi i(\theta - \mathbb{1})} = e^{-2\pi i \theta}$ as diagonal part.

1.2 Middle convolution functor and Killing factorization

Katz [26] introduced the middle convolution functor $\mathscr{M}_\chi$ to prove an existence theorem for irreducible rigid local systems, i.e., when the global behaviour of the solutions under analytic continuation on the punctured Riemann sphere is just determined by the local one at finite singularities and ∞. Any such system was shown be obtained from just a one-

[3] See [1], proof of Theorem I adapted to our *decreasing* lexicographic order of the singularities.

dimensional local system by applying iteratively a suitable (and invertible) sequence of middle convolutions and scalar multiplications, leading simultaneously to a classification and an existence algorithm. Such functor preserves important properties like the index of rigidity and irreducibility, but in general changes the rank and the monodromy group.

Following [10], we detail a purely algebraic analogue of this functor, whose properties mimic those of $\mathscr{M}_\chi$. Such algebraic counterpart is defined as the endofunctor

$$\mathscr{M}_\lambda : \mathsf{Mod}(\mathbb{C}[F_r]) \longrightarrow \mathsf{Mod}(\mathbb{C}[F_r]), \tag{1.2.1}$$

where $\mathsf{Mod}(\mathbb{C}[F_r])$ is the category of finite-dimensional (left) $\mathbb{C}[F_r]$-modules, F_r denoting the free group on r generators. In particular, objects in $\mathsf{Mod}(\mathbb{C}[F_r])$ can be viewed as couples $(\mathbf{M}, V)$, $\mathbf{M} = (M_1, M_2, \dots, M_r) \in \mathsf{GL}(V)^r$ where each M_i represents the action of the respective generator on the vector space V. Thus, we can detail the functor algebraically as a map $(\mathbf{M}, V) \mapsto (\mathbf{N}, W)$, $\mathbf{N} \in \mathsf{GL}(W)^r$, between r-tuples of matrices.

First, construct the object $(\mathscr{C}_\lambda(\mathbf{M}), V^r) \in \mathsf{Mod}(\mathbb{C}[F_r])$, $\mathscr{C}_\lambda(\mathbf{M}) = (N_1, \dots, N_r) \in \mathsf{GL}(V^r)^r$: for $i = 1, \dots, r$,

$$N_i = \begin{pmatrix} \mathbb{1} & \mathbb{0} & & \dots & & \mathbb{0} & \\ & \ddots & & & & & \\ & & \mathbb{1} & & & & \\ \lambda(M_1 - \mathbb{1}) & \dots & \lambda(M_{i-1} - \mathbb{1}) & \lambda M_i & M_{i+1} - \mathbb{1} & \dots & M_r - \mathbb{1} \\ & & & & \mathbb{1} & & \\ & & & & & \ddots & \\ \mathbb{0} & & & \dots & & \mathbb{0} & \mathbb{1} \end{pmatrix}. \tag{1.2.2}$$

The middle convolution is then obtained as a restriction of this enlarged tuple on the quotient

space $V^r/(\mathcal{K}+\mathcal{L})$, where $\mathcal{K} := \bigoplus_{i=1}^{r} \mathcal{K}_i$,

$$\mathcal{K}_i = \begin{pmatrix} 0 \\ \vdots \\ 0 \\ \ker(M_i - \mathbb{1}) \\ 0 \\ \vdots \\ 0 \end{pmatrix} \quad (i\text{-th entry}),$$

and

$$\mathcal{L} = \bigcap_{i=1}^{r} \ker(N_i - \mathbb{1}) = \ker(N_1 \cdots N_r - \mathbb{1})$$

are $\langle N_1, \ldots, N_r \rangle$-invariant subspaces of V^r.

Definition 1.2.1 *The object* $(\mathscr{C}_\lambda(\mathbf{M}), V^r)$ *is called the* convolution *of* V *with* λ. *The object* $(\mathscr{M}_\lambda(\mathbf{M}), V^r/(\mathcal{K}+\mathcal{L}))$ *is called the* middle convolution *of* $\mathbf{M}$ *with* λ, *where the matrix tuple* $\mathscr{M}_\lambda(\mathbf{M}) := \left(\tilde{N}_1, \ldots, \tilde{N}_r\right) \in \mathsf{GL}(V^r/(\mathcal{K}+\mathcal{L}))^r$ *has each* $\tilde{N}_k$ *induced by the action of the corresponding element of* $\mathscr{C}_\lambda(\mathbf{M})$ *on the quotient.*

Remark 1.2.2 *In general,* $\dim(V^r/(\mathcal{K}+\mathcal{L})) \neq \dim(V)$*; when the matrix tuple* $\mathbf{M}$ *comes from monodromy, this mismatch allows to map between monodromy data of Fuchsian systems in form* (I.1) *having different dimensions. Moreover, for* $\lambda \neq 1$,

$$\mathcal{L} = \left\langle \begin{pmatrix} M_2 \cdots M_r v \\ M_3 \cdots M_r v \\ \vdots \\ v \end{pmatrix} \;\middle|\; v \in \ker(\lambda M_1 \cdots M_r - \mathbb{1}) \right\rangle \qquad \textit{and} \qquad \mathcal{K} + \mathcal{L} = \mathcal{K} \oplus \mathcal{L}.$$

Among its many properties, the functor is multiplicative, allowing for an inversion formula:

Theorem 1.2.3 ([10], Theorem 2.4) *Let $\lambda_1, \lambda_2 \in \mathbb{C}^*$ be such that $\lambda = \lambda_1\lambda_2$. If $\langle M_1, \ldots, M_r\rangle$ generates an irreducible subgroup of $\mathsf{GL}(V)$ for at least two M_is different from the identity, then*

$$\mathscr{M}_{\lambda_1} \circ \mathscr{M}_{\lambda_2} \cong \mathscr{M}_{\lambda}. \tag{1.2.3}$$

In particular,

$$\mathscr{M}_{\lambda^{-1}} \circ \mathscr{M}_{\lambda} = \mathrm{Id}. \tag{1.2.4}$$

For the core functorial construction of this thesis, we need to combine the middle convolution with a classical factorization result that traces its origin back to Killing [7]:

Theorem 1.2.4 ([7], Corollary 3.4) *Let $R_1, R_2, \ldots, R_n \in \mathsf{GL}(V)$ be pseudo-reflections of the n-dimensional $\mathbb{C}$-vector space V, i.e., $R_i = \mathbb{1} + e_i \otimes \alpha_i$, $\{e_i\}$ forming a basis in V and $\alpha_i \in V^*$. Then, their product can be uniquely factorized as*[4]

$$R_1R_2\cdots R_n = U_+^{-1}\Lambda U_-, \tag{1.2.5}$$

for U_+, U_- respectively upper and lower unitriangular, and Λ diagonal.

Remark 1.2.5 *As pointed out by Boalch [3], this factorization connects the Stokes data of the irregular system (I.3) with the monodromy matrices of the Fuchsian connection*

$$\mathrm{d} - \left(\sum_{k=1}^{3} \frac{\tilde{B}_k}{\lambda - u_k}\right), \tag{1.2.6}$$

where each $\tilde{B}_k \in \mathrm{End}(\mathbb{C}^3)$ is a rank 1 matrix. Appendix A.3 shows that such 3-dimensional connection is obtained from the 2-dimensional Fuchsian system (I.1) via the additive middle convolution.

[4] Due to our opposite (decreasing) lexicographic order of the singularities, formula (1.2.5) is the reversed of the paper's one.

Chapter 2

The GDAHA functor

The Deligne-Simpson problem offers a natural link between monodromy and the family of generalized double affine Hecke algebras (GDAHA). We thus start the Chapter introducing GDAHAs through such problem, providing full details for our two algebras of interest corresponding to the affine Dynkin diagrams $\tilde{D}_4$ and $\tilde{E}_6$.

By introducing a quantum analogue of both Katz's middle convolution and the Killing factorization, we then construct a functor sending representations of the GDAHA of type $\tilde{D}_4$ into representations of the $\tilde{E}_6$-type one.

As a direct application, we send the quantum Fuchsian monodromy data to a triple of quantum matrices whose classical limit gives genuine (generalized) monodromy for the irregular system, achieving the desired quantization of the irregular data.

The whole Chapter is an adaptation of the homonym section from the arXiv preprint

> D. Dal Martello and M. Mazzocco. Generalized double affine Hecke algebras, their representations, and higher Teichmüller theory. *arXiv:2307.06803v2*, 2023.

Throughout the Chapter, $\mathsf{Rep}(\mathcal{A})$ denotes the category of representations of the algebra $\mathcal{A}$: objects are pairs (ρ, V), for V a vector space and $\rho : \mathcal{A} \to \mathrm{End}(V)$ an algebra homomorphism, while arrows are homomorphisms of representations.

2.1 Deligne-Simpson problem and GDAHAs

For any algebraically closed field k, let V be a n-dimensional k-vector space and fix a d-tuple of scalars $\tau = (\tau_1, \dots, \tau_d) \in k^d$. An endomorphism $M \in \mathsf{End}(V)$ has type τ if

$$\prod_{i=1}^{d} (M - \tau_i \mathbb{1}) = 0, \tag{2.1.1}$$

with corresponding dimension vector $(n_0 = n, n_1, \dots, n_{d-1}, n_d = 0) \in \mathbb{Z}^{d+1}$ collecting the rank of the partial products $n_k = \operatorname{rank} \prod_{i=1}^{k} (M - \tau_i \mathbb{1})$.

On top of being invariant with respect to conjugation, type and dimension vector together uniquely fix a conjugacy class in $\mathsf{End}(V)$:

- M has type τ if and only if its Jordan form has blocks $J_{\lambda,r}$, $r \leqslant \#\{k \,|\, 1 \leqslant k \leqslant d,\ \tau_k = \lambda\}$;
- $n_{i-1} - n_i$ counts the number of Jordan blocks $J_{\tau_i,r}$, $r \geqslant \#\{k \,|\, 1 \leqslant k \leqslant i,\ \tau_k = \tau_i\}$.

After this preamble, we can formulate the Deligne-Simpson problem as follows:

> "For a group G and conjugacy classes $C_i \in \mathrm{G}$, $i = 1, \dots, r$, find an irreducible r-tuple of matrices $\mathbf{M} = (M_1, M_2, \dots, M_r)$, $M_i \in C_i$, such that $M_1 \cdots M_r = \mathbb{1}$."

Here 'irreducible' means that the matrices have no common invariant subspace.

Remark 2.1.1 ([29]) *Despite not emerging as a natural requirement, irreducibility has several good reasons to be part of the formulation of the problem. E.g., for almost all types of the conjugacy classes, the tuple is indeed irreducible and this feature eases the resolution of the problem that depends now only on the Jordan normal forms of the classes.*

As anticipated, the problem connects with both monodromy and quantum algebra. On the one hand, data (1.1.12) are truly relevant only up to global conjugation: their cyclic defining equation is manifestly neutral to such operation, and the whole monodromy depends on the choice of base point. Therefore, it is natural to consider equivalence classes of

matrices instead, and the resulting monodromy space coincides—up to irreducibility that is almost always free from the formulation—with solutions to the Deligne-Simpsons problem for $G = \mathsf{SL}_n(\mathbb{C})$. On the other hand, the problem incorporates the classical representation theory of a special family of quantum algebras known as generalized double affine Hecke algebras (GDAHA).

To fully appreciate this second connection, let us introduce these algebras explicitly.

For any simply laced Dynkin diagram $\mathscr{D}$ with star-shaped affinization $\tilde{\mathscr{D}}$, GDAHAs were introduced by Etingof, Oblomkov and Rains [12] as flat deformations of $\mathbb{C}[G_l]$, the group algebra of the 2-dimensional crystallographic group $G_l := \mathbb{Z}_l \ltimes \mathbb{Z}^2$, for $l = 2, 3, 4, 6$. In detail, for any Dynkin diagram $\mathscr{D} \in \{D_4, E_6, E_7, E_8\}$, a family $H_{\mathscr{D}}(t, q)$ of GDAHAs can be defined, depending on parameters $q \in \mathbb{C}^*$ (not a root of unity) and a tuple t of non-zero complex numbers.

For the monodromic purpose of this thesis, we focus on the two cases $l = 2, 3$, which correspond respectively to $\tilde{D}_4$ and $\tilde{E}_6$.

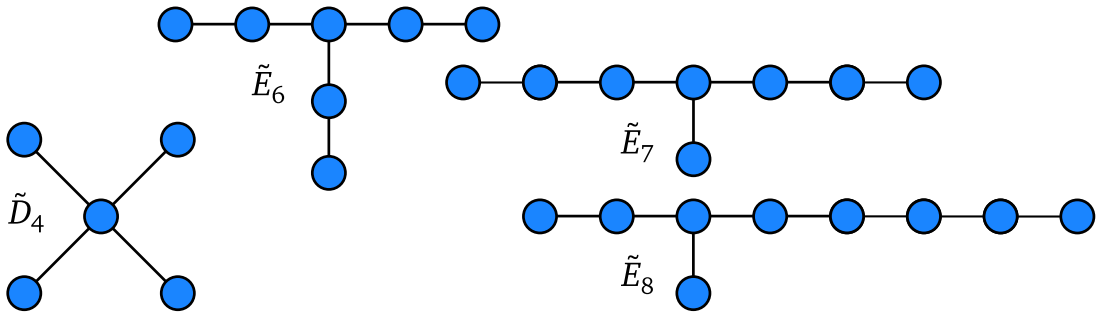

Figure 2.1: All simply laced star-shaped affine Dynkin diagrams.

On the one hand, $H_{D_4}(t, q)$ is defined as the family of algebras depending on parameters $t_1, t_2, t_3, t_4, q \in \mathbb{C}^*$ by generators K_1, K_2, K_3, K_4 and relations

$$(K_i - t_i)\left(K_i - \frac{1}{t_i}\right) = 0, \quad i = 1, 2, 3, 4; \qquad K_1 K_2 K_3 K_4 = q^{-1/2}. \tag{2.1.2}$$

On the other hand, $H_{E_6}(t, q)$ is the family of algebras depending on $q, t_i^{(j)} \in \mathbb{C}^*$, $i = 1, 2, 3$

and $j = 1, 2$, generated by J_1, J_2, J_3 subject to the relations

$$\left(J_i - t_i^{(1)}\right)\left(J_i - t_i^{(2)}\right)\left(J_i - \frac{1}{t_i^{(1)} t_i^{(2)}}\right) = 0, \quad i = 1, 2, 3; \qquad J_1 J_2 J_3 = q^{-1/3}. \tag{2.1.3}$$

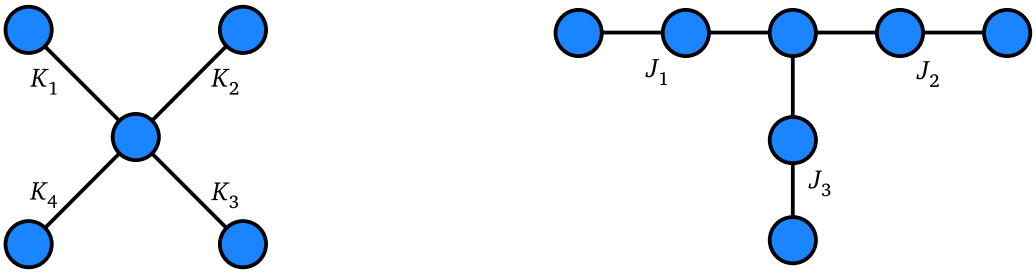

Figure 2.2: Affine Dynkin diagrams: $\tilde{D}_4$ on the left and $\tilde{E}_6$ on the right. Each leg contributes a generator and its length determines the order of the corresponding Hecke relation. These two cases are special in that all legs have same length.

Remark 2.1.2 *Denote by $\mathbb{T}$ the algebraic torus formed by the tuple t, namely $\mathbb{T} = (\mathbb{C}^*)^4$ in the case of H_{D_4} and $\mathbb{T} = (\mathbb{C}^*)^6$ in the case of H_{E_6}. Then, each family of GDAHAs can be obtained by specializations of a universal algebra $\mathsf{H}_{\mathscr{D}}$ over $\mathbb{C}[\mathbb{T}] \otimes \mathbb{C}[q^{\pm 1/l}]$, in which q and all elements of t are central.*

From Definition I.3, $H_{D_4}(t, q)$ coincides (up to rescalings by the imaginary unit) with $CC_1^\vee$ so that the E-type families are meant as true generalizations of this DAHA.

By just looking at the definitions, irreducible representations of $H_{\mathscr{D}}(t, 1)$ give solutions to the corresponding $\mathsf{G} = \mathsf{SL}_n(\mathbb{C})$ Deligne-Simpson problem. E.g., for $\mathscr{D} = D_4$, all conjugacy classes C_i, $i = 1, 2, 3, 4$, share the same $d = 2$ and have $\tau_1 = \tau_2^{-1} = t_i$. In other words, the classical limit of the GDAHA of type $\tilde{D}_4$ algebraically encodes the monodromic features of the Fuchsian system (I.1).

The rest of the Chapter upgrades to quantum this dictionary between monodromy and GDAHAs, encompassing the irregular case in the process.

2.2 Quantum middle convolution

This section turns noncommutative the algebraic middle convolution of Section 1.2, tailoring to our GDAHA $H_{D_4}(t,q)$ case of interest.

For convenience, we rescale the generators in (2.1.2) as

$$\widehat{K}_i = \frac{1}{t_i} K_i, \quad i=1,2,3; \qquad \widehat{K}_4 = t_1 t_2 t_3 K_4, \tag{2.2.1}$$

so that the Hecke relations can be written as follows:

$$\begin{aligned} (\widehat{K}_i - 1)\left(\widehat{K}_i - \frac{1}{t_i^2}\right) &= 0, \quad i=1,2,3; \\ (\widehat{K}_4 - t_1 t_2 t_3 t_4)\left(\widehat{K}_4 - \frac{t_1 t_2 t_3}{t_4}\right) &= 0. \end{aligned} \tag{2.2.2}$$

In doing so, the cyclic relation in preserved:

$$\widehat{K}_1 \widehat{K}_2 \widehat{K}_3 \widehat{K}_4 = q^{-1/2}. \tag{2.2.3}$$

For an object $(\rho, V) \in \mathsf{Rep}\big(H_{D_4}(t,q)\big)$, we denote $\rho(\widehat{K}_j)$ by $\widehat{K}_j$, namely we use the same notation for the generator and its representation $\widehat{K}_i \in \mathrm{End}(V)$.

Introducing the triple $\widehat{\mathbf{K}} := (\widehat{K}_1, \widehat{K}_2, \widehat{K}_3)$, the first map we define is

$$\begin{array}{rccc} \mathscr{C} : & \mathrm{End}(V)^3 & \to & \mathrm{End}(\bigoplus_3 V)^3 \\ & (\widehat{K}_1, \widehat{K}_2, \widehat{K}_3) & \mapsto & (N_1, N_2, N_3) \end{array}$$

where

$$N_1 = \begin{pmatrix} \widehat{K}_1 & \widehat{K}_2 - 1 & \widehat{K}_3 - 1 \\ 0 & 1 & 0 \\ 0 & 0 & 1 \end{pmatrix}, \quad N_2 = \begin{pmatrix} 1 & 0 & 0 \\ \widehat{K}_1 - 1 & \widehat{K}_2 & \widehat{K}_3 - 1 \\ 0 & 0 & 1 \end{pmatrix}, \quad N_3 = \begin{pmatrix} 1 & 0 & 0 \\ 0 & 1 & 0 \\ \widehat{K}_1 - 1 & \widehat{K}_2 - 1 & \widehat{K}_3 \end{pmatrix}.$$

Notice that $(\mathscr{C}(\widehat{\mathbf{K}}), \bigoplus_3 V)$ no longer defines a representation of $H_{D_4}(t,q)$.
The algebra structure in $\mathrm{End}(\bigoplus_3 V)$ is given by the usual matrix multiplication, combined with the algebra operations in $H_{D_4}(t,q)$. In particular, the ordering is dictated by that of matrix multiplication.

The following operation is a 'quantum' quotient to a subspace encoding the Hecke-type properties of $\widehat{\mathbf{K}}$.

Lemma 2.2.1 *The subspace $W \subset \bigoplus_3 V$, defined as*

$$W := \bigoplus_{i=1}^{3} \ker(\widehat{K}_i - 1), \tag{2.2.4}$$

is invariant under the action of N_1, N_2 and N_3.

Proof. For any $\mathbf{v} = (v_1, v_2, v_3) \in W$, $N_1(\mathbf{v}) = (\widehat{K}_1(v_1) + (\widehat{K}_2 - 1)(v_2) + (\widehat{K}_3 - 1)(v_3), v_2, v_3)$. Since v_i is in the kernel of $(\widehat{K}_i - 1)$, $(\widehat{K}_2 - 1)(v_2) + (\widehat{K}_3 - 1)(v_3) = 0$ while $\widehat{K}_1(v_1) = v_1$. Analogous computations can be repeated for N_2 and N_3. □

The quantum middle convolution is the restriction of $\mathscr{C}(\widehat{\mathbf{K}})$ to the quotient $(\bigoplus_3 V)/W$. To construct this quotient, we take advantage of the properties entailed by the Hecke relations. In particular, each operator $\widehat{K}_i : V \to V$ carries a natural direct sum decomposition of V into eigenspaces:

$$V = V_1^{(i)} \oplus V_2^{(i)}, \tag{2.2.5}$$

where $V_1^{(i)}$ corresponds to the eigenvalue 1 and $V_2^{(i)}$ to the other eigenvalue t_i^{-2}.

Lemma 2.2.2 *The operators e_i, defined as*

$$e_i := \frac{t_i^2}{1 - t_i^2}(\widehat{K}_i - 1),$$

are idempotent and project onto the eigenspace $V_2^{(i)}$*:*

$$e_i^2 = e_i, \quad \widehat{K}_i e_i = \frac{1}{t_i^2} e_i. \tag{2.2.6}$$

Moreover, denoting $\overline{e}_i := \frac{t_i^2}{t_i^2-1}(\widehat{K}_i - t_i^{-2})$ *the complement idempotent element projecting onto* $V_1^{(i)}$*, the following relations hold for* $i = 1, 2, 3$*:*

$$e_i \overline{e}_i = \overline{e}_i e_i = 0, \quad e_i + \overline{e}_i = 1. \tag{2.2.7}$$

Proof. It all stems from the Hecke relation $(\widehat{K}_i - 1)(\widehat{K}_i - t_i^{-2}) = (\widehat{K}_i - t_i^{-2})(\widehat{K}_i - 1) = 0$:

$$\begin{aligned}
e_i^2 &= \frac{t_i^4}{(1-t_i^2)^2}(\widehat{K}_i - 1)^2 = \frac{t_i^4}{(1-t_i^2)^2}(t_i^{-2} - 1)(\widehat{K}_i - 1) = e_i, \\
\widehat{K}_i e_i &= \frac{t_i^2}{1-t_i^2}\widehat{K}_i(\widehat{K}_i - 1) = \frac{t_i^2}{1-t_i^2}\frac{1}{t_i^2}(\widehat{K}_i - 1) = \frac{1}{t_i^2} e_i, \\
e_i \overline{e}_i &= -\frac{t_i^4}{(1-t_i^2)^2}(\widehat{K}_i - 1)(\widehat{K}_i - t_i^{-2}) = 0, \\
e_i + \overline{e}_i &= \frac{t_i^2}{1-t_i^2}(\widehat{K}_i - 1) + \frac{t_i^2}{t_i^2-1}(\widehat{K}_i - t_i^{-2}) = \frac{t_i^2}{t_i^2-1} - \frac{1}{t_i^2-1} = 1.
\end{aligned}$$

□

Introducing the operator

$$E := e_1 \oplus e_2 \oplus e_3 \in \mathrm{End}(\bigoplus_3 V),$$

we can finally give the following

Definition 2.2.3 *Let* VECT^2 *be the arrow category of all vector spaces. The* quantum middle convolution *is the map*

$$\mathscr{M}_q : \mathsf{Rep}\big(H_{D_4}(t,q)\big) \to \mathsf{VECT}^2$$

sending an object $(\widehat{\mathbf{K}}, V) \in \mathsf{Rep}\big(H_{D_4}(t,q)\big)$ *to a triple* $(EN_1, EN_2, EN_3) \in \mathrm{End}(E(V))^3$*, where* $E(V) := e_1(V) \oplus e_2(V) \oplus e_3(V)$*.*

Proposition 2.2.4 *$\mathscr{M}_q$ is a functor whose image consists of quantum pseudo-reflections.*

Proof. Let us first characterize $\mathscr{C}(\widehat{\mathbf{K}})$ explicitly in $\mathrm{End}(E(V))$: since $\widehat{K}_i$ acts as the multiplication by t_i^{-2} on $e_i(V)$, it is immediate to obtain the pseudo-reflection formulae

$$
\begin{aligned}
EN_1\big|_{E(V)} &= \begin{pmatrix} t_1^{-2} & (t_2^{-2}-1)e_1 & (t_3^{-2}-1)e_1 \\ 0 & 1 & 0 \\ 0 & 0 & 1 \end{pmatrix}, \\
EN_2\big|_{E(V)} &= \begin{pmatrix} 1 & 0 & 0 \\ (t_1^{-2}-1)e_2 & t_2^{-2} & (t_3^{-2}-1)e_2 \\ 0 & 0 & 1 \end{pmatrix}, \\
EN_3\big|_{E(V)} &= \begin{pmatrix} 1 & 0 & 0 \\ 0 & 1 & 0 \\ (t_1^{-2}-1)e_3 & (t_2^{-2}-1)e_3 & t_3^{-2} \end{pmatrix}.
\end{aligned}
\tag{2.2.8}
$$

Now let $(\mathbf{K}, V), (\mathbf{K}', V')$ be objects in $\mathsf{Rep}\big(H_{D_4}(t,q)\big)$ and $\varphi : V \to V'$ be a homomorphism of representations, i.e. for $i = 1,2,3$ the following diagram commutes:

$$
\begin{array}{ccc} V & \xrightarrow{\varphi} & V' \\ {\scriptstyle K_i}\downarrow & & \downarrow{\scriptstyle K_i'} \\ V & \xrightarrow{\varphi} & V' \end{array}
\tag{2.2.9}
$$

Since representations in the same category have the same parameters (q,t), φ also commutes with the rescaled representations.

In order to define the functor on arrows, we first introduce the map

$$
\mathscr{C}(\varphi) := (\bigoplus_3 \varphi)^3 : (\bigoplus_3 V)^3 \to (\bigoplus_3 V')^3
\tag{2.2.10}
$$

as the arrow in VECT^2 making the diagram

$$\begin{array}{ccc} (\bigoplus_3 V)^3 & \xrightarrow{\mathscr{C}(\varphi)} & (\bigoplus_3 V')^3 \\ {\scriptstyle (N_1,N_2,N_3)}\downarrow & & \downarrow{\scriptstyle (N_1',N_2',N_3')} \\ (\bigoplus_3 V)^3 & \xrightarrow{\mathscr{C}(\varphi)} & (\bigoplus_3 V')^3 \end{array} \tag{2.2.11}$$

commute. E.g.,

$$(\bigoplus_3 \varphi)N_1 = \begin{pmatrix} \varphi\widehat{K}_1 & \varphi\widehat{K}_2-\varphi & \varphi\widehat{K}_3-\varphi \\ 0 & \varphi & 0 \\ 0 & 0 & \varphi \end{pmatrix} \overset{(2.2.9)}{=\!=} \begin{pmatrix} \widehat{K}_1'\varphi & \widehat{K}_2'\varphi-\varphi & \widehat{K}_3'\varphi-\varphi \\ 0 & \varphi & 0 \\ 0 & 0 & \varphi \end{pmatrix} = N_1'(\bigoplus_3 \varphi). \tag{2.2.12}$$

Analogously, $(\bigoplus_3 \varphi)N_i = N_i'(\bigoplus_3 \varphi)$ holds for $i = 2, 3$.

Since $(\bigoplus_3 \varphi)E = E'(\bigoplus_3 \varphi)$ given that $\varphi e_i = e_i'\varphi$, the map (2.2.10) restricts to $E(V)^3$ as

$$\mathscr{M}_q(\varphi) := (\bigoplus_3 \varphi)^3 : E(V)^3 \to E'(V')^3,$$

defining the functor $\mathscr{M}_q$ on arrows. Indeed, the diagram

$$\begin{array}{ccc} E(V)^3 & \xrightarrow{\mathscr{M}_q(\varphi)} & E'(V')^3 \\ {\scriptstyle (EN_1,EN_2,EN_3)}\downarrow & & \downarrow{\scriptstyle (E'N_1',E'N_2',E'N_3')} \\ E(V)^3 & \xrightarrow{\mathscr{M}_q(\varphi)} & E'(V')^3 \end{array} \tag{2.2.13}$$

commutes given that (2.2.12) restricts as

$$(\bigoplus_3 \varphi)EN_1 = E'(\bigoplus_3 \varphi)N_1 = E'N_1'(\bigoplus_3 \varphi). \tag{2.2.14}$$

Functoriality is a straightforward consequence of the definitions: for the identity $\mathrm{id} : V \to V$, the relation $\mathscr{M}_q(\mathrm{id}) = \mathrm{id}$ is obvious while given two arrows $\varphi : V \to V'$ and $\psi : V' \to V''$,

$\mathscr{M}_q(\psi\varphi) = \mathscr{M}_q(\psi)\mathscr{M}_q(\varphi)$ follows from

$$\bigoplus_3(\psi\varphi) = (\bigoplus_3\psi)(\bigoplus_3\varphi) \in \mathrm{Hom}(E(V), E''(V'')). \qquad \square$$

Remark 2.2.5 *In the language of Katz [26], Definition 2.2.3 is the quantum algebraic analogue of $M(\infty, \mathscr{F})$. It corresponds to quotient by only the $\mathcal{K}$ subspace (equivalently, to assume λ generic and set it to 1 after the restriction is performed).*

A quantum construction taking full account of the other subspace would be useless for our purpose: for a nontrivial $\mathcal{L}$, the image of such a quantum middle convolution would remain an object in $\mathsf{Rep}\big(H_{D_4}(t,q)\big)$, with no hope of being mapped to a different GDAHA.

2.3 Quantum Killing factorization

The Killing factorization is readily extended to the noncommutative realm:

Lemma 2.3.1 *For a noncommutative ring $\mathcal{R}$ with unit group $\mathcal{R}^\times$, let $R_1, R_2, R_3 \in \mathsf{Mat}_3(\mathcal{R})$ be pseudo-reflections: for $a_{ij} \in \mathcal{R}$,*

$$R_1 = \begin{pmatrix} a_{11} & a_{12} & a_{13} \\ 0 & 1 & 0 \\ 0 & 0 & 1 \end{pmatrix}, \quad R_2 = \begin{pmatrix} 1 & 0 & 0 \\ a_{21} & a_{22} & a_{23} \\ 0 & 0 & 1 \end{pmatrix}, \quad R_3 = \begin{pmatrix} 1 & 0 & 0 \\ 0 & 1 & 0 \\ a_{31} & a_{32} & a_{33} \end{pmatrix}. \tag{2.3.1}$$

Their product can be uniquely factorized as

$$R_1R_2R_3 = UL, \tag{2.3.2}$$

for U upper unitriangular and L lower triangular given by

$$L - (U^{-1} - 1) = A, \quad (A)_{ij} = a_{ij}. \tag{2.3.3}$$

Moreover, when $a_{ii} \in \mathcal{R}^\times$, R_i is invertible in $\mathsf{Mat}_3(\mathcal{R})$.

Proof. With the ordering in the entries induced by the matrix multiplication one, by direct computation we obtain

$$R_1R_2R_3 = \begin{pmatrix} a_{11} + a_{12}a_{21} + a_{13}a_{31} + a_{12}a_{23}a_{31} & a_{12}a_{22} + a_{13}a_{32} + a_{12}a_{23}a_{32} & a_{13}a_{33} + a_{12}a_{23}a_{33} \\ a_{21} + a_{23}a_{31} & a_{22} + a_{23}a_{32} & a_{23}a_{33} \\ a_{31} & a_{32} & a_{33} \end{pmatrix}. \tag{2.3.4}$$

Multiplying this formula on the left by a suitable upper unitriangular matrix U^{-1}, we obtain a lower triangular result:

$$\underbrace{\begin{pmatrix} 1 & -a_{12} & -a_{13} \\ 0 & 1 & -a_{23} \\ 0 & 0 & 1 \end{pmatrix}}_{U^{-1}} R_1R_2R_3 = \underbrace{\begin{pmatrix} a_{11} & 0 & 0 \\ a_{21} & a_{22} & 0 \\ a_{31} & a_{32} & a_{33} \end{pmatrix}}_{L}. \tag{2.3.5}$$

To calculate U, we use the fact that U^{-1} is unipotent: $(U^{-1} - \mathbb{1})^3 = \mathbb{0}$ implies

$$U = U^{-2} + 3U^{-1} - 3\mathbb{1} = \begin{pmatrix} 1 & a_{12} & a_{13} + a_{12}a_{23} \\ 0 & 1 & a_{23} \\ 0 & 0 & 1 \end{pmatrix}. \tag{2.3.6}$$

Assuming that $a_{11} \in \mathcal{R}^\times$ and denoting by a_{11}^{-1} its multiplicative inverse,

$$R_1^{-1} = \begin{pmatrix} a_{11}^{-1} & -a_{11}^{-1}a_{12} & -a_{11}^{-1}a_{13} \\ 0 & 1 & 0 \\ 0 & 0 & 1 \end{pmatrix} \tag{2.3.7}$$

and analogous formulae hold for R_2 and R_3. When $a_{ii} \in \mathcal{R}^\times$ for $i = 1, 2, 3$, the triple product

$R_1R_2R_3$ can be inverted too. Doing so via the factorisation, since U^{-1} is known it suffices to invert L:

$$L^{-1} = \begin{pmatrix} a_{11}^{-1} & 0 & 0 \\ -a_{22}^{-1}a_{21}a_{11}^{-1} & a_{22}^{-1} & 0 \\ -a_{33}^{-1}a_{31}a_{11}^{-1} + a_{33}^{-1}a_{32}a_{22}^{-1}a_{21}a_{11}^{-1} & -a_{33}^{-1}a_{32}a_{22}^{-1} & a_{33}^{-1} \end{pmatrix}. \tag{2.3.8}$$

□

Applying Lemma 2.3.1 to each $R_i = EN_i\big|_{E(V)}$, the factorization (2.3.2) takes the form

$$U = \begin{pmatrix} 1 & (t_2^{-2}-1)e_1 & (t_3^{-2}-1)e_1 + (t_2^{-2}-1)(t_3^{-2}-1)e_1e_2 \\ 0 & 1 & (t_3^{-2}-1)e_2 \\ 0 & 0 & 1 \end{pmatrix}, \tag{2.3.9}$$

$$L = \begin{pmatrix} t_1^{-2} & 0 & 0 \\ (t_1^{-2}-1)e_2 & t_2^{-2} & 0 \\ (t_1^{-2}-1)e_3 & (t_2^{-2}-1)e_3 & t_3^{-2} \end{pmatrix}. \tag{2.3.10}$$

Moreover, defining $h_i := (t_i^{-2}-1)$,

$R_1R_2R_3 =$

$$\begin{pmatrix} t_1^{-2} + h_1h_2e_1e_2 + h_1h_3e_1(1+h_2e_2)e_3 & t_2^{-2}h_2e_1 + h_2h_3e_1(1+h_2e_2)e_3 & t_3^{-2}h_3e_1 + t_3^{-2}h_2h_3e_1e_2 \\ h_1e_2 + h_1h_3e_2e_3 & t_2^{-2} + h_2h_3e_2e_3 & t_3^{-2}h_3e_2 \\ h_1e_3 & h_2e_3 & t_3^{-2} \end{pmatrix}.$$

2.4 The functorial composition

Composing the noncommutative analogues of the Killing factorization and the middle convolution provides a tool to construct representations of the E_6-type GDAHA, provided a special choice for some of its parameters:

Lemma 2.4.1 *Given an object $(\rho, V) \in \mathsf{Rep}\big(H_{D_4}(t,q)\big)$, let U and L be the quantum Killing*

factors of $EN_1EN_2EN_3$*, where* (EN_1, EN_2, EN_3) *is the triple of pseudo-reflections* (2.2.8). *Denoting by* $\Pi := (EN_1EN_2EN_3)^{-1}$ *the inverse triple product, the following relations hold:*

$$\begin{aligned}(U-1)(U-1)(U-1) &= 0,\\ \left(L-t_1^{-2}\right)\left(L-t_2^{-2}\right)\left(L-t_3^{-2}\right) &= 0,\\ (\Pi-1)\left(\Pi-\sqrt{q}\,t_1t_2t_3t_4\right)\left(\Pi-\sqrt{q}\,\frac{t_1t_2t_3}{t_4}\right) &= 0.\end{aligned} \tag{2.4.1}$$

In particular, the rescaled operators

$$\widehat{L} := (t_1t_2t_3)^{2/3}L, \quad \widehat{\Pi} := \frac{1}{q^{1/3}(t_1t_2t_3)^{2/3}}\Pi, \tag{2.4.2}$$

satisfy the Hecke relations

$$\begin{aligned}\left(\widehat{L}-t_1^{-4/3}t_2^{2/3}t_3^{2/3}\right)\left(\widehat{L}-t_1^{2/3}t_2^{-4/3}t_3^{2/3}\right)\left(\widehat{L}-t_1^{2/3}t_2^{2/3}t_3^{-4/3}\right) &= 0,\\ \left(\widehat{\Pi}-\frac{1}{q^{1/3}t_1^{2/3}t_2^{2/3}t_3^{2/3}}\right)\left(\widehat{\Pi}-q^{1/6}t_1^{1/3}t_2^{1/3}t_3^{1/3}t_4\right)\left(\widehat{\Pi}-q^{1/6}\frac{t_1^{1/3}t_2^{1/3}t_3^{1/3}}{t_4}\right) &= 0,\end{aligned} \tag{2.4.3}$$

together with the cyclic one

$$U\,\widehat{L}\,\widehat{\Pi} = q^{-1/3}. \tag{2.4.4}$$

Proof. By construction, $U\,L\,\Pi = 1$ and (2.4.4) follows immediately. As an *upper* triangular matrix of operators, U automatically satisfies a Hecke relation with its diagonal entries as parameters—which are forced to be unities by the quantum factorization. Being lower triangular, L satisfies the analogous Hecke relation if and only if its diagonal is made of invertible elements—which is the case for the factorization of (EN_1, EN_2, EN_3), see (2.3.10).

To prove the remaining Hecke relation for Π, we use the basic (faithful) representation of $H_{D_4}(t,q)$ [31]. This is given by the operators T_0, T_1, Z acting on the space of Laurent

polynomials $f[z] \in V := \mathbb{C}[z^{\pm 1}]$ as follows:

$$(Zf)[z] := z f[z], \tag{2.4.5}$$

$$(T_1(a,b)f)[z] := \frac{(a+b)z-(1+ab)}{1-z^2} f[z] + \frac{(1-az)(1-bz)}{1-z^2} f[z^{-1}], \tag{2.4.6}$$

$$(T_0(a,b,c,d)f)[z] := \frac{q^{-1}z((cd+q)z-(c+d)q)}{q-z^2} f[z] - \frac{(c-z)(d-z)}{q-z^2} f[qz^{-1}]. \tag{2.4.7}$$

These operators satisfy the algebra relations

$$\begin{aligned} (T_1+ab)(T_1+1) &= 0, \\ (T_0+q^{-1}cd)(T_0+1) &= 0, \\ (T_1Z+a)(T_1Z+b) &= 0, \\ (qT_0Z^{-1}+c)(qT_0Z^{-1}+d) &= 0. \end{aligned} \tag{2.4.8}$$

To put these relations in form (2.2.2), we set

$$\begin{gathered} \widehat{K}_1 = -T_1, \quad \widehat{K}_2 = -aT_1^{-1}Z^{-1}, \quad \widehat{K}_3 = -T_0, \quad \widehat{K}_4 = -\frac{1}{a\sqrt{q}} T_0^{-1}Z, \\ t_1^2 = \frac{1}{ab}, \qquad t_2^2 = \frac{b}{a}, \qquad t_3^2 = \frac{q}{cd}, \qquad t_4^2 = \frac{c}{d}. \end{gathered} \tag{2.4.9}$$

Notice that with this choice, among the new relations we have the cyclic one as (2.2.3).

Despite the fact that the operators $\widehat{K}_i$ act on the infinite dimensional $\mathbb{C}$-vector space of Laurent polynomials $\mathbb{C}[z^{\pm 1}]$, we can give an explicit characterization to their eigenspaces:

Lemma 2.4.2 ([27]) *Let* Sym *denote the space of symmetric Laurent polynomials,*

$$\mathsf{Sym} = \left\{ f \in \mathbb{C}[z^{\pm 1}] \,|\, f[z] = f[z^{-1}] \right\},$$

and Sym_q *denote the space of q-symmetric Laurent polynomials,*

$$\mathsf{Sym}_q = \left\{ f \in \mathbb{C}[z^{\pm 1}] \,|\, f[z] = f[qz^{-1}] \right\}.$$

Then,

$$\begin{aligned}
&\widehat{K}_1 f[z] = abf[z] \iff f[z] \in \mathsf{Sym},\\
&\widehat{K}_2 f[z] = \frac{a}{b} f[z] \iff f[z] = (bz-1)p[z], \quad p[z] \in \mathsf{Sym},\\
&\widehat{K}_3 f[z] = \frac{cd}{q} f[z] \iff f[z] \in \mathsf{Sym}_q.
\end{aligned} \tag{2.4.10}$$

Thanks to Lemma 2.4.2, we have that

$$e_1(V) = \mathsf{Sym}, \quad e_2(V) = (bz-1)\,\mathsf{Sym}, \quad e_3(V) = \mathsf{Sym}_q,$$

allowing to give an explicit restriction of the triple of operators resulting from applying $\mathscr{M}_q$ to $(\widehat{K}_1, \widehat{K}_2, \widehat{K}_3)$ from (2.4.9). The restricted operators act on a generic element in the quotient $(v_1[z], v_2[z], v_3[z]) \in E(V) = e_1(V) \oplus e_2(V) \oplus e_3(V)$ as follows:

$$\begin{aligned}
EN_1(v_1[z], v_2[z], v_3[z]) = \Bigg(& abv_1[z] + \frac{(a-b)(b-z)}{b(ab-1)z} v_2[z] \\
& + \frac{(cd-q)}{(ab-1)q(z^2-1)} \left((az-1)(bz-1)v_3[z^{-1}] - (a-z)(b-z)v_3[z] \right), v_2[z],\, v_3[z] \Bigg),
\end{aligned} \tag{2.4.11}$$

$$\begin{aligned}
EN_2(v_1[z], v_2[z], v_3[z]) = \Bigg(& v_1[z], -\frac{a(ab-1)(bz-1)}{(a-b)} v_1[z] + \frac{a}{b} v_2[z] \\
& + \frac{(cd-q)(bz-1)}{(a-b)q(z^2-1)} \left((a-z)v_3[z] - z(az-1)v_3[z^{-1}] \right), v_3[z] \Bigg),
\end{aligned} \tag{2.4.12}$$

$$\begin{aligned}
EN_3(v_1[z], v_2[z], v_3[z]) = \Bigg(& v_1[z],\, v_2[z], \\
& \frac{(ab-1)}{(cd-q)(q-z^2)} \left(q(c-z)(z-d)v_1[qz^{-1}] - (cz-q)(dz-q)v_1[z] \right) \\
& + \frac{(a-b)}{b(cd-q)(q-z^2)} \left(q(c-z)(d-z)v_2[qz^{-1}] - (cz-q)(dz-q)v_2[z] \right) + \frac{cd}{q} v_3[z] \Bigg).
\end{aligned} \tag{2.4.13}$$

It is immediate to put these operators in matrix form and read off their Killing factors as explained in Section 2.3.

We obtain the following operators:

$$L(v_1[z],v_2[z],v_3[z]) = \Big(ab\,v_1[z],\ \frac{a(ab-1)(bz-1)}{a-b}v_1[z] + \frac{a}{b}v_2[z],$$
$$\frac{(ab-1)}{(cd-q)(q-z^2)}\big(q(c-z)(d-z)v_1[qz^{-1}] - (cz-q)(dz-q)v_1[z]\big)$$
$$+ \frac{(a-b)}{b(cd-q)(q-z^2)}\big(q(c-z)(d-z)v_2[qz^{-1}] - (cz-q)(dz-q)v_2[z]\big) + \frac{q}{cd}v_3[z]\Big), \tag{2.4.14}$$

and

$$U(v_1[z],v_2[z],v_3[z]) = \Big(v_1[z] + \frac{(a-b)(b-z)}{b(ab-1)z}v_2[z]$$
$$+ \frac{(cd-q)}{q(ab-1)b(z^2-1)}\big(z(az-1)(bz-1)v_3[z^{-1}] - \frac{(a-z)(b-z)}{z}v_3[z]\big),$$
$$v_2[z] + \frac{(cd-q)(bz-1)}{(a-b)q(z^2-1)}\big((a-z)v_3[z] - z(az-1)v_3[z^{-1}]\big),\ v_3[z]\Big). \tag{2.4.15}$$

Moreover, we set $\Pi = L^{-1}U^{-1}$, where L^{-1} and U^{-1} are computed as prescribed in Section 2.3:

$$\Pi(v_1[z],v_2[z],v_3[z]) = \Big(\frac{1}{ab}v_1[z] + \frac{(a-b)(z-b)(bz-1)}{ab^2(ab-1)z}v_2[z]$$
$$+ \frac{(cd-q)}{ab(ab-1)q(z^2-1)}\big((z-a)(z-b)v_3[z] - (az-1)(bz-1)v_3[z^{-1}]\big),$$
$$\frac{(ab-1)(bz-1)}{a(a-b)}v_1[z] + \frac{(bz-1)(b-z+bz^2)}{abz}v_2[z]$$
$$+ \frac{(cd-q)(bz-1)}{a(a-b)q(z^2-1)}\big((az-1)v_3[z^{-1}] - (a-z)v_3[z]\big),$$
$$\frac{(ab-1)q}{acd(cd-q)(z^2-q)}\Big(\frac{q^2}{z}(c-z)(d-z)v_1[qz^{-1}] - z(cz-q)(dz-q)v_1[z]\Big)$$
$$+ \frac{(a-b)q}{abcd(cd-q)(z^2-q)}\Big(\frac{q^2}{z^2}(bq-z)(c-z)(d-z)v_2[qz^{-1}] - z(bz-1)(cz-q)(dz-q)v_2[z]\Big)$$
$$- \frac{q(c-z)(d-z)(az-q)}{acdz(z^2-q)}v_3[qz^{-1}] - \frac{z\,(aq(d-z)+(ac+q-cz)(q-dz))}{acd(z^2-q)}\Big). \tag{2.4.16}$$

The Hecke relations for L and U can be checked directly using formulae (2.4.14-2.4.15), while $U\,L\,\Pi = 1$ holds by construction. Verifying the Hecke relation for Π is a heavy computation best performed with symbolic calculation [8].

This concludes the proof of formulae (2.4.1) with parameters (2.4.9). □

Theorem 2.4.3 *The quantum Killing factorization of the quantum middle convolution gives a functor of (faithful) representations*

$$\begin{array}{rccc} \mathscr{F}_q : & \mathsf{Rep}\big(H_{D_4}(t,q)\big) & \to & \mathsf{Rep}\big(H_{E_6}(\tilde{t},q)\big), \\ & (\rho, V) & \mapsto & (\eta, E(V)), \end{array}$$

where

$$E(V) := e_1(V) \oplus e_2(V) \oplus e_3(V),$$

with e_i defined in Lemma 2.2.2, and $\eta : H_{E_6}(\tilde{t},q) \to \mathrm{End}(E(V))$ is the algebra homomorphism acting on the generators J_1, J_2, J_3 of $H_{E_6}(\tilde{t},q)$ as

$$\eta(J_1) = U, \quad \eta(J_2) = \widehat{L}, \quad \eta(J_3) = \widehat{\Pi},$$

with U, $\widehat{L}$ and $\widehat{\Pi}$ defined in Lemma 2.4.1 and the parameters $\tilde{t}$ given by

$$\begin{aligned} &\tilde{t}_1^{(1)} = \tilde{t}_1^{(2)} = 1, \qquad \tilde{t}_2^{(1)} = t_1^{-4/3} t_2^{2/3} t_3^{2/3}, \quad \tilde{t}_2^{(2)} = t_1^{2/3} t_2^{-4/3} t_3^{2/3}, \\ &\qquad\qquad \tilde{t}_3^{(1)} = \frac{q^{-1/3}}{t_1^{2/3} t_2^{2/3} t_3^{2/3}}, \quad \tilde{t}_3^{(2)} = q^{1/6} t_1^{1/3} t_2^{1/3} t_3^{1/3} t_4. \end{aligned} \tag{2.4.17}$$

Proof. In Lemma 2.4.1, we have already proven that $\mathscr{F}_q$ maps objects $(\rho, V) \in \mathsf{Rep}\big(H_{D_4}(t,q)\big)$ to objects $(\eta, E(V)) \in \mathsf{Rep}\big(H_{E_6}(\tilde{t},q)\big)$. The faithfulness of $(\eta, E(V))$ is proven with the very same argument used in the proof of Theorem 3.2.3.

Now, let (ρ, V) and (ρ', V') be two objects in $\mathsf{Rep}\big(H_{D_4}(t,q)\big)$ and $\varphi : V \to V'$ a homomorphism of representations. The map of arrows defined in the proof of Proposition 2.2.4 carries

through the factorization: for $i=1,2,3$, $\mathscr{F}_q(\varphi):=\bigoplus_3\varphi$ gives the commutative diagram

$$\begin{array}{ccc} E(V) & \xrightarrow{\mathscr{F}_q(\varphi)} & E'(V') \\ {\scriptstyle \eta(J_i)}\downarrow & & \downarrow{\scriptstyle \eta'(J_i)} \\ E(V) & \xrightarrow{\mathscr{F}_q(\varphi)} & E'(V') \end{array} \tag{2.4.18}$$

Indeed, each Killing factor's entry is a (linear combination of) composition of entries from EN_1, EN_2, EN_3 and these suitably commute with φ: as previously observed, $\varphi e_i = e_i'\varphi$.
To conclude, functoriality holds unaffected: for the identity $\mathrm{id}: V\to V$, $\mathscr{F}_q(\mathrm{id})=\mathrm{id}$ manifestly while for $\psi: V'\to V''$ satisfying $\psi\rho'(K_i)=\rho''(K_i)\psi$, $\mathscr{F}_q(\psi\varphi)=\bigoplus_3(\psi\varphi)=(\bigoplus_3\psi)(\bigoplus_3\varphi)$ as maps in $\mathrm{Hom}(E(V),E''(V''))$. □

Remark 2.4.4 *In principle, one can obtain a wealth of representations of $H_{E_6}(\tilde{t},q)$ by feeding the functor $\mathscr{F}_q$ with the representation theory of H_{D_4}. We provide two examples of distinct nature with the basic representation above and the quantum matricial one in the following section.*

Notice also that $\tilde{t}$ specializes only the two parameters $t_1^{(1)}$ and $t_1^{(2)}$: the remaining four are free, as confirmed by the following inversion formulae

$$t_1=q^{-1/6}\tilde{t}_2^{(1)-1/2}\tilde{t}_3^{(1)-1/2},\quad t_2=q^{-1/6}\tilde{t}_2^{(2)-1/2}\tilde{t}_3^{(1)-1/2},\quad t_3=q^{-1/6}\tilde{t}_2^{(1)1/2}\tilde{t}_2^{(2)1/2}\tilde{t}_3^{(1)-1/2},\quad t_4=\tilde{t}_3^{(1)1/2}\tilde{t}_3^{(2)}. \tag{2.4.19}$$

This specialization is deeply connected with monodromy, in that it achieves the unitriangular requirement of the irregular data (see the last paragraph of Section 1.1.2).

2.5 Application: quantum irregular monodromy data

In this section, by applying the functor $\mathscr{F}_q$ to the quantum Fuchsian monodromy matrices, we finally construct an explicit quantization of the irregular data (1.1.26).

As prescribed in Section 2.2, we start by rescaling the triple (I.10) of $\mathsf{SL}_2(\mathbb{T}^3_q)$ matrices:

$$\widehat{K}_1 = -e^{\frac{p_1}{2}} M_1^{\hbar} = \begin{pmatrix} 0 & e^{S_1+p_1} \\ -e^{-S_1} & 1+e^{p_1} \end{pmatrix},$$
$$\widehat{K}_2 = -e^{\frac{p_2}{2}} M_2^{\hbar} = \begin{pmatrix} 1+e^{p_2}+e^{S_2+p_2} & 1+e^{p_2}+e^{S_2+p_2}+e^{-S_2} \\ -e^{S_2+p_2} & -e^{S_2+p_2} \end{pmatrix}, \tag{2.5.1}$$
$$\widehat{K}_3 = -e^{\frac{p_3}{2}} M_3^{\hbar} = \begin{pmatrix} 1+e^{p_3}+e^{-S_3} & e^{-S_3} \\ -1-e^{p_3}-e^{S_3+p_3}-e^{-S_3} & -e^{-S_3} \end{pmatrix}.$$

As our input to $\mathscr{F}_q$ is given by 2×2 matrices, the map $\mathscr{C}$ will produce 6×6 matrices N_1, N_2, N_3.

In order to perform concretely the quotient at the core of the quantum middle convolution, we need an explicit characterization of the eigenspaces $V_2^{(1)}, V_2^{(2)}, V_2^{(3)}$ (2.2.5) we have to restrict to. Selecting a representation of $\mathbb{T}^3_q$ on a vector space $\mathcal{V}$, we fit the framework of genuine representations on vector spaces developed in Section 2.2: indeed, this allows to view the matrices $\widehat{K}_i$ as elements in $\mathrm{End}(\mathcal{V}\oplus\mathcal{V})$, namely $V := \mathcal{V}\oplus\mathcal{V}$. Now, solving for eigenspaces is more conveniently carried out by reading formulae (2.5.1) as arrows in $\mathrm{Hom}_{\mathsf{Mod}\text{-}\mathbb{T}^3_q}(\oplus_2\mathbb{T}^3_q, \oplus_2\mathbb{T}^3_q)$, where $\mathsf{Mod}\text{-}\mathbb{T}^3_q$ denotes the category of right $\mathbb{T}^3_q$-modules, namely having the rescaled matrices act in the usual way on the columns in $\mathsf{Mat}_{2\times 1}(\mathbb{T}^3_q)$. Indeed, computing eigenspaces in $\mathcal{V}\oplus\mathcal{V}$ amounts to solving $\mathbb{T}^3_q$-linear equations.

Remark 2.5.1 *The quantum n-torus, $n\in\mathbb{Z}_{>0}$, is known to be an Ore domain [2] whose ring of fractions* $\mathrm{Frac}(\mathbb{T}^n_q)$ *is a division algebra. Therefore, $\oplus_2\mathbb{T}^3_q$ is well-defined as the free rank* 2 *$\mathbb{T}^3_q$-module.*

Proposition 2.5.2 *As rank* 1 *$\mathbb{T}^3_q$-submodules of $\oplus_2\mathbb{T}^3_q$, the eigenspaces $V_2^{(i)}$ read*

$$V_2^{(1)} = \left\langle (e^{S_1}, 1)^T \right\rangle, \quad V_2^{(2)} = \left\langle (-1-e^{-S_2}, 1)^T \right\rangle, \quad V_2^{(3)} = \left\langle (-1, 1+e^{S_3})^T \right\rangle. \tag{2.5.2}$$

Then,

$$E(\mathcal{V}\oplus\mathcal{V}) = \left\langle (e^{S_1},1,0,0,0,0)^T,\, (0,0,-1-e^{-S_2},1,0,0)^T,\, (0,0,0,0,-1,1+e^{S_3})^T \right\rangle \quad (2.5.3)$$

Proof. It is a straightforward computation: e.g., looking for $(a,b)^T \in \oplus_2 \mathbb{T}^3_q$ such that

$$\begin{pmatrix} 1+e^{p_2}+e^{S_2+p_2} & 1+e^{p_2}+e^{S_2+p_2}+e^{-S_2} \\ -e^{S_2+p_2} & -e^{S_2+p_2} \end{pmatrix} \begin{pmatrix} a \\ b \end{pmatrix} = e^{p_2} \begin{pmatrix} a \\ b \end{pmatrix}, \quad (2.5.4)$$

one immediately obtains $a = -b - e^{-S_2} b$ from the second equation and this tautologically satisfies the first one. Notice that all three pairs of equations can be solved in $\mathbb{T}^3_q$, providing each a rank-1 submodule, due to the very special entries of the triple. In general, one must resort to $\mathrm{Frac}(\mathbb{T}^3_q)$ to invert generic entries. □

Reading $\mathscr{C}(\widehat{\mathbf{K}})$ over the generators (2.5.3), we obtain a triple of pseudo-reflections (R_1, R_2, R_3) encoded by the following A matrix (see Section 2.3):

$$A = \begin{pmatrix} e^{p_1} & (1-e^{p_2})\frac{1+e^{-S_1-p_1}(1+e^{-S_2})}{e^{-p_1}-1} & (1-e^{p_3})\frac{1+e^{-S_1-p_1}+e^{S_3}}{e^{-p_1}-1} \\ (e^{p_1}-1)\frac{e^{-p_2}+(1+q^2e^{S_1})e^{S_2}}{e^{-p_2}-1} & e^{p_2} & (e^{p_3}-1)\frac{e^{-p_2}+(e^{-p_2}+e^{S_2})e^{S_3}}{e^{-p_2}-1} \\ (e^{p_1}-1)\frac{e^{-S_3-p_3}+e^{S_1}(1+q^2e^{-S_3-p_3})}{e^{-p_3}-1} & (1-e^{p_2})\frac{1+e^{-S_2}(1+q^2e^{-S_3-p_3})}{e^{-p_3}-1} & e^{p_3} \end{pmatrix}. \quad (2.5.5)$$

We choose a more polished $(\overline{R}_1, \overline{R}_2, \overline{R}_3)$ by performing a global diagonal conjugation, which manifestly preserves the pseudo-reflection structure of the whole triple:

$$\overline{R}_1 := CR_1C^{-1} = \begin{pmatrix} e^{p_1} & -1-(1+e^{S_1+p_1})e^{S_2} & -q^{-1}e^{S_2}-q^{-1}e^{S_1+p_1}e^{S_2}(1+q^2e^{S_3}) \\ 0 & 1 & 0 \\ 0 & 0 & 1 \end{pmatrix},$$

$$\overline{R}_2 := CR_2C^{-1} = \begin{pmatrix} 1 & 0 & 0 \\ e^{p_2} + e^{-S_1+p_2} + q^2e^{-S_1}e^{-S_2} & e^{p_2} & -q^{-1} - q(1+e^{S_2+p_2})e^{S_3} \\ 0 & 0 & 1 \end{pmatrix},$$

$$\overline{R}_3 := CR_3C^{-1} = \begin{pmatrix} 1 & 0 & 0 \\ 0 & 1 & 0 \\ qe^{-S_2+p_3} + q(e^{-S_1}+1)e^{-S_2}e^{-S_3} & qe^{p_3}(1+e^{-S_2}) + qe^{-S_2}e^{-S_3} & e^{p_3} \end{pmatrix},$$

for $C := \mathrm{diag}(e^{S_1} - e^{S_1+p_1}, -e^{-S_2} + e^{-S_2+p_2}, -qe^{-S_2} + qe^{-S_3+p_2}) \in \mathsf{GL}_3(\mathbb{T}^3_q)$.

Remark 2.5.3 *As fully detailed in Theorem 3.3.3, this special choice selects in the conjugacy class of pseudo-reflections the triple allowing for a direct match with the representation from higher Teichmüller theory.*

The quantum Killing factorization of $\overline{R}_1\overline{R}_2\overline{R}_3$ reads

$$U = \begin{pmatrix} 1 & -1-(1+e^{S_1+p_1})e^{S_2} & q^{-1} + qe^{S_3} + q(1+e^{p_2}+e^{S_2+p_2}+e^{S_1+p_1}e^{S_2+p_2})e^{S_2}e^{S_3} \\ 0 & 1 & -q^{-1} - qe^{S_3} - qe^{S_2+p_2}e^{S_3} \\ 0 & 0 & 1 \end{pmatrix},$$

$$L = \begin{pmatrix} e^{p_1} & 0 & 0 \\ e^{p_2} + e^{-S_1+p_2} + q^2e^{-S_1}e^{-S_2} & e^{p_2} & 0 \\ q(e^{-S_2+p_3} + e^{-S_2}e^{-S_3} + e^{-S_1}e^{-S_2}e^{-S_3}) & q(e^{p_3} + e^{-S_2+p_3} + e^{-S_2}e^{-S_3}) & e^{p_3} \end{pmatrix}, \tag{2.5.6}$$

with inverse triple product $\Pi = L^{-1}U^{-1}$ obtained by formulae (2.3.5-2.3.8), see [8].

Performing the rescalings (2.4.2), we obtain

$$\widehat{L} := e^{-\frac{p_1}{3}}e^{-\frac{p_2}{3}}e^{-\frac{p_3}{3}}L, \quad \widehat{\Pi} := q^{-\frac{2}{3}}e^{\frac{p_1}{3}}e^{\frac{p_2}{3}}e^{\frac{p_3}{3}}\Pi. \tag{2.5.7}$$

Proposition 2.5.4 *The matrices* $U, \widehat{L}, \widehat{\Pi} \in \mathsf{SL}_3(\mathbb{T}_q^3)$ *satisfy the relations*

$$\begin{aligned}
(U-\mathbb{1})(U-\mathbb{1})(U-\mathbb{1}) &= \mathbb{0}, \\
\left(\widehat{L}-e^{\frac{2}{3}p_1-\frac{p_2}{3}-\frac{p_3}{3}}\mathbb{1}\right)\left(\widehat{L}-e^{-\frac{p_1}{3}+\frac{2}{3}p_2-\frac{p_3}{3}}\mathbb{1}\right)\left(\widehat{L}-e^{-\frac{p_1}{3}-\frac{p_2}{3}+\frac{2}{3}p_3}\mathbb{1}\right) &= \mathbb{0}, \\
\left(\widehat{\Pi}-q^{-\frac{2}{3}}e^{\frac{p_1}{3}+\frac{p_2}{3}+\frac{p_3}{3}}\mathbb{1}\right)\left(\widehat{\Pi}-q^{\frac{4}{3}}e^{-\frac{2}{3}p_1-\frac{2}{3}p_2-\frac{2}{3}p_3}e^{-S_1}e^{-S_2}e^{-S_3}\mathbb{1}\right) & \\
\left(\widehat{\Pi}-q^{\frac{4}{3}}e^{\frac{p_1}{3}+\frac{p_2}{3}+\frac{p_3}{3}}e^{S_1}e^{S_2}e^{S_3}\mathbb{1}\right) &= \mathbb{0}, \\
U\,\widehat{L}\,\widehat{\Pi} &= q^{-2/3}\mathbb{1}.
\end{aligned} \tag{2.5.8}$$

The map $J_1 \to U$, $J_2 \to \widehat{L}$, $J_3 \to \widehat{\Pi}$ *gives a faithful representation of* $H_{E_6}(\tilde{t}, q^2)$.

Proof. The whole statement follows as a corollary of Theorem 2.4.3. All relations can be checked directly in the Mathematica companion [9]. □

To conclude, the classical limit $q \to 1$ reads as

$$U \longrightarrow S_1, \quad L \longrightarrow S_2, \quad \Pi \longrightarrow M_0^L, \tag{2.5.9}$$

proving that the triple (Π, U, L) gives the desired quantum realization of the (generalized) irregular monodromy data. In particular [33], $e^{p_i} \equiv e^{2\pi i \theta_i}$, confirming the diagonal part of L matches the expected one of S_2, and the eigenvalues of Π match the expected form as $e^{s_1+s_2+s_3} \equiv e^{-\pi i(\theta_1+\theta_2+\theta_3+\theta_\infty)}$.

Chapter 3

The higher Teichmüller approach

We start the Chapter recalling the basics of higher Teichmüller theory and the moduli space of pinnings. We give a brief self-consistent summary of the Fock-Goncharov coordinates for the moduli space of $\mathsf{PGL}_n(\mathbb{R})$-local systems and their extension to the moduli space of pinnings due to Goncharov and Shen. We describe the so-called snake calculus, detailing how to compute transport matrices and glue triangles by amalgamations. After giving a recipe to represent fat graph loops by strings of transport matrices, we explain the quantization of the Fock-Goncharov coordinates.

Using this toolkit, the Chapter's main theorem constructs the first explicit representation of the universal GDAHA H_{E_6}. As a primer to this theorem, we recast in cluster terms the $\mathsf{SL}_2(\mathbb{T}^3_q)$-embedding (I.10), promoting it to the universal H_{D_4} by replacing the quantum 3-torus with a more general quantum algebra. This way, we rediscover the quantum Fuchsian monodromy data through the lens of higher Teichmüller geometry.

After introducing the quiver seizure operation, we conclude the Chapter by showing that the representation of the universal H_{E_6} can be reduced to recover the quantum irregular monodromy data generated by the GDAHA functor.

The whole Chapter is an adaptation of sections 2, 3 and 4 from the arXiv preprint

> D. Dal Martello and M. Mazzocco. Generalized double affine Hecke algebras, their representations, and higher Teichmüller theory. *arXiv:2307.06803v2,* 2023.

Throughout the Chapter, we mainly deal with the three quivers $\mathcal{Q}_1$, $\mathcal{Q}_2$, $\mathcal{Q}_3$ in Figure 3.1.

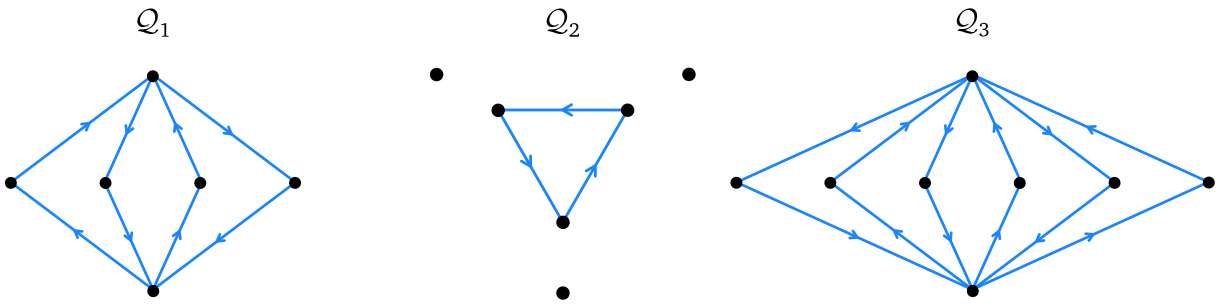

Figure 3.1: The main quivers starring in this thesis. $\mathcal{Q}_{2,3}$ emerge from the rank $n = 2, 3$ higher Teichmüller theory, respectively. $\mathcal{Q}_1$ is a full subquiver of $\mathcal{Q}_3$, obtained by evaluating at 1 specific central elements in $\mathcal{X}_{\mathcal{Q}_3}$, the quantum torus associated with $\mathcal{Q}_3$.

3.1 Higher Teichmüller theory

Let $\Sigma_{g,s,m}$ be a genus g topological surface with s boundary components and m marked points on the boundaries having negative Euler characteristic. In the absence of marked points, the Teichmüller space $\mathcal{T}_{\mathsf{PSL}_2}(\Sigma_{g,s,0})$, i.e., the moduli space of complex structures on $\Sigma_{g,s,0}$ modulo diffeomorphisms isotopic to the identity, is identified with the space of discrete faithful representations $\pi_1(\Sigma_{g,s,0}) \to \mathsf{PSL}_2(\mathbb{R})$ modulo conjugation.

This moduli space admits a *higher* generalization, replacing PSL_2 with any split semisimple algebraic group G, given by the *moduli space of pinnings* $\mathcal{P}_{\mathsf{G}}(\Sigma_{g,s,m})$ introduced by Goncharov and Shen [19]. The latter is defined as an extension by additional data of the moduli space $\mathcal{X}_{\mathsf{G}}(\Sigma_{g,s,m})$ of *framed* G-local systems, i.e., principal G-bundles with framed flat connections defined by attaching an invariant flag to each marked point.

3.1.1 Combinatorial description of the moduli space of pinnings

In this section, we recall the main ingredients of the combinatorial description of the moduli space $\mathcal{P}_{\mathsf{G}}(\Sigma_{g,s,m})$ and its quantization [6, 19], restricting to $\mathsf{G} = \mathsf{PGL}_n(\mathbb{R})$. We closely follow the former paper as well as [22]: since notations have been tailored to our needs, for the sake of the reader the exposition is self-consistent.

In subsection 3.1.1, we describe the moduli space of framed $\mathsf{PGL}_n(\mathbb{R})$-local systems for the disk with three marked points $1,2,3$ on its boundary. We picture such surface $\Sigma_{0,1,3}$ as the equilateral triangle $\triangle 123$ in Figure 3.9 and assign a clockwise orientation. In subsection 3.1.1, we introduce pinnings on $\triangle 123$ and explain how to glue triangles together to form the moduli space $\mathscr{P}$ for any Riemann surface $\Sigma_{g,s,m}$.

The snake calculus on a triangle

For a given $n \in \mathbb{Z}_{>0}$, we cover $\triangle 123$ by its unique tessellation of n^2 identical equilateral triangular tiles, arranged between upward and downward. Each vertex of this tessellation is labelled by a triple of non-negative integers (i,j,k) by the minimum number of tiles connecting it to the sides of $\triangle 123$: i for side 23, j for side 31 and k for side 12 (Figure 3.2). Since $i+j+k=n$, these triples are called *barycentric coordinates*. This coordinatization

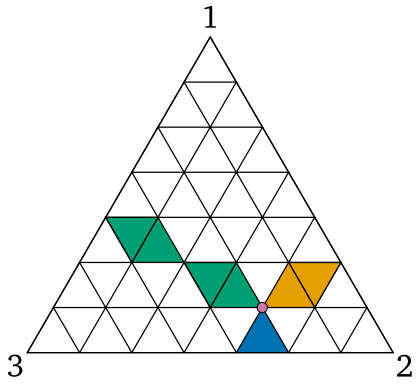

Figure 3.2: $n=7$ tessellation of $\triangle 123$ and barycentric coordinates $(1,4,2)$ for the pink vertex, with colors highlighting the tile-counting ruling the coordinatization. The total n^2 tiles are all similar to $\triangle 123$ and arranged between $\binom{n+1}{2}$ upward and $\binom{n}{2}$ downward ones.

naturally extends to a tile by assigning a triple (a,b,c) to its *center*:

- $a+b+c=n-1$ in the upward case, where vertices appear in the form

$$\big\{(a+1,b,c),(a,b+1,c),(a,b,c+1)\big\};$$

- $a+b+c=n-2$ in the downward case, where vertices appear in the form

$$\big\{(a,b+1,c+1),\,(a+1,b,c+1),\,(a+1,b+1,c)\big\}.$$

Remark 3.1.1 *Let us highlight the resulting combinatorics: barycentric coordinates are assigned to vertices of the tessellation and centers of the tiles so that the type of object they label can be detected by just inspecting the (integral) result of their sum.*

Since any flat connection on the contractible $\triangle 123$ is trivial, $\mathscr{X}_{\mathsf{PGL}_n(\mathbb{R})}(\triangle 123)$ is identified with the space of triples of invariant complete flags in $\mathbb{R}^n$.

Snake calculus is a way to construct elementary change-of-basis matrices between projective bases of $\mathbb{R}^n$ induced by a choice of flags in generic position. Let us detail the combinatorial features of this construction.

Definition 3.1.2 *A* complete flag $F_\bullet$ *in a vector space V is a collection of consecutively embedded subspaces*

$$\{0=F_0\subset F_1\subset\ldots\subset F_{n-1}\subset F_n=V\},\quad \dim(F_k)=k.$$

Let $F^1_\bullet, F^2_\bullet, F^3_\bullet$ be the (generic) complete flags in $\mathbb{R}^n$ attached to the vertices of $\triangle 123$. To any center (a,b,c) of a tile in the tessellation of $\triangle 123$, we attach the subspace $F^1_{n-a}\cap F^2_{n-b}\cap F^3_{n-c}$: a line λ_{abc} for upward tiles and a plane π_{abc} for downward ones. By construction, a plane π_{abc} contains the lines $\lambda_{(a+1)bc}, \lambda_{a(b+1)c}, \lambda_{ab(c+1)}$ attached to the three upward tiles adjacent to the downward one it is attached to. Let us visually highlight this correspondence: after labelling each center with its subspace, we stick on each plane a grey upward triangle whose vertices match the three coplanar lines it contains. Figure 3.3 gives a step-by-step display of the resulting configuration on $\triangle 123$.

For the rest of this section, we forget the tessellation focusing on these $\binom{n}{2}$ grey triangles—and the resulting $\binom{n-1}{2}$ white downward ones among them—looking at specific paths called

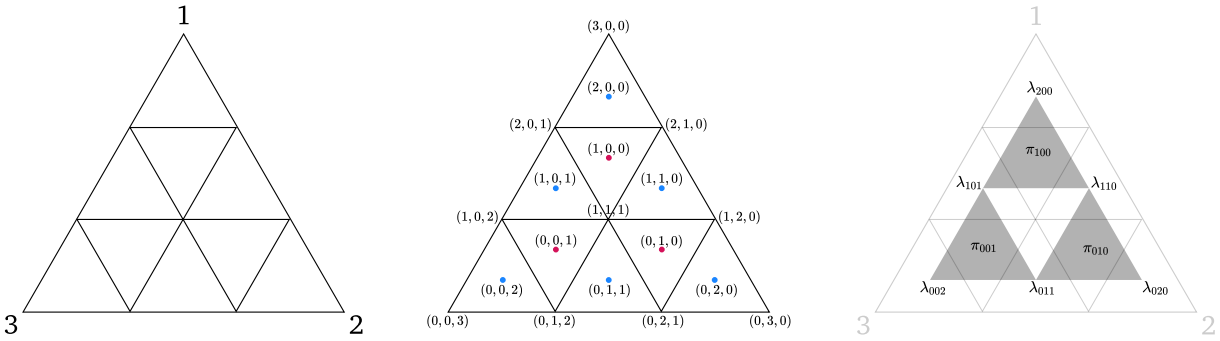

Figure 3.3: For $n = 3$, from left to right: tessellation of $\triangle 123$, barycentric coordinates for vertices of the tessellation and centers of the tiles, configuration of subspaces with the grey triangles (and one white triangle enclosed by them).

snakes that run over their sides. Notice that the upward grey and downward white triangles gives nothing but the $n-1$ tessellation of a triangle connecting $\{\lambda_{(n-1)00}, \lambda_{0(n-1)0}, \lambda_{00(n-1)}\}$.

Definition 3.1.3 *A* snake $\mathbf{p}$ *is an oriented piece-wise path composed by exactly* $n-1$ *sides of grey triangles, which starts from a tile sharing a vertex with* $\triangle 123$ *and ends on a tile in contact with the opposite side.*

Notice that the length requirement implies no segment can be parallel to the snake's target side of $\triangle 123$. We call $\mathbf{p}_{IJ}$, the unique snake running parallel to side IJ of $\triangle 123$, a ∂-snake. Let Greek letters denote a generic triple of barycentric coordinates: e.g., λ_{ijk} is equally denoted by λ_α. As shown in Figure 3.5, each segment of a snake connects two vertices α, β of a grey triangle. The corresponding lines $\lambda_\alpha, \lambda_\beta$ are coplanar to λ_γ, where γ is the remaining vertex of the grey triangle. By coplanarity, a choice of vector $\mathbf{v}_\alpha \in \lambda_\alpha$ uniquely determines $\mathbf{v}_\beta \in \lambda_\beta$ by the following orientation rule

$$\lambda_\gamma \ni \mathbf{v}_\gamma = \begin{cases} \mathbf{v}_\beta + \mathbf{v}_\alpha, & \circlearrowright \\ \mathbf{v}_\beta - \mathbf{v}_\alpha, & \circlearrowleft . \end{cases} \tag{3.1.1}$$

Therefore, a snake inductively determines a projective basis of $\mathbb{R}^n$: chosen the first vector

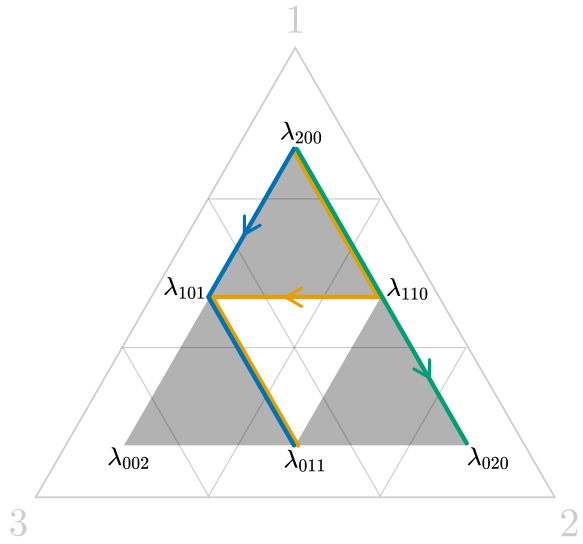

Figure 3.4: For $n = 3$, two snakes and a forbidden ochre path. The green snake $\mathbf{p}_{12}$ has basis $\{\mathbf{v}_{200}, \mathbf{v}_{110}, \mathbf{v}_{020}\}$ in $\mathbb{R}^3$, whose vectors satisfy $\mathbf{v}_{101} = \mathbf{v}_{110} + \mathbf{v}_{200}, \mathbf{v}_{011} = \mathbf{v}_{020} + \mathbf{v}_{110}$. The blue snake has basis $\{\mathbf{v}_{200}, \mathbf{v}_{101}, \mathbf{v}_{011}\}$, with $\mathbf{v}_{110} = \mathbf{v}_{101} - \mathbf{v}_{200}, \mathbf{v}_{002} = \mathbf{v}_{011} + \mathbf{v}_{101}$.

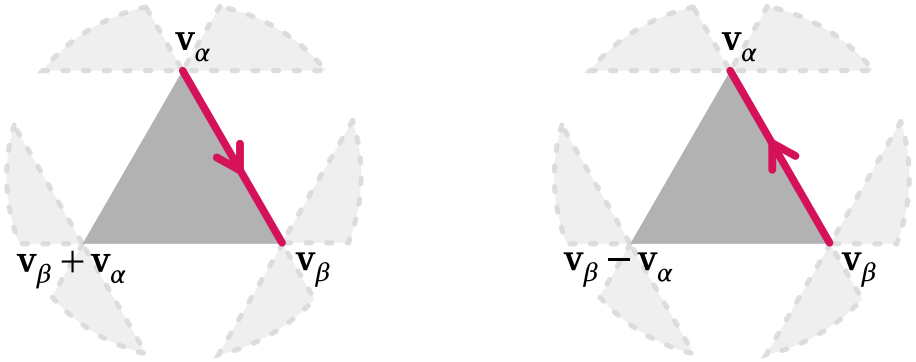

Figure 3.5: Segments of two oppositely oriented snakes. The vertices of the grey triangle correspond to 3 coplanar lines $\lambda_\alpha, \lambda_\beta, \lambda_\gamma$ and $\mathbf{v}_\gamma = \mathbf{v}_\beta \pm \mathbf{v}_\alpha$ depending on whether the segment is oriented clockwise or counterclockwise with respect to its grey triangle.

and iteratively applying the rule, the resulting n vectors are defined up to a global scaling factor. Their linear independence is a consequence of the flags being assumed generic.

Given any two snakes, a change-of-basis matrix maps between their corresponding projective bases. The snake calculus gives a simple recipe to write down these matrices: since the elementary moves in Figure 3.6 suffice to decompose any snake transformation, they are constructed out of the elementary building blocks in the following

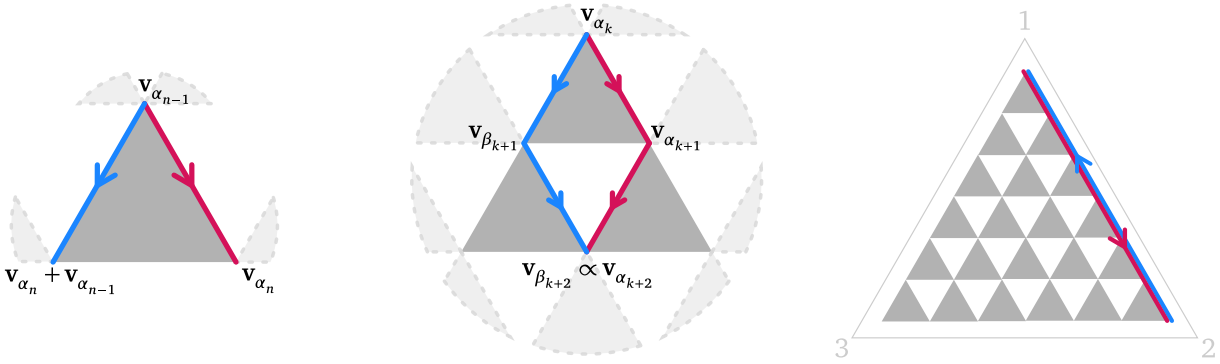

Figure 3.6: From left to right, elementary snake moves I, II and III mapping red to blue segments of a sample snake with $\mathbf{v}_1 \in \lambda_{n00}$. Notice that move I can only be performed on the last segment of a snake, i.e. when no subsequent segments can be affected. In this sense, move II can be thought of as the extension of move I to any other segment.

Definition 3.1.4 *Let E_{rs} be the matrix unit, i.e., $(E_{rs})_{ij} = \delta_{ri}\delta_{sj}$. For $\mathbb{1}$ denoting the identity matrix, $k \in \{1,\dots,n\}$ and a parameter $t \in \mathbb{R}_{>0}$, define the $\mathsf{SL}_n(\mathbb{R}_{>0})$ matrices*

$$L_k = \mathbb{1} + E_{k+1,k}, \tag{3.1.2}$$

$$H_k(t) = t^{-\frac{n-k}{n}}\operatorname{diag}\big(\underbrace{1,\dots,1}_{k\text{ times}},t,\dots,t\big), \tag{3.1.3}$$

and the $\mathsf{SL}_n(\mathbb{R})$ antidiagonal matrix

$$(S)_{ij} = (-1)^{n-i}\delta_{i,n+1-j}. \tag{3.1.4}$$

Let us sketch the origin of this advantageous feature, adapting Appendix A in [22]. Move I flips the last segment pivoting its source center across a grey triangle, by rule (3.1.1) yielding:

$$\begin{bmatrix}\mathbf{v}_{\alpha_1}\\ \vdots\\ \mathbf{v}_{\alpha_{n-1}}\\ \mathbf{v}_{\alpha_n}\end{bmatrix} \mapsto \begin{bmatrix}\mathbf{v}_{\alpha_1}\\ \vdots\\ \mathbf{v}_{\alpha_{n-1}}\\ \mathbf{v}_{\alpha_n}+\mathbf{v}_{\alpha_{n-1}}\end{bmatrix} = \underbrace{\begin{pmatrix}\mathbb{1}_{n-2} & & \\ & 1 & 0\\ & 1 & 1\end{pmatrix}}_{L_{n-1}}\begin{bmatrix}\mathbf{v}_{\alpha_1}\\ \vdots\\ \mathbf{v}_{\alpha_{n-1}}\\ \mathbf{v}_{\alpha_n}\end{bmatrix}. \tag{3.1.5}$$

Move II flips any two non-parallel consecutive segments. Analogously to move I, sweeping the grey triangle yields $\mathbf{v}_{\alpha_{k+1}} \mapsto \mathbf{v}_{\beta_{k+1}} = \mathbf{v}_{\alpha_{k+1}} + \mathbf{v}_{\alpha_k}$. However, this drags the second segment in a flip that pivots its target center: we expect the transformed 2-segment portion of the snake to end on a different vector within the same line, i.e. $\mathbf{v}_{\beta_{k+2}} \propto \mathbf{v}_{\alpha_{k+2}}$. Denoting by Z the proportionality constant,

$$\begin{bmatrix} \mathbf{v}_{\alpha_1} \\ \vdots \\ \mathbf{v}_{\alpha_k} \\ \mathbf{v}_{\alpha_{k+1}} \\ \mathbf{v}_{\alpha_{k+2}} \\ \vdots \\ \mathbf{v}_{\alpha_n} \end{bmatrix} \mapsto \begin{bmatrix} \mathbf{v}_{\alpha_1} \\ \vdots \\ \mathbf{v}_{\alpha_k} \\ \mathbf{v}_{\beta_{k+1}} \\ \mathbf{v}_{\beta_{k+2}} \\ \vdots \\ \mathbf{v}_{\alpha_n} \end{bmatrix} = \begin{pmatrix} \mathbb{1}_{k-1} & & & & \\ & 1 & 0 & 0 & \\ & 1 & 1 & 0 & \\ & 0 & 0 & Z & \\ & & & & Z\ \mathbb{1}_{n-k-2} \end{pmatrix} \begin{bmatrix} \mathbf{v}_{\alpha_1} \\ \vdots \\ \mathbf{v}_{\alpha_k} \\ \mathbf{v}_{\alpha_{k+1}} \\ \mathbf{v}_{\alpha_{k+2}} \\ \vdots \\ \mathbf{v}_{\alpha_n} \end{bmatrix}. \tag{3.1.6}$$

Since the elementary blocks L_i and $H_j(t)$ commute for $i \neq j$, this change-of-basis matrix can be factorized, inside $\mathsf{PGL}_n(\mathbb{R})$, as $L_k H_{k+1}(Z)$ and the move as a whole is well-defined. Finally, move III, inverting a clockwise oriented ∂-snake, is unravelled tracking segment reversals:

$$\begin{bmatrix} \mathbf{v}_{\alpha_1} \\ \mathbf{v}_{\alpha_2} \\ \vdots \\ \mathbf{v}_{\alpha_{n-1}} \\ \mathbf{v}_{\alpha_n} \end{bmatrix} \mapsto \begin{bmatrix} \mathbf{v}_{\alpha_n} \\ -\mathbf{v}_{\alpha_{n-1}} \\ \vdots \\ (-1)^{n-2}\mathbf{v}_{\alpha_2} \\ (-1)^{n-1}\mathbf{v}_{\alpha_1} \end{bmatrix} = S^{-1} \begin{bmatrix} \mathbf{v}_{\alpha_1} \\ \vdots \\ \mathbf{v}_{\alpha_{n-1}} \\ \mathbf{v}_{\alpha_n} \end{bmatrix}. \tag{3.1.7}$$

Notice that $S^{-1} = (-1)^{n-1}S = S^T$.

There are $\binom{n-1}{2}$ type II moves, one for each downward white triangle, and the corresponding proportionality constants are the so-called (positive) Fock-Goncharov variables. Topologically, notice that Fock-Goncharov variables are in bijection with inner vertices of

the tessellation of $\triangle_{123}$: there is exactly one such vertex inside any white triangle. We thus denote them Z_{ijk} by the barycentric coordinates of the unique corresponding vertex, $i, j, k \in \mathbb{Z}_{>0}$.

Taking advantage of this calculus, the general formula for the change-of-basis matrix corresponding to the ∂-snake map $\mathbf{p}_{12} \mapsto \mathbf{p}_{31}$ reads

$$\mathsf{PSL}_n(\mathbb{R}) \ni C_{12\to 31} = S\ L_{n-1} \prod_{j=1}^{n-2} \left[\prod_{i=1}^{j} \left[L_{n-i-1} H_{n-i}(Z_{n-j-i,i,j}) \right] L_{n-1} \right]. \tag{3.1.8}$$

Example 3.1.5 *For $n = 2$, there are no inner vertices and formula (3.1.8) simplifies to*

$$C_{12\to 31} = S\ L_1 = \begin{pmatrix} 0 & -1 \\ 1 & 0 \end{pmatrix} \begin{pmatrix} 1 & 0 \\ 1 & 1 \end{pmatrix}. \tag{3.1.9}$$

For $n = 3$, there is just a single Fock-Goncharov variable Z_{111}:

$$\begin{aligned} C_{12\to 31} &= S\ L_2 L_1 H_2(Z_{111}) L_2 \\ &= \begin{pmatrix} 0 & 0 & 1 \\ 0 & -1 & 0 \\ 1 & 0 & 0 \end{pmatrix} \begin{pmatrix} 1 & 0 & 0 \\ 0 & 1 & 0 \\ 0 & 1 & 1 \end{pmatrix} \begin{pmatrix} 1 & 0 & 0 \\ 1 & 1 & 0 \\ 0 & 0 & 1 \end{pmatrix} \begin{pmatrix} Z_{111}^{-1/3} & 0 & 0 \\ 0 & Z_{111}^{-1/3} & 0 \\ 0 & 0 & Z_{111}^{2/3} \end{pmatrix} \begin{pmatrix} 1 & 0 & 0 \\ 0 & 1 & 0 \\ 0 & 1 & 1 \end{pmatrix}. \end{aligned} \tag{3.1.10}$$

Transport matrices and amalgamation

In order to glue triangles together, we need to attach additional variables to the sides of $\triangle 123$. This is formally done by extending $\mathscr{X}_{\mathsf{PGL}_n(\mathbb{R})}(\triangle 123)$ to the *moduli space of pinnings* $\mathscr{P}_{\mathsf{PGL}_n(\mathbb{R})}(\triangle 123)$, in which each oriented side of the triangle comes equipped with a 1-dimensional subspace of $\mathbb{R}^n$ in generic position to the corresponding pair of flags. A *pinning*

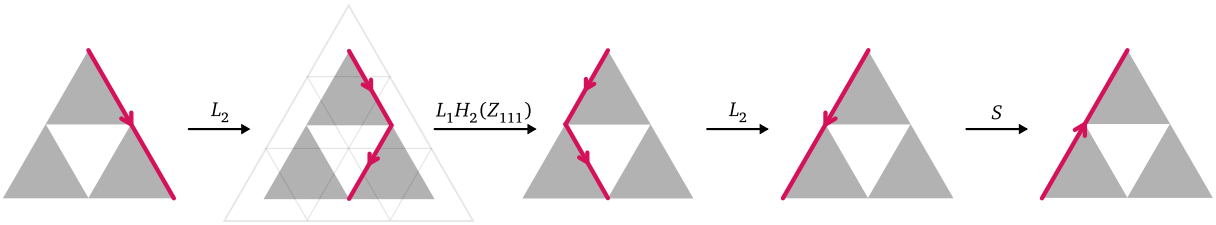

Figure 3.7: Sequence of snake moves factorizing $C_{12\to 31}$ for $n = 3$. At step 2, the tessellation's only inner vertex of barycentric coordinates $(1,1,1)$ labels the Fock-Goncharov variable Z_{111}. At step 4, the ∂-snake runs counterclockwise and an S matrix is needed.

on side IJ is given by the triple $\{F^I_\bullet, F^J_\bullet, \Lambda\}$ with $\Lambda \subset \mathbb{R}^n, \dim(\Lambda) = 1$. A choice of Λ equals a choice of projective basis $\{\mathbf{v}_{\alpha_1}, \dots \mathbf{v}_{\alpha_n}\}$ in $\mathbb{R}^n$, a vector for each vertex along IJ from the corresponding line, via the condition $\sum_{i=1}^n \mathbf{v}_{\alpha_i} \in \Lambda$. Therefore, each oriented side IJ comes with two projective bases, one from the pinning and the other from the corresponding ∂-snake $\mathbf{p}_{IJ}$, and the unimodular change-of-basis matrix between them takes the form $\prod_{i=1}^{n-1} H_i(t_i)$. These $n-1$ proportionality constants are thought of as additional Fock-Goncharov variables Z_{ijk}, labelled by the vertices on the interior of IJ. Adding these extra variables from all three sides to the ones birthed by type II moves, we get a total of $3(n-1) + \binom{n-1}{2} = \frac{(n+4)(n-1)}{2}$ Fock-Goncharov variables (Figure 3.8). As a whole, they parametrize $\mathscr{P}_{\mathsf{PGL}_n(\mathbb{R})}(\triangle 123)$ and are in bijection with the tessellation's vertices except $1, 2, 3$.

Remark 3.1.6 *We impose all Fock-Goncharov variables to be strictly positive: this restriction is known [6] to provide a parametrization of the moduli space describing its positive connected component* $\mathscr{P}^+_{\mathsf{PGL}_n(\mathbb{R})}(\Sigma)$. *In particular, this choice makes the transport matrices* (3.1.11) *genuine elements of* $\mathsf{PSL}_n(\mathbb{R}) \subseteq \mathsf{PGL}_n(\mathbb{R})$.

We finally define the transport matrices T_i in Figure 3.9. They correspond to the special change-of-basis matrices between the pinning-induced projective bases associated to the oriented sides of $\triangle 123$. For example, T_1 maps the pinning of side 12 first to the snake $\mathbf{p}_{12}$, then maps the snake $\mathbf{p}_{12}$ to the snake $\mathbf{p}_{31}$, and finally maps the snake $\mathbf{p}_{31}$ to the pinning of side 31.

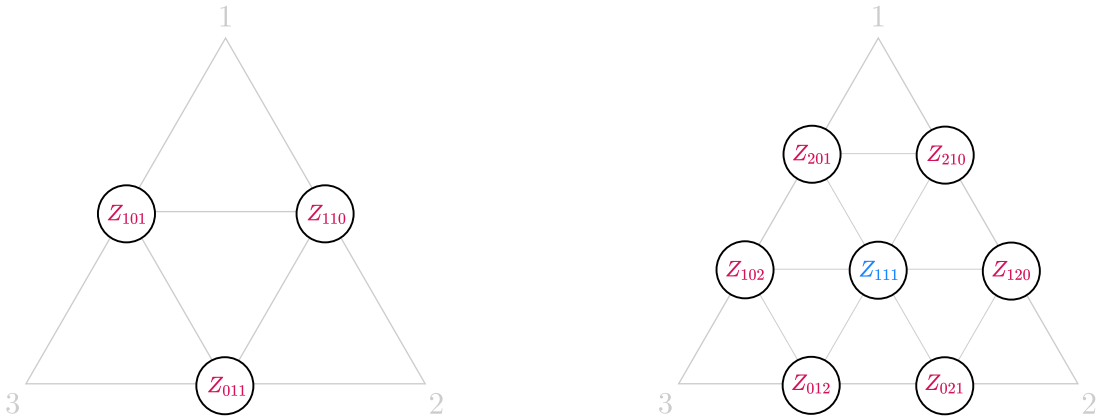

Figure 3.8: From left to right, Fock-Goncharov variables Z_α for $\mathscr{P}_{\mathsf{PGL}_2(\mathbb{R})}(\triangle 123)$ and $\mathscr{P}_{\mathsf{PGL}_3(\mathbb{R})}(\triangle 123)$. Blue variables are associated with moves II and red ones with side pinnings.

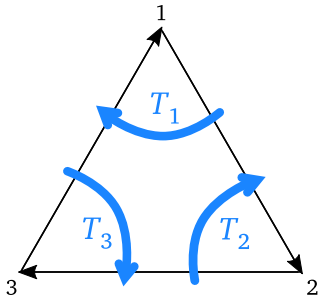

Figure 3.9: The triple of transport matrices on the oriented triangle $\triangle 123$. T_1 corresponds to the map of oriented sides $12 \mapsto 31$, T_2 to $23 \mapsto 12$ and T_3 to $31 \mapsto 23$.

Definition 3.1.7 *The* transport matrices T_1, T_2, T_3 *are the following* $n \times n$ *matrices*

$$
\begin{aligned}
T_1 &= S \prod_{k=1}^{n-1} \Big[H_{n-k}(Z_{k,0,n-k}) \Big] \; L_{n-1} \prod_{j=1}^{n-2} \Bigg[\prod_{i=1}^{j} \Big[L_{n-i-1} H_{n-i}(Z_{n-j-i,i,j}) \Big] L_{n-1} \Bigg] \; \prod_{k=1}^{n-1} H_k(Z_{n-k,k,0}), \\
T_2 &= S \prod_{k=1}^{n-1} \Big[H_{n-k}(Z_{n-k,k,0}) \Big] \; L_{n-1} \prod_{j=1}^{n-2} \Bigg[\prod_{i=1}^{j} \Big[L_{n-i-1} H_{n-i}(Z_{j,n-j-i,i}) \Big] L_{n-1} \Bigg] \; \prod_{k=1}^{n-1} H_k(Z_{0,n-k,k}), \\
T_3 &= S \prod_{k=1}^{n-1} \Big[H_{n-k}(Z_{0,n-k,k}) \Big] \; L_{n-1} \prod_{j=1}^{n-2} \Bigg[\prod_{i=1}^{j} \Big[L_{n-i-1} H_{n-i}(Z_{i,j,n-j-i}) \Big] L_{n-1} \Bigg] \; \prod_{k=1}^{n-1} H_k(Z_{k,0,n-k}).
\end{aligned}
\tag{3.1.11}
$$

Together with their inverses, T_1, T_2, T_3 suffice to map between any two sides. Notice that the permutation map σ acts on matrices $T(Z_{ijk})$ depending on Fock-Goncharov variables Z_{ijk} as $\sigma T(Z_{ijk}) := T(Z_{jki})$, so that we have $T_2 = \sigma T_1$ and $T_3 = \sigma^2 T_1$.

We introduce the following shorthand notation:

$$T_1 = H^{31}_{out}\ C_{12\to 31}\ H^{12}_{in}$$

where

$$H^{12}_{in} := \prod_{k=1}^{n-1} H_k(Z_{n-k,k,0}), \tag{3.1.12}$$

$$H^{31}_{out} := (H^{31}_{in})^{-1} = \prod_{k=1}^{n-1}\Big[H_k^{-1}(Z_{k,0,n-k})\Big] = S\prod_{k=1}^{n-1}\Big[H_{n-k}(Z_{k,0,n-k})\Big]S^{-1}. \tag{3.1.13}$$

Remark 3.1.8 *These diagonal factors modifying the change-of-basis matrix can be visualized as passing from the side's pinning to the inner ∂-snake and vice versa: H^{12}_{in} for the oriented side* 12 *the path crosses to enter the triangle (pinning-to-snake), H^{31}_{out} for the oriented side of exit (snake-to-pinning).*

Example 3.1.9 *Explicitly, for $n = 2$ and $n = 3$ we get*

$$T_1 = S\ H_1(Z_{101})L_1H_1(Z_{110}) = \begin{pmatrix} -Z_{101}^{1/2}Z_{110}^{-1/2} & -Z_{101}^{1/2}Z_{110}^{1/2} \\ Z_{101}^{-1/2}Z_{110}^{-1/2} & 0 \end{pmatrix}, \tag{3.1.14}$$

$$\begin{aligned} T_1 &= S\ H_2(Z_{102})H_1(Z_{201})L_2L_1H_2(Z_{111})L_2H_1(Z_{210})H_2(Z_{120}) \\ &= \begin{pmatrix} Z_{102}^{2/3}Z_{111}^{-1/3}Z_{120}^{1/3}Z_{201}^{1/3}Z_{210}^{-2/3} & Z_{102}^{2/3}(Z_{111}^{-1/3}+Z_{111}^{2/3})Z_{120}^{-1/3}Z_{201}^{1/3}Z_{210}^{1/3} & Z_{102}^{2/3}Z_{111}^{2/3}Z_{120}^{2/3}Z_{201}^{1/3}Z_{210}^{1/3} \\ -Z_{102}^{-1/3}Z_{111}^{-1/3}Z_{120}^{-1/3}Z_{201}^{1/3}Z_{210}^{-2/3} & -Z_{102}^{-1/3}Z_{111}^{-1/3}Z_{120}^{-1/3}Z_{201}^{1/3}Z_{210}^{1/3} & 0 \\ Z_{102}^{-1/3}Z_{111}^{-1/3}Z_{120}^{-1/3}Z_{201}^{-2/3}Z_{210}^{-2/3} & 0 & 0 \end{pmatrix}. \end{aligned} \tag{3.1.15}$$

Notice that, in both cases, no Fock-Goncharov variables from side 23 *appear, in accordance with the crossing of $\triangle$*123 *associated with T_1. Cyclically permute the indices once and twice to get*

the expressions for T_2 and T_3.

As anticipated, pinnings allow to *amalgamate* variables of two adjacent triangles, creating the set of parameters describing the moduli space $\mathscr{P}_{\mathsf{PGL}_n(\mathbb{R})}(\square)$ of the quadrangle obtained by gluing the pair along the common side. The amalgamation procedure orderly identifies the two $(n-1)$-tuples of vertices on the interior of the sides to be glued, assigning to each resulting vertex a Fock-Goncharov amalgamated variable via the product of the parent ones: if the identified vertices α_1, α_2 result in the single vertex α, $Z_\alpha := Z_{\alpha_1} Z_{\alpha_2}$ (Figure 3.10).

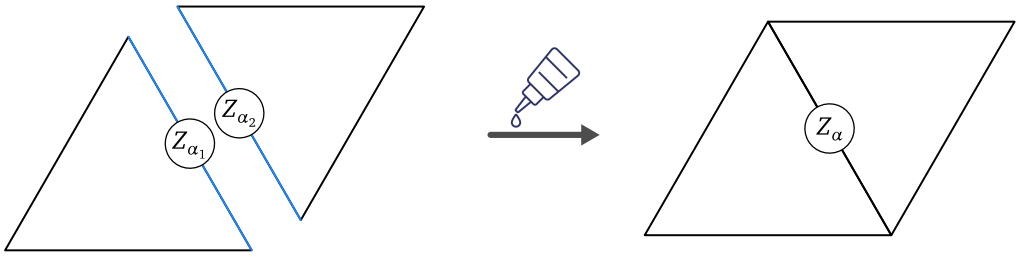

Figure 3.10: Amalgamation example $Z_\alpha = Z_{\alpha_1} Z_{\alpha_2}$, with the sides to be glued in blue.

This operation allows to parameterize $\mathscr{P}_{\mathsf{PGL}_n(\mathbb{R})}(\mathbb{S})$, for any (suitable) triangulated surface $\mathbb{S}$, by amalgamation of the moduli spaces of pinnings assigned to the individual triangles.

3.1.2 Fat graph loops via transport matrices

Using the machinery of Section 3.1.1, we here explain how to assign sequences of transport matrices to loops running over a fat graph. In order to explain this transport matrix factorization of fat graph paths, we assume a clockwise labelling of vertices from the set $\{1,2,3\}$ is chosen for each triangle coming from the dual fat graph $\Gamma^\vee_{g,s,m}$ of the surface $\Sigma_{g,s,m}$, where $\Gamma_{g,s,m}$ is constructed following the recipe in [5].

One should picture a path as transporting an oriented side along the triangulation by the action of transport matrices. In order to consistently compose two transport matrices—that we defined as maps between the *clockwise* oriented sides of a triangle—a reversal of the transported side must be performed. This is done by inserting a S block between the

matrices.

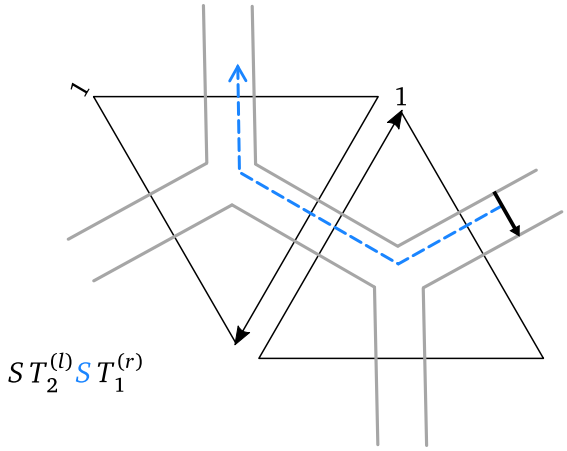

Figure 3.11: The blue path transports the oriented side indicated by the thick black arrow. When constructing its representation, the transport composition rule prescribes the insertion of the S block between the transport matrices. The orientation is explicitly indicated on those sides interacting via the composition: the 31 oriented side of the right (r) triangle is reversed by S to match the 23 one of the left (l) triangle. The leftmost S block performs a final reversal: without it, the path would flip the side it is just allowed to transport.

In terms of Fock-Goncharov variables, this transport composition rule enforces the amalgamation, performed in the language of transport matrices by letting the diagonal pinning factors multiply each other. Notice that the side reversal is exactly the operation needed to absorb the leftmost S factor of a transport matrix and let the H blocks generate the amalgamated variable.

Example 3.1.10 *For $n = 2$, the composition in Figure 3.11 is the amalgamation $Z' := Z^{(l)}_{011} Z^{(r)}_{101}$:*

$$\begin{aligned} T_2^{(l)}\ S\ T_1^{(r)} &= SH_1(Z^{(l)}_{110})L_1H_1(Z^{(l)}_{011})\ S\ SH_1(Z^{(r)}_{101})L_1H_1(Z^{(r)}_{110}) \\ &= -S\ H_1(Z^{(l)}_{110})L_1 \underbrace{H_1(Z^{(l)}_{011})H_1(Z^{(r)}_{101})}_{H_1(Z^{(l)}_{011}Z^{(r)}_{101})} L_1H_1(Z^{(r)}_{110}) \\ &= -S\ H_1(Z^{(l)}_{110})L_1H_1(Z')L_1H_1(Z^{(r)}_{110}), \end{aligned} \tag{3.1.16}$$

i.e. $H_1(Z_{\alpha_2})H_1(Z_{\alpha_1}) = H_1(Z_{\alpha_1}Z_{\alpha_2}) = H_1(Z_\alpha)$, for Z_α the amalgamated variable. For $n = 3$, the

mechanism reads

$$H_1(Z_{\beta_2})H_2(Z_{\alpha_2})H_2(Z_{\alpha_1})H_1(Z_{\beta_1}) = H_1(Z_{\beta_2}Z_{\beta_1})H_2(Z_{\alpha_2}Z_{\alpha_1})$$
$$= H_2(Z_{\alpha_2}Z_{\alpha_1})H_1(Z_{\beta_2}Z_{\beta_1}) = H_2(Z_\alpha)H_1(Z_\beta),$$

with Z_α, Z_β as the two amalgamated variables.

Remark 3.1.11 *When dealing with loops, the amalgamation at the base-point cannot be captured by the mere factorization over transport matrices: the unavoidable choice of a starting point prevents the composition between the first and last transport matrices from happening. Nevertheless, this issue is easily fixed by a* global *conjugation. E.g., the path in Figure 3.11 can be closed into a loop conjugating its factorization $ST_2^{(l)}ST_1^{(r)}$ by $C = H_1(Z_{110}^{(r)})$: denoting by $Z'' := Z_{110}^{(r)}Z_{110}^{(l)}$ the new amalgamated variable due to the closure,*

$$CST_2^{(l)}ST_1^{(r)}C^{-1} = H_1(Z_{110}^{(r)})H_1(Z_{110}^{(l)})L_1H_1(Z')L_1H_1(Z_{110}^{(r)})H_1^{-1}(Z_{110}^{(r)}) = H_1(Z'')L_1H_1(Z')L_1.$$

Notice that in this last factorization none of the variables forming Z'' remains.

Summing up, once the sequence of transport matrices associated to the directed crossings of triangles is read off, each loop's matrix is assembled by transport compositions and finalized by a global conjugation.

3.1.3 Quantization

The triangle's moduli space of pinnings $\mathscr{P}_{\mathsf{PGL}_n(\mathbb{R})}(\triangle 123)$ is quantized by promoting the Fock-Goncharov variables to generators of a quantum torus, with relations encoded by a quiver constructed from the tessellation of $\triangle 123$. Provided the removal of $1, 2, 3$, the quiver's vertices coincide with the tessellation's ones and arrows are defined by consistently extending the clockwise orientation of $\triangle 123$ to the tiles: upward ones are clockwise and downward

ones counterclockwise. Arrows from the sides of $\triangle 123$ are dashed. The resulting quiver is displayed in Figure 3.12.

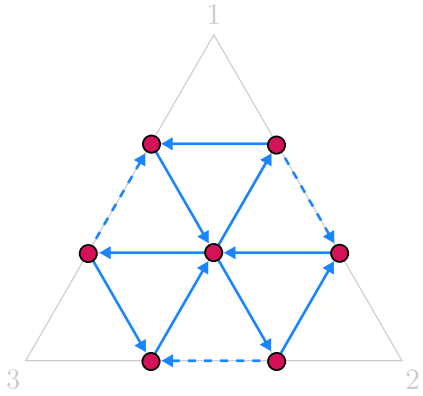

Figure 3.12: $n = 3$ quiver for $\triangle 123$.

The set of vertices of the quiver is in bijection with quantum Fock-Goncharov variables Z_α and arrows rule their commutation relations: for a central invertible variable q,

$$\begin{cases} Z_\beta Z_\alpha = q^{-2} Z_\alpha Z_\beta & \alpha \bullet \longrightarrow \bullet \beta \\ Z_\beta Z_\alpha = q^{-1} Z_\alpha Z_\beta & \alpha \bullet \dashrightarrow \bullet \beta \\ Z_\beta Z_\alpha = Z_\alpha Z_\beta & \alpha \bullet \quad \bullet \beta \end{cases} \tag{3.1.17}$$

Denoting by $\mathcal{Q}$ the ruling quiver, the resulting noncommutative algebra, known as a quantum $\mathcal{X}$-torus [15], reads

$$\mathcal{X}_\mathcal{Q} := \mathbb{C}[q^{\pm 1/2}]\big\langle \{Z_\alpha^{\pm 1}\} \big\rangle \big/ (Z_\beta Z_\alpha - q^{-2\#} Z_\alpha Z_\beta), \tag{3.1.18}$$

where $\#$ counts the number of arrows from α to β ($1/2$ for a dashed one). It naturally carries the *Weyl quantum ordering*: for any monomial $Z_{\alpha_1} \cdots Z_{\alpha_n}$, we denote it by double bullets

$$:\!Z_{\alpha_1} \cdots Z_{\alpha_n}\!: := q^W Z_{\alpha_1} \cdots Z_{\alpha_n}, \quad W := \sum_{\substack{k=2 \\ j<k}}^{n} w_{jk} \ \text{ for } \ Z_{\alpha_j} Z_{\alpha_i} = q^{2w_{ij}} Z_{\alpha_i} Z_{\alpha_j}. \tag{3.1.19}$$

A handy way to master rule (3.1.19) is to imagine the weight $w_{ij} = -w_{ji}$ measuring a flow carried by the arrows: -1 for an outgoing arrow $\alpha_i \to \alpha_j$ (outflow) and $+1$ for an incoming arrow $\alpha_i \leftarrow \alpha_j$ (inflow), with dashed arrows corresponding to half flows. Notice that *inside* the double bullets the order does not matter, e.g., $\overset{\bullet}{\bullet} Z_\alpha Z_\beta \overset{\bullet}{\bullet} = \overset{\bullet}{\bullet} Z_\beta Z_\alpha \overset{\bullet}{\bullet}$. This is the very reason this definition provides a well-defined ordering for quantum variables.

Remark 3.1.12 *A quantum $\mathcal{X}$-torus can be defined for any (weighted) quiver $\mathcal{Q}$ having no loops or 2-cycles. In particular, $\mathcal{X}_{\mathcal{Q}_1}$, $\mathcal{X}_{\mathcal{Q}_2}$ and $\mathcal{X}_{\mathcal{Q}_3}$ are the quantum tori for the three quivers in Figure 3.1*

Due to the normalized H_k block, we need an extension of $\mathcal{X}_{\mathcal{Q}}$ containing n-th roots of Fock-Goncharov variables:

$$\mathcal{X}_{\mathcal{Q}}^{1/n} := \mathbb{C}[q^{\pm\frac{1}{2n^2}}]\big\langle\{Z_\alpha^{\pm 1/n}\}\big\rangle\Big/\big(Z_\beta^{1/n} Z_\alpha^{1/n} - q^{-\frac{2\#}{n^2}} Z_\alpha^{1/n} Z_\beta^{1/n}\big).$$

The n^2 denominator is found by factorizing each Z_α as $\prod_{i=1}^{n} Z_\alpha^{1/n}$, while the quantum ordering formula remains valid.

Transport matrices are quantized following a straightforward recipe:

Definition 3.1.13 *For the diagonal matrix $(Q)_{ii} := q^{2-i-\frac{n+1}{n^2}}$, the triplet of* quantum transport matrices *is given by*

$$T_i^q = Q \overset{\bullet}{\bullet} T_i \overset{\bullet}{\bullet}, \quad i = 1, 2, 3, \tag{3.1.20}$$

where the Weyl quantum ordering acts linearly on each entry.

The matrix Q is uniquely defined by enforcing the quantum groupoid relation [6]

$$T_1^q T_2^q T_3^q = \mathbb{1}.$$

Within the framework of Section 3.1.2, this translates to the topological consistency visualized by Figure 3.13. In the classical case, $T_1 T_2 T_3 = \mathbb{1}$ follows automatically from (3.1.11).

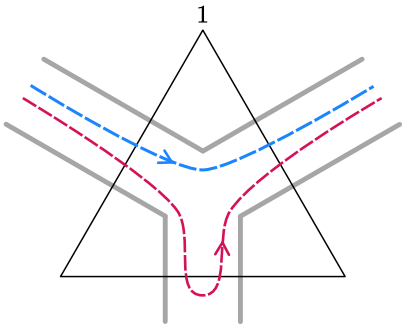

Figure 3.13: Interpretation of the quantum groupoid relation for paths: being topologically equivalent, blue and red must be assigned the same matrix, i.e. $(T_1^q)^{-1} = T_2^q T_3^q$.

Notice that the quantum correction introduced with the matrix Q causes the entries of the quantum transport matrices *not* to be Weyl-ordered monomials. Moreover, interpreting this correction as the quantization

$$S \mapsto S^q := QS,$$

we quantize the transport composition rule (Figure 3.11) by prescribing the insertion of a S^q block instead.

Finally, the quantum extension of the amalgamation procedure is straightforward: under the simplest rule prescribing commutation for quantum Fock-Goncharov variables coming from different triangles, a quantum amalgamated variable reads $Z_\alpha := {}^{\bullet}_{\bullet} Z_{\alpha_2} Z_{\alpha_1} {}^{\bullet}_{\bullet} = Z_{\alpha_2} Z_{\alpha_1} = Z_{\alpha_1} Z_{\alpha_2}$. For the special self-gluing case where two sides of the *same* triangle are identified, only the first equality holds and the amalgamated variable must be taken as the quantum ordering.

3.2 GDAHAs from higher Teichmüller theory

For a special pair of fat graphs, we prove that the matrix algebras resulting from the transport matrix factorization provide embeddings of GDAHAs. The $n = 2$ case recovers the known representation for type $\tilde{D}_4$ in the form of quantum Fuchsian monodromy data, serving as both a showcase of the machinery developed in Section 3.1.2 and an appetizer

for the more involved $n = 3$ one.

Our proofs are supported by the `NCAlgebra` extension for Mathematica [21]. This package allows to perform noncommutative multiplications and simplify symbolic expressions by repeated substitution of a prescribed set of relations. All Mathematica-aided computations can be found in [8].

In the following two sections, the notation drops the q superscript for better readability, namely T_i and S stay for the respective quantum matrices.

3.2.1 The matrix algebra for H_{D_4}

For $n = 2$, the fat graph is chosen as the four-holed Riemann sphere $\Sigma_{0,4,0}$, which is exactly the domain of the Fuchsian system (I.1).

The transport matrix (3.1.14), computed in Example 3.1.9, needs to be quantized and multiplied by the quantum correction $Q = \mathrm{diag}(q^{1/4}, q^{-3/4})$:

$$T_1 = Q \begin{pmatrix} -{}^{\bullet}_{\bullet}Z^{1/2}_{101}Z^{-1/2}_{110}{}^{\bullet}_{\bullet} & -{}^{\bullet}_{\bullet}Z^{1/2}_{101}Z^{1/2}_{110}{}^{\bullet}_{\bullet} \\ {}^{\bullet}_{\bullet}Z^{-1/2}_{101}Z^{-1/2}_{110}{}^{\bullet}_{\bullet} & 0 \end{pmatrix} = \begin{pmatrix} -Z^{1/2}_{101}Z^{-1/2}_{110} & -q^{\frac{1}{2}}Z^{1/2}_{101}Z^{1/2}_{110} \\ q^{-\frac{1}{2}}Z^{-1/2}_{101}Z^{-1/2}_{110} & 0 \end{pmatrix}. \tag{3.2.1}$$

Quantum T_2 and T_3 follow the same recipe.

The transport matrix factorization can be read off from Figure 3.14: denoting by O the matrix corresponding to the ochre loop, B the matrix of the blue loop, G the one of the green loop and P that of the pink one, we have

$$\begin{aligned} O &= -q\, S\, T_3^{(r)}\, S\, T_2^{(r)}\, S, \\ B &= -q\, T_2^{(c)}\, S\, T_3^{(d)}\, S\, T_2^{(d)}\, S\, T_2^{(c)-1}, \\ G &= -q\, T_1^{(c)-1}\, S\, T_3^{(l)}\, S\, T_2^{(l)}\, S\, T_1^{(c)}, \\ P &= \sqrt{q}\, T_1^{(c)-1}\, S\, T_2^{(l)-1}\, S\, T_3^{(l)-1}\, S\, T_3^{(c)-1}\, S\, T_2^{(d)-1}\, S\, T_3^{(d)-1}\, S\, T_2^{(c)-1}\, S\, T_2^{(r)-1}\, S\, T_3^{(r)-1}\, S, \end{aligned} \tag{3.2.2}$$

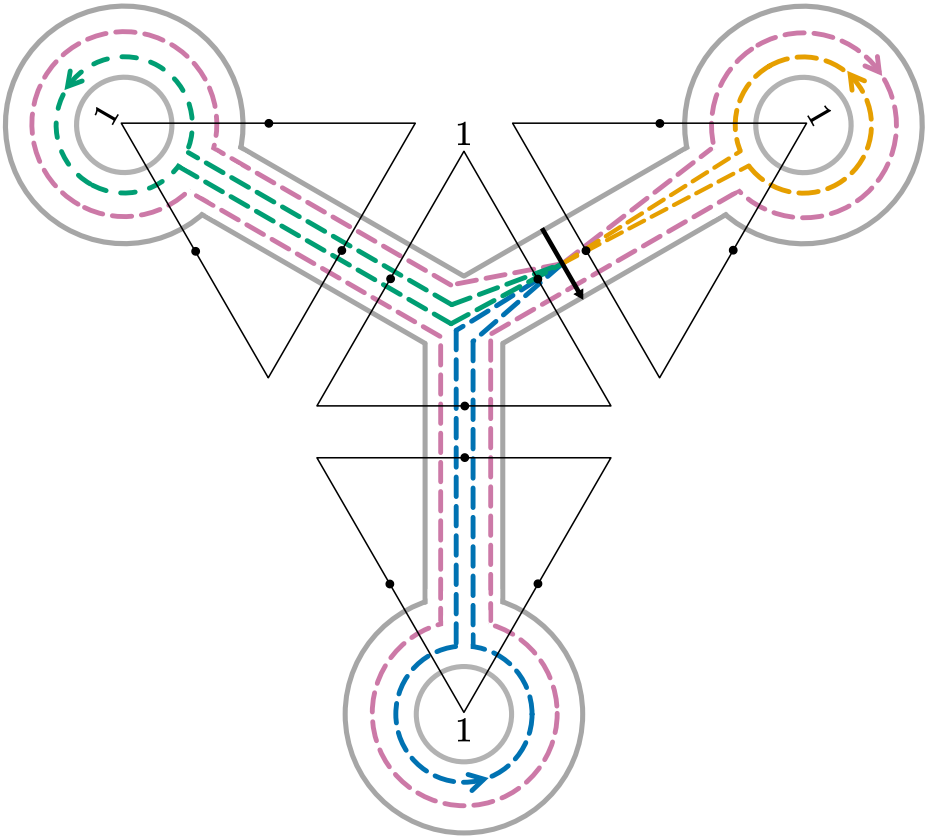

Figure 3.14: Fat graph $\Gamma_{0,4,0}$, its dual and relevant loops for $n = 2$, with the transported edge displayed by the thick black arrow. The four triangles are labelled as follows: (c) for the central one, (r) for the rightmost one, (l) for the leftmost one and (d) for the downmost one. For each triangle, the 1 indicates the choice of labelling and thus dictates its triple of transport matrices as in Figure 3.9.

where $T_i^{(a)}$ stays for the quantum transport matrix T_i in the Fock-Goncharov variables $Z_\alpha^{(a)}$ of the triangle (a). The q and $\sqrt{q}$ factors have been introduced in (3.2.2) to set the product of each pair of Hecke parameters to the unit.

The base-point amalgamation is achieved conjugating formulae (3.2.2) by the diagonal matrix

$$C = H_1(\sqrt{q}Z_{110}^{(c)}) = \begin{pmatrix} q^{-1/4}Z_{110}^{(c)-1} & 0 \\ 0 & q^{1/4}Z_{110}^{(c)} \end{pmatrix}. \tag{3.2.3}$$

For a matrix M representing a path in a fat graph, we denote by $\overline{M} := CMC^{-1}$ the one conjugated by the C in (3.2.3).

The final matrices $\overline{O}, \overline{B}, \overline{G}, \overline{P}$ depend only on the amalgamated variables

$$\begin{aligned} Z_{O1} &= qZ^{(r)}_{101}Z^{(r)}_{110}, & Z_{O2} &= Z^{(c)}_{110}Z^{(r)}_{011}, \\ Z_{B1} &= qZ^{(d)}_{101}Z^{(d)}_{110}, & Z_{B2} &= Z^{(c)}_{011}Z^{(d)}_{011}, \\ Z_{G1} &= qZ^{(l)}_{101}Z^{(l)}_{110}, & Z_{G2} &= Z^{(c)}_{101}Z^{(l)}_{011}, \end{aligned} \tag{3.2.4}$$

whose algebra relations are encoded by the triangular-shaped quiver in Figure 3.15.

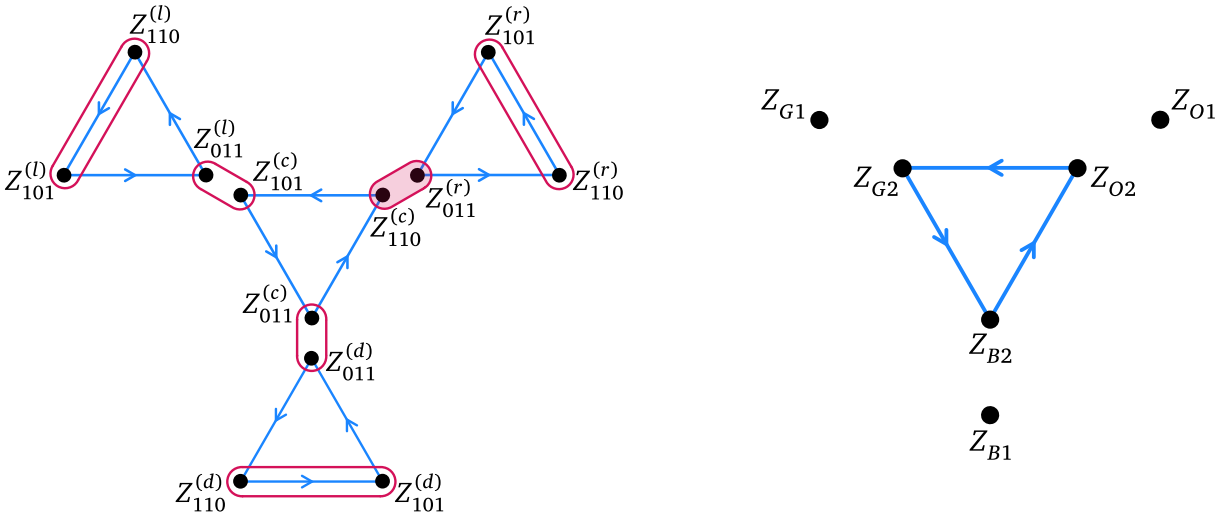

Figure 3.15: On the left, amalgamated pairs are highlighted in red, the shaded one triggered by the global conjugation. No variables from the original four triangles remain. On the right, the resulting quiver $\mathcal{Q}_2$ of amalgamated variables. The variables Z_{O1}, Z_{B1}, Z_{G1} together with $Z_{O2}Z_{B2}Z_{G2}$ generate the subalgebra of Casimir elements.

Remark 3.2.1 *On the one hand, being isolated vertices in the amalgamated quiver, the variables Z_{O1}, Z_{B1}, Z_{G1} are central elements. On the other hand, despite the transport matrices involve square roots of Fock-Goncharov variables, no fractional Z_{O2}, Z_{B2} or Z_{G2} appear in the whole quadruple $(\overline{O}, \overline{B}, \overline{G}, \overline{P})$.*

As anticipated, the next theorem recovers the $\mathsf{Mat}_2(\mathbb{T}^3_q)$-embedding of the $\tilde{D}_4$-type GDAHA found by the second author in [33]. This match is expected: the embedding was constructed using classical Teichmüller theory, which is exactly the case of $n = 2$.

Theorem 3.2.2 *Let $\mathcal{X}_{\mathcal{Q}_2}$ be the quantum $\mathcal{X}$-torus with coordinates $Z_{O1}, Z_{O2}, Z_{B1}, Z_{B2}, Z_{G1}, Z_{G2}$ and q-commutations encoded by the quiver in Figure 3.15. The $\mathsf{SL}_2(\mathcal{X}^{1/2}_{\mathcal{Q}_2})$ matrices*

$$\begin{aligned}
\overline{O} &= \begin{pmatrix} 0 & Z_{O1}^{-1/2} Z_{O2}^{-1} \\ -Z_{O1}^{1/2} Z_{O2} & Z_{O1}^{1/2} + Z_{O1}^{-1/2} \end{pmatrix}, \\
\overline{B} &= \begin{pmatrix} Z_{B1}^{1/2} + Z_{B1}^{-1/2} + Z_{B1}^{-1/2} Z_{B2}^{-1} & Z_{B1}^{1/2} + Z_{B1}^{-1/2} + Z_{B1}^{-1/2} Z_{B2}^{-1} + Z_{B1}^{1/2} Z_{B2} \\ -Z_{B1}^{-1/2} Z_{B2}^{-1} & -Z_{B1}^{-1/2} Z_{B2}^{-1} \end{pmatrix}, \\
\overline{G} &= \begin{pmatrix} Z_{G1}^{1/2} + Z_{G1}^{-1/2} + Z_{G1}^{1/2} Z_{G2} & Z_{G1}^{1/2} Z_{G2} \\ -Z_{G1}^{1/2} - Z_{G1}^{-1/2} - Z_{G1}^{-1/2} Z_{G2}^{-1} - Z_{G1}^{1/2} Z_{G2} & -Z_{G1}^{1/2} Z_{G2} \end{pmatrix}, \\
\overline{P} &= \begin{pmatrix} q Z_{O1}^{1/2} Z_{B1}^{1/2} Z_{G1}^{1/2} Z_{O2} Z_{B2} Z_{G2} & 0 \\ -qz & q Z_{O1}^{-1/2} Z_{B1}^{-1/2} Z_{G1}^{-1/2} Z_{O2}^{-1} Z_{B2}^{-1} Z_{G2}^{-1} \end{pmatrix},
\end{aligned} \tag{3.2.5}$$

with

$$\begin{aligned}
z =& (Z_{O1}^{1/2} - Z_{O1}^{-1/2}) Z_{B1}^{-1/2} Z_{G1}^{-1/2} Z_{B2}^{-1} Z_{G2}^{-1} + (Z_{B1}^{1/2} - Z_{B1}^{-1/2}) Z_{G1}^{-1/2} Z_{O1}^{-1/2} Z_{O2} Z_{G2}^{-1} \\
&+ (Z_{G1}^{1/2} - Z_{G1}^{-1/2}) Z_{O1}^{-1/2} Z_{B1}^{-1/2} Z_{O2} Z_{B2} + Z_{O1}^{1/2} Z_{B1}^{1/2} Z_{G1}^{1/2} Z_{O2} Z_{B2} Z_{G2} \\
&+ Z_{O1}^{1/2} Z_{B1}^{1/2} Z_{G1}^{-1/2} Z_{O2} Z_{B2} Z_{G2}^{-1} + Z_{O1}^{1/2} Z_{B1}^{-1/2} Z_{G1}^{-1/2} Z_{O2} Z_{B2}^{-1} Z_{G2}^{-1},
\end{aligned} \tag{3.2.6}$$

satisfy the relations

$$\begin{aligned}
\left(\overline{O} - Z_{O1}^{1/2} \mathbb{1}\right)\left(\overline{O} - Z_{O1}^{-1/2} \mathbb{1}\right) &= \mathbb{0}, \\
\left(\overline{B} - Z_{B1}^{1/2} \mathbb{1}\right)\left(\overline{B} - Z_{B1}^{-1/2} \mathbb{1}\right) &= \mathbb{0}, \\
\left(\overline{G} - Z_{G1}^{1/2} \mathbb{1}\right)\left(\overline{G} - Z_{G1}^{-1/2} \mathbb{1}\right) &= \mathbb{0}, \\
\left(\overline{P} - q Z_{O1}^{1/2} Z_{B1}^{1/2} Z_{G1}^{1/2} Z_{O2} Z_{B2} Z_{G2} \mathbb{1}\right)\left(\overline{P} - q Z_{O1}^{-1/2} Z_{B1}^{-1/2} Z_{G1}^{-1/2} Z_{O2}^{-1} Z_{B2}^{-1} Z_{G2}^{-1} \mathbb{1}\right) &= \mathbb{0}, \\
\overline{O}\,\overline{B}\,\overline{G}\,\overline{P} &= q^{-1} \mathbb{1}.
\end{aligned} \tag{3.2.7}$$

The map $K_1 \to \overline{O},\ K_2 \to \overline{B},\ K_3 \to \overline{G}, K_4 \to \overline{P}, q \to q^2$ embeds H_{D_4} into $\mathsf{Mat}_2(\mathcal{X}^{1/2}_{\mathcal{Q}_2})$.

Proof. Specializing the variables in $\mathbb{C}$, this result was proved in [33], Theorem 3. For the formulae to match, we need to replace our q by $\sqrt{q}$ and perform the following substitutions:

$$\overline{O} \mapsto M_1^{\hbar}, \quad \overline{B} \mapsto M_2^{\hbar}, \quad \overline{G} \mapsto M_3^{\hbar}, \quad \overline{P} \mapsto M_{\infty}^{\hbar}, \tag{3.2.8}$$

as

$$\begin{aligned} Z_{O1} &\mapsto e^{-p_1}, & Z_{O2} &\mapsto e^{-s_1}, \\ Z_{B1} &\mapsto e^{-p_2}, & Z_{B2} &\mapsto e^{-s_2}, \\ Z_{G1} &\mapsto e^{-p_3}, & Z_{G2} &\mapsto e^{-s_3}. \end{aligned} \tag{3.2.9}$$

A direct computation in $\mathcal{X}_{\mathcal{Q}_2}^{1/2}$ of all four relations (3.2.7) can be found in the Mathematica companion [8].

The parameters in the Hecke relations are manifestly central: as previously noticed, the variables Z_{O1}, Z_{B1}, Z_{G1} are isolated vertices while $Z_{O2}Z_{B2}Z_{G2}$ forms an isolated quiver cycle—as it involves just one-in one-out vertices. Moreover, one easily checks that in $\mathcal{X}_{\mathcal{Q}_2}^{1/2}$ the Hecke parameters of $\overline{P}$ multiply to the unit:

$$\left(qZ_{O1}^{1/2}Z_{B1}^{1/2}Z_{G1}^{1/2}Z_{O2}Z_{B2}Z_{G2}\right)\left(qZ_{O1}^{-1/2}Z_{B1}^{-1/2}Z_{G1}^{-1/2}Z_{O2}^{-1}Z_{B2}^{-1}Z_{G2}^{-1}\right) = 1.$$

Finally, notice that (3.2.9) evaluates the central variables Z_{O1}, Z_{B1}, Z_{G1} to the respective parameter e^{p_i}, setting all four matrices free from fractional coordinates (see Remark 3.2.1). This evaluation indeed reduces to the quantum 3-torus $\mathbb{T}_q^3$. □

3.2.2 The matrix algebra for H_{E_6}

For $n = 3$, we take the fat graph shown in Figure 3.16; insights on this choice can be found in Remark 3.3.4. The matrix algebra resulting from the transport matrix factorization indeed delivers a representation of the universal $\tilde{E}_6$-type GDAHA.

The transport matrix (3.1.15), computed in Example 3.1.9, needs to be quantized and

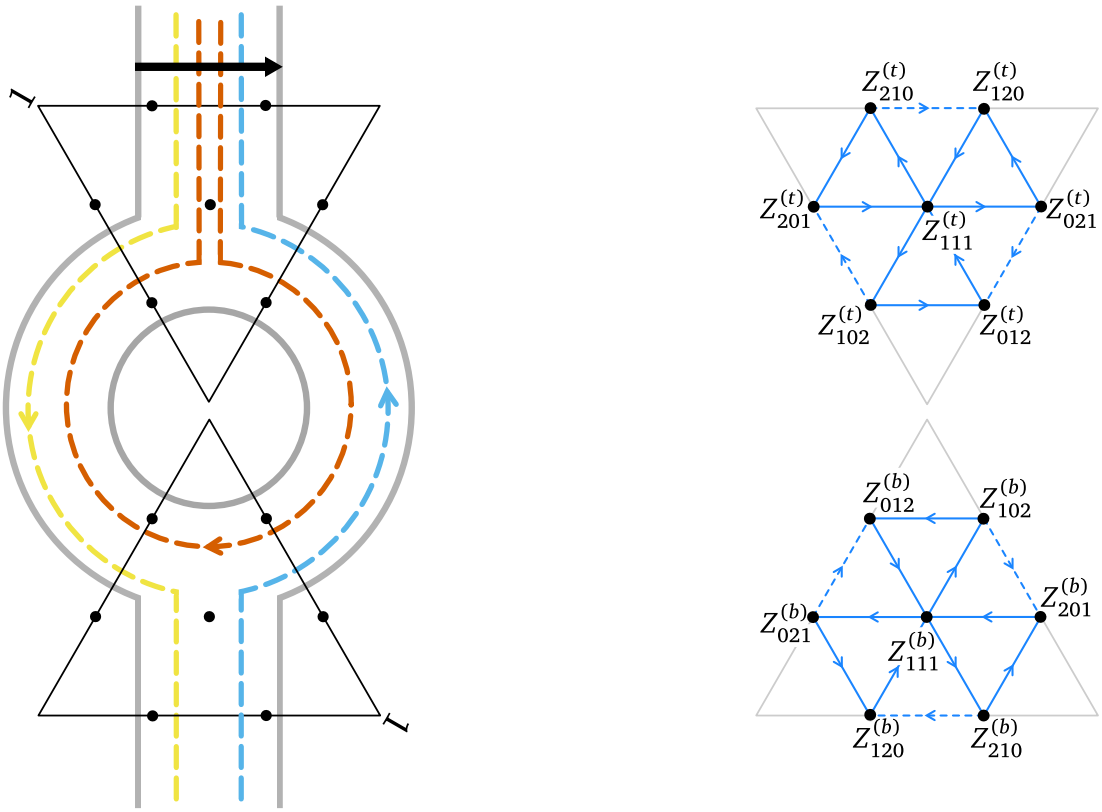

Figure 3.16: On the left: fat graph, triangles and relevant paths for $n = 3$, with the transported edge displayed by the thick black arrow. The triangles are labelled as follows: (t) for the top one and (b) for the bottom one. 1's indicate the choice of labelling on the triangles. On the right: variables and corresponding quivers for each triangle *before* any amalgamation is performed.

multiplied by the quantum correction $Q = \mathrm{diag}(q^{5/9}, q^{-4/9}, q^{-13/9})$. We get the following formula:

$$T_1 = \begin{pmatrix} q^{\frac{5}{9}} Z_{111}^{-1/3} Z_{102}^{2/3} Z_{210}^{-2/3} Z_{201}^{1/3} Z_{120}^{-1/3} & q^{\frac{13}{18}} \left(Z_{111}^{-1/3} + q^{-1} Z_{111}^{2/3}\right) Z_{102}^{2/3} Z_{210}^{2/3} Z_{120}^{-1/3} & q^{\frac{2}{9}} Z_{111}^{2/3} Z_{102}^{2/3} Z_{210}^{1/3} Z_{201}^{1/3} Z_{120}^{2/3} \\ -q^{-\frac{11}{18}} Z_{111}^{-1/3} Z_{102}^{-1/3} Z_{210}^{-2/3} Z_{201}^{2/3} & -q^{-\frac{4}{9}} Z_{111}^{-1/3} Z_{102}^{-1/3} Z_{210}^{1/3} Z_{201}^{1/3} Z_{120}^{-1/3} & 0 \\ q^{-\frac{19}{9}} Z_{111}^{-1/3} Z_{102}^{-1/3} Z_{210}^{-2/3} Z_{201}^{-2/3} Z_{120}^{-1/3} & 0 & 0 \end{pmatrix}.$$

Quantum T_2 and T_3 follow the same recipe.

The matrices corresponding to the paths can be read off from Figure 3.16. Denoting by Y the matrix corresponding to the yellow path, C the one of the cyan path and R that of the

red one, we have

$$\begin{aligned} Y &= q^{\frac{10}{9}}\ S\ T_2^{(b)}\ S\ T_1^{(t)}, \\ C &= q^{\frac{10}{9}}\ T_2^{(t)}\ S\ T_1^{(b)}\ S, \\ R &= q^{\frac{10}{9}}\ T_1^{(t)-1}\ S\ T_3^{(b)}\ S\ T_2^{(t)-1}, \end{aligned} \tag{3.2.10}$$

with $q^{10/9}$ factors introduced to set the product of each triple of Hecke parameters to the unit.

We then glue together the two open edges in Figure 3.16, closing all paths into loops. Notice that the fat graph now corresponds to $\Sigma_{0,3,0}$, the three punctured Riemann sphere. In order to amalgamate glued triangle sides properly, we perform a global conjugation by the following element in the Cartan subgroup (the so-called *outer monodromy* in [19]):

$$\mathrm{diag}(1, q^{5/6}, q^{1/3}) H_1(Z_{210}^{(t)}) H_2(Z_{120}^{(t)}) = \begin{pmatrix} Z_{210}^{(t)-2/3} Z_{120}^{(t)-1/3} & 0 & 0 \\ 0 & q^{5/6} Z_{210}^{(t)1/3} Z_{120}^{(t)-1/3} & 0 \\ 0 & 0 & q^{1/3} Z_{210}^{(t)1/3} Z_{120}^{(t)2/3} \end{pmatrix}, \tag{3.2.11}$$

the diagonal of q-factors chosen to simplify the resulting expressions.

The conjugated matrices, denoted with the overline notation, depend only on $Z_{111}^{(t)}$, $Z_{111}^{(b)}$ and the following amalgamated variables

$$\begin{aligned} Z_{Y1} &= Z_{201}^{(t)} Z_{021}^{(b)}, \quad Z_{Y2} = Z_{102}^{(t)} Z_{012}^{(b)}, \quad Z_{Y3} = Z_{210}^{(t)} Z_{120}^{(b)}, \\ Z_{C1} &= Z_{201}^{(b)} Z_{021}^{(t)}, \quad Z_{C2} = Z_{102}^{(b)} Z_{012}^{(t)}, \quad Z_{C3} = Z_{210}^{(b)} Z_{120}^{(t)}. \end{aligned}$$

The algebra relations are encoded by the diamond-shaped quiver in Figure 3.17.

Before we finally state the main theorem of this Chapter by giving the explicit representation of the universal $\tilde{E}_6$-type GDAHA, let us anticipate that, unlike for $n = 2$, the matrix entries involve fractional powers of *all* variables.

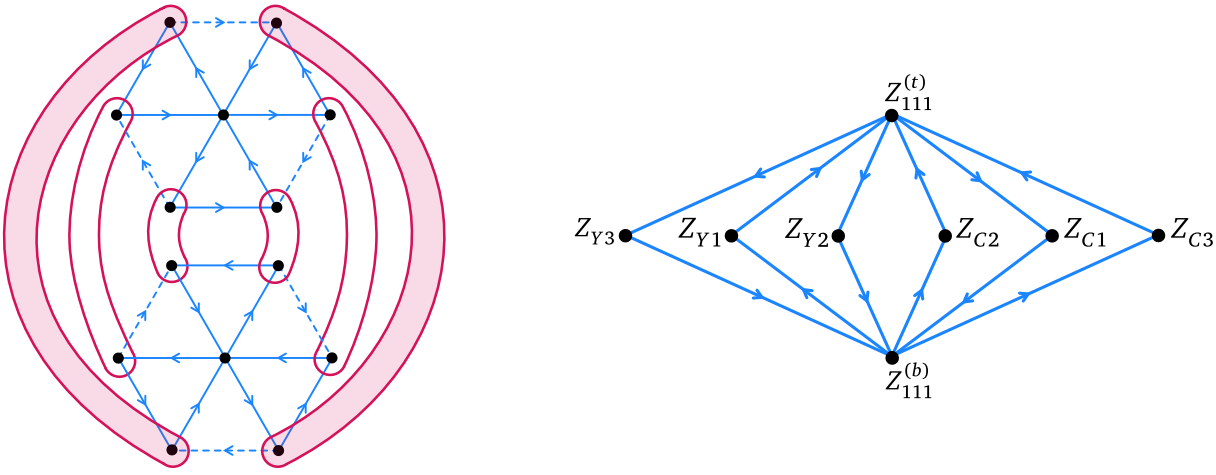

Figure 3.17: On the left, amalgamated pairs are highlighted in red, the shaded ones triggered by the global conjugation. Only the inner variables survive the amalgamations, one from each triangle. On the right, the resulting quiver $\mathcal{Q}_3$ of amalgamated variables: generators for the subalgebra of Casimir elements are given by $Z^{(t)}_{111}Z^{(b)}_{111}$ and all quiver cycles.

Theorem 3.2.3 *Let $\mathcal{X}_{\mathcal{Q}_3}$ be the quantum $\mathcal{X}$-torus with coordinates*

$$Z_{Y1},\, Z_{Y2},\, Z_{Y3},\, Z_{C1},\, Z_{C2},\, Z_{C3},\, Z^{(t)}_{111},\, Z^{(b)}_{111}$$

and q-commutations encoded by the quiver in Figure 3.17. The $\mathsf{SL}_3(\mathcal{X}^{1/3}_{\mathcal{Q}_3})$ matrices

$$\overline{C} = \begin{pmatrix} Z_{C1}^{1/3}Z_{C2}^{2/3}Z_{Y3}^{2/3}Z_{C3}^{1/3}Z_{111}^{(t)2/3}Z_{111}^{(b)2/3} & \overline{C}_{12} & \overline{C}_{13} \\ 0 & Z_{C1}^{1/3}Z_{C2}^{-1/3}Z_{Y3}^{-1/3}Z_{C3}^{1/3}Z_{111}^{(t)-1/3}Z_{111}^{(b)-1/3} & \overline{C}_{23} \\ 0 & 0 & Z_{C1}^{-2/3}Z_{C2}^{-1/3}Z_{Y3}^{-1/3}Z_{C3}^{-2/3}Z_{111}^{(t)-1/3}Z_{111}^{(b)-1/3} \end{pmatrix},$$

$$\overline{Y} = \begin{pmatrix} Z_{Y1}^{-2/3}Z_{Y2}^{-1/3}Z_{Y3}^{-2/3}Z_{C3}^{-1/3}Z_{111}^{(t)-1/3}Z_{111}^{(b)-1/3} & 0 & 0 \\ \overline{Y}_{21} & Z_{Y1}^{1/3}Z_{Y2}^{-1/3}Z_{Y3}^{1/3}Z_{C3}^{-1/3}Z_{111}^{(t)-1/3}Z_{111}^{(b)-1/3} & 0 \\ \overline{Y}_{31} & \overline{Y}_{32} & Z_{Y1}^{1/3}Z_{Y2}^{2/3}Z_{Y3}^{1/3}Z_{C3}^{2/3}Z_{111}^{(t)2/3}Z_{111}^{(b)2/3} \end{pmatrix},$$

$$\overline{R} = q^{2/3}(\overline{C}\,\overline{Y})^{-1}, \tag{3.2.12}$$

whose entries are given by Appendix C and

$$\overline{C}_{12} = -q^{\frac{1}{3}} Z_{C1}^{1/3} Z_{C2}^{-1/3} Z_{Y3}^{-1/3} Z_{C3}^{1/3} Z_{111}^{(t)-1/3} Z_{111}^{(b)-1/3} - Z_{C1}^{1/3}\big(Z_{C2}^{-1/3} + q^{-1} Z_{C2}^{2/3}\big) Z_{Y3}^{-1/3} Z_{C3}^{1/3} Z_{111}^{(t)2/3} Z_{111}^{(b)-1/3}$$
$$- Z_{C1}^{1/3} Z_{C2}^{2/3} Z_{Y3}^{-1/3} Z_{C3}^{1/3} Z_{111}^{(t)2/3} Z_{111}^{(b)2/3},$$

$$\overline{C}_{13} = \big(Z_{C1}^{1/3} + q^{\frac{1}{3}} Z_{C1}^{-2/3}\big) Z_{C2}^{-1/3} Z_{Y3}^{-1/3} Z_{C3}^{-2/3} Z_{111}^{(t)-1/3} Z_{111}^{(b)-1/3} + Z_{C1}^{1/3}\big(q^{\frac{5}{3}} Z_{C2}^{-1/3} + q^{\frac{2}{3}} Z_{C2}^{2/3}\big) Z_{Y3}^{-1/3} Z_{C3}^{-2/3} Z_{111}^{(t)2/3} Z_{111}^{(b)-1/3},$$

$$\overline{C}_{23} = -\big(q^{-\frac{1}{3}} Z_{C1}^{1/3} + Z_{C1}^{-2/3}\big) Z_{C2}^{-1/3} Z_{Y3}^{-1/3} Z_{C3}^{-2/3} Z_{111}^{(t)-1/3} Z_{111}^{(b)-1/3};$$

$$\overline{Y}_{21} = \big(q^{\frac{1}{3}} Z_{Y1}^{1/3} + Z_{Y1}^{-2/3}\big) Z_{Y2}^{-1/3} Z_{Y3}^{1/3} Z_{C3}^{-1/3} Z_{111}^{(t)-1/3} Z_{111}^{(b)-1/3},$$

$$\overline{Y}_{31} = \big(Z_{Y1}^{1/3} + q^{\frac{1}{3}} Z_{Y1}^{-2/3}\big) Z_{Y2}^{-1/3} Z_{Y3}^{1/3} Z_{C3}^{2/3} Z_{111}^{(t)-1/3} Z_{111}^{(b)-1/3} + Z_{Y1}^{1/3}\big(q Z_{Y2}^{-1/3} + Z_{Y2}^{2/3}\big) Z_{Y3}^{1/3} Z_{C3}^{2/3} Z_{111}^{(t)-1/3} Z_{111}^{(b)2/3},$$

$$\overline{Y}_{32} = q^{\frac{1}{3}} Z_{Y1}^{1/3} Z_{Y2}^{-1/3} Z_{Y3}^{1/3} Z_{C3}^{2/3} Z_{111}^{(t)-1/3} Z_{111}^{(b)-1/3} + Z_{Y1}^{1/3}\big(q^{\frac{4}{3}} Z_{Y2}^{-1/3} + q^{\frac{1}{3}} Z_{Y2}^{2/3}\big) Z_{Y3}^{1/3} Z_{C3}^{2/3} Z_{111}^{(t)-1/3} Z_{111}^{(b)2/3}$$
$$+ Z_{Y1}^{1/3} Z_{Y2}^{2/3} Z_{Y3}^{1/3} Z_{C3}^{2/3} Z_{111}^{(t)2/3} Z_{111}^{(b)2/3};$$

satisfy the relations

$$\big(\overline{C} - Z_{C1}^{-2/3} Z_{C2}^{-1/3} Z_{Y3}^{-1/3} Z_{C3}^{-2/3} Z_{111}^{(t)-1/3} Z_{111}^{(b)-1/3} \mathbb{1}\big)\big(\overline{C} - Z_{C1}^{1/3} Z_{C2}^{-1/3} Z_{Y3}^{-1/3} Z_{C3}^{1/3} Z_{111}^{(t)-1/3} Z_{111}^{(b)-1/3} \mathbb{1}\big)$$
$$\big(\overline{C} - Z_{C1}^{1/3} Z_{C2}^{2/3} Z_{Y3}^{2/3} Z_{C3}^{1/3} Z_{111}^{(t)2/3} Z_{111}^{(b)2/3} \mathbb{1}\big) = \mathbb{0},$$
$$\big(\overline{Y} - Z_{Y1}^{-2/3} Z_{Y2}^{-1/3} Z_{Y3}^{-2/3} Z_{C3}^{-1/3} Z_{111}^{(t)-1/3} Z_{111}^{(b)-1/3} \mathbb{1}\big)\big(\overline{Y} - Z_{Y1}^{1/3} Z_{Y2}^{-1/3} Z_{Y3}^{1/3} Z_{C3}^{-1/3} Z_{111}^{(t)-1/3} Z_{111}^{(b)-1/3} \mathbb{1}\big)$$
$$\big(\overline{Y} - Z_{Y1}^{1/3} Z_{Y2}^{2/3} Z_{Y3}^{1/3} Z_{C3}^{2/3} Z_{111}^{(t)2/3} Z_{111}^{(b)2/3} \mathbb{1}\big) = \mathbb{0},$$
$$\big(\overline{R} - Z_{Y1}^{-1/3} Z_{Y2}^{-2/3} Z_{C1}^{-1/3} Z_{C2}^{-2/3} Z_{111}^{(t)-1/3} Z_{111}^{(b)-1/3} \mathbb{1}\big)\big(\overline{R} - Z_{Y1}^{-1/3} Z_{Y2}^{1/3} Z_{C1}^{-1/3} Z_{C2}^{1/3} Z_{111}^{(t)-1/3} Z_{111}^{(b)-1/3} \mathbb{1}\big)$$
$$\big(\overline{R} - Z_{Y1}^{2/3} Z_{Y2}^{1/3} Z_{C1}^{2/3} Z_{C2}^{1/3} Z_{111}^{(t)2/3} Z_{111}^{(b)2/3} \mathbb{1}\big) = \mathbb{0},$$
$$\overline{C}\,\overline{Y}\,\overline{R} = q^{2/3}\mathbb{1}. \tag{3.2.13}$$

The map $J_1 \to \overline{C}$, $J_2 \to \overline{Y}$, $J_3 \to \overline{R}$, $q \to q^{-2}$ *embeds* H_{E_6} *into* $\mathsf{Mat}_3(\mathcal{X}_{Q_3}^{1/3})$.

Proof. Proving that $\overline{Y}$, $\overline{C}$ and $\overline{R}$ satisfy relations (3.2.13) is a direct computation, which can be reproduced in the Mathematica companion [8]. The Hecke parameters are central being

products of pairs of variables having arrows with opposite directions. As an example, take

$$\begin{aligned}\overline{C}_{11} = Z_{C1}^{1/3}Z_{C2}^{2/3}Z_{Y3}^{2/3}Z_{C3}^{1/3}Z_{111}^{(t)2/3}Z_{111}^{(b)2/3} &= (Z_{C2}^{2/3}Z_{Y3}^{2/3})(Z_{C1}^{1/3}Z_{C3}^{1/3})(Z_{111}^{(t)2/3}Z_{111}^{(b)2/3}) \\ &= (Z_{C2}Z_{Y3})^{2/3}(Z_{C1}Z_{C3})^{1/3}(Z_{111}^{(t)}Z_{111}^{(b)})^{2/3}.\end{aligned}$$

For each bracketed pair, arrows cancel out: e.g., the q-factors due to arrows $Z_{C2} \to Z_{111}^{(b)}$ and $Z_{C2} \leftarrow Z_{111}^{(t)}$ are respectively absorbed by the ones due to $Z_{Y3} \leftarrow Z_{111}^{(b)}$ and $Z_{Y3} \to Z_{111}^{(t)}$.

The following inversion formulae, expressing central elements of $\mathcal{X}_{\mathcal{Q}_3}$ in terms of the tuple t, prove that this representation fully recovers the universal H_{E_6}:

$$\begin{aligned}&Z_{C1}Z_{Y3}^{-1} = \frac{t_1^{(2)}}{t_2^{(1)}t_2^{(2)}t_3^{(1)}t_3^{(2)}}, \qquad Z_{C2}Z_{Y3} = t_1^{(1)}t_2^{(2)}t_3^{(2)}, \qquad Z_{Y1}Z_{Y3} = t_2^{(1)}t_2^{(2)}, \\ &Z_{Y2}Z_{Y3}^{-1} = \frac{1}{t_1^{(1)}t_2^{(2)}t_3^{(1)}}, \quad Z_{C3}Z_{Y3} = t_1^{(1)}t_1^{(2)}t_2^{(1)}t_2^{(2)}t_3^{(1)}t_3^{(2)}, \quad Z_{111}^{(t)}Z_{111}^{(b)} = \frac{1}{t_1^{(2)}t_2^{(2)}t_3^{(2)}}.\end{aligned} \tag{3.2.14}$$

The fact that the map is an embedding can be proved by choosing a faithful representation of $\mathcal{X}_{\mathcal{Q}_3}^{1/3}$, namely a vector space V and an algebra homomorphism $\rho : \mathcal{X}_{\mathcal{Q}_3}^{1/3} \to \mathrm{End}(V)$. The resulting map $\tilde{\rho} : \mathsf{H}_{E_6} \to \mathsf{Mat}_3(\mathrm{End}(V))$ gives a representation of H_{E_6} on $\bigoplus_3 V$. Now, the rank 1 GDAHA of type $\tilde{E}_6$ is prime. Indeed, for generic values of parameters, it is Morita equivalent to its spherical subalgebra, whose associated graded algebra is a twisted homogeneous coordinate ring of an irreducible curve, and therefore is a domain (Theorems 6.5, 6.10 in [12]). Furthermore, for $q \neq 1$ it has no finite dimensional representations and is in fact simple[1]. This proves that $\tilde{\rho}$ is injective, thus so is our map. □

3.3 Quiver seizure

We start the section introducing a new concept. It involves the choice of specific central elements c_i in $\mathcal{X}_{\mathcal{Q}}$ such that the quotient $\mathcal{X}_{\mathcal{Q}}/(c_1 - c_1^{(0)}, \dots, c_l - c_l^{(0)})$ is given by $\mathcal{X}_{\tilde{\mathcal{Q}}}$, where the subquiver $\tilde{\mathcal{Q}}$ is obtained from $\mathcal{Q}$ by a new operation we name *quiver seizure*.

[1] Thanks to P. Etingof for clarifying this argument.

Let us explain this operation. We call rhombus in $\mathcal{Q}$ a 4-cycle with vertices labelled cyclicly by variables $Z_1, Z_2, Z_3, Z_4 \in \mathcal{X}_\mathcal{Q}$ such that the indegree and outdegree of both Z_2 and Z_4 equal one, namely $\deg^+(Z_i) = \deg^-(Z_i) = 1$ for $i = 2, 4$.

Definition 3.3.1 *The* quiver seizure *at vertex Z_i is the map*

$$\mathcal{Q} \mapsto \mathcal{Q} \backslash Z_i,$$

where $\mathcal{Q}\backslash Z_i \subset \mathcal{Q}$ is the full subquiver obtained by removing Z_i together with its two arrows.

This operation is illustrated in Figure 3.18.

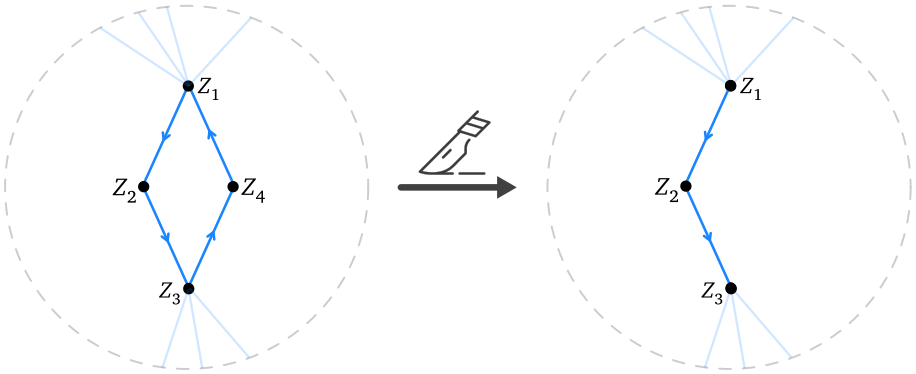

Figure 3.18: A quiver seizure removing Z_4.

Given a rhombus in $\mathcal{Q}$, the monomial Z_2Z_4 is automatically central in $\mathcal{X}_\mathcal{Q}$. Then, for any $c^{(0)} \in \mathbb{C}^*$, the assignment

$$\begin{cases} Z_4^{-1} \longmapsto \frac{1}{c^{(0)}} Z_2, \\ Z_j \longmapsto Z_j, \quad j \neq 2, \end{cases} \tag{3.3.1}$$

extends to a quantum torus isomorphism $\mathcal{X}_\mathcal{Q} \big/ \left(Z_2Z_4 - c^{(0)}\right) \xrightarrow{\sim} \mathcal{X}_{\mathcal{Q}\backslash Z_4}$, where $\mathcal{Q} \setminus Z_4$ is the full subquiver of $\mathcal{Q}$ obtained by erasing Z_4 and the two arrows incident with it. Analogously, we get $\mathcal{Q} \setminus Z_2$ by resolving Z_2^{-1} instead.

Remark 3.3.2 *The monomial Z_2Z_4 always allows for a seizure, but does not cover all the ways a seizure can manifest: when the rhombus attaches to the rest of $\mathcal{Q}$ so that even Z_1Z_3 is central, the whole monomial $Z_1Z_2Z_3Z_4$ can be also chosen.*

With the quiver seizure defined, we are now ready to show that the (scaled) quantum irregular data $(U, \widehat{L}, \widehat{\Pi})$, generated by the GDAHA functor, can be found within the representation $(\overline{C}, \overline{Y}, \overline{R})$ of H_{E_6} from our higher Teichmüller machinery.

Theorem 3.3.3 *Let $\mathcal{X}_{\mathcal{Q}_1} := \mathcal{X}_{\mathcal{Q}_3}\big/I$ be the quotient by the ideal*

$$I = (Z_{C1}Z_{C3} - 1,\, Z^{(t)}_{111}Z^{(b)}_{111}Z_{C2}Z_{Y3} - 1)$$

and denote by $(\overline{C}_I, \overline{Y}_I, \overline{R}_I)$ the restriction of the triple (3.2.12) to $\mathcal{X}_{\mathcal{Q}_1}$. Then, provided the dictionary (3.2.9) expressing the quantum irregular data in the Fock-Goncharov coordinates $\{Z_{O1}, Z_{O2}, Z_{B1}, Z_{B2}, Z_{G1}, Z_{G2}\}$,

$$(\overline{C}_I, \overline{Y}_I, \overline{R}_I) = \mu\iota\tau(U, \widehat{L}, \widehat{\Pi}) \tag{3.3.2}$$

via the entry-wise action of the following three maps:

- *the algebra isomorphism*

$$\tau : \mathcal{X}_{\mathcal{Q}_2} \xrightarrow{\sim} \mathcal{X}_{\mathcal{Q}_2}$$

  reversing q, i.e.,

$$\begin{gathered}\tau(Z_{O1}) = Z_{O1}, \quad \tau(Z_{B1}) = Z_{B1}, \quad \tau(Z_{G1}) = Z_{G1},\\ \tau(Z_{O2}) = Z_{O2}, \quad \tau(Z_{B2}) = Z_{B2}, \quad \tau(Z_{G2}) = Z_{G2},\\ \tau(q) = q^{-1};\end{gathered} \tag{3.3.3}$$

- *the algebra isomorphism*

$$\iota : \tau(\mathcal{X}_{\mathcal{Q}_2}) \xrightarrow{\sim} \mathcal{X}'_{\mathcal{Q}_1}$$

given by

$$\begin{aligned} Z_{O2}^{-1} &\mapsto q^{-1/3} Z'_{Y1}, & Z_{O1}^{-1} &\mapsto q^{-2/3} Z'_{C2} Z'^{-1}_{Y1}, \\ Z_{B2}^{-1} &\mapsto q^{-1/3} Z'^{(t)}_{111}, & Z_{B1}^{-1} &\mapsto q^{-2/3} Z'^{(b)}_{111} Z'^{(t)-1}_{111}, \\ Z_{G2}^{-1} &\mapsto q^{5/3} Z'_{C1}, & Z_{G1}^{-1} &\mapsto q^{-2/3} Z'_{Y2} Z'^{-1}_{C1}; \end{aligned} \tag{3.3.4}$$

- *the quantum cluster mutation*

$$\mu : \mathrm{Frac}(\mathcal{X}'_{\mathcal{Q}_1}) \xrightarrow{\sim} \mathrm{Frac}(\mathcal{X}_{\mathcal{Q}_1})$$

at vertex $Z_{111}^{(b)}$*:*

$$\begin{aligned} \mu(Z'^{(b)}_{111}) &= Z_{111}^{(b)-1}, & \mu(Z'^{(t)}_{111}) &= Z_{111}^{(t)} \\ \mu(Z'_{C1}) &= Z_{C1}\left(1 + qZ_{111}^{(b)-1}\right)^{-1}, & \mu(Z'_{Y2}) &= Z_{Y2}\left(1 + qZ_{111}^{(b)-1}\right)^{-1}, \\ \mu(Z'_{Y1}) &= Z_{Y1}\left(1 + qZ_{111}^{(b)}\right), & \mu(Z'_{C2}) &= Z_{C2}\left(1 + qZ_{111}^{(b)}\right). \end{aligned} \tag{3.3.5}$$

Proof. We start by noticing that $\mathcal{X}_{\mathcal{Q}_1}$ is obtained by a well-defined quantum quotient: both $Z_{C1}Z_{C3}$ and $Z_{111}^{(t)}Z_{111}^{(b)}Z_{C2}Z_{Y3}$ are central in $\mathcal{X}_{\mathcal{Q}_3}$.

These monomials in $\mathcal{X}_{\mathcal{Q}_3}$ can be recognized as seizures for the quiver in Figure 3.17: the former at vertex Z_{C3} for the rhombus $\{Z_{111}^{(t)}, Z_{C1}, Z_{111}^{(b)}, Z_{C3}\}$, the latter at vertex Z_{Y3} for the rhombus $\{Z_{111}^{(t)}, Z_{Y3}, Z_{111}^{(b)}, Z_{C2}\}$ (see also Remark 3.3.5). By the seizure's properties, the q-commutations for $\mathcal{X}_{\mathcal{Q}_1}$ are encoded by the reduced quiver in which we have erased the vertices Z_{Y3} and Z_{C3} together with their incident arrows. This is indeed $\mathcal{Q}_1$, labelled in two equivalent shapes in Figure 3.19.

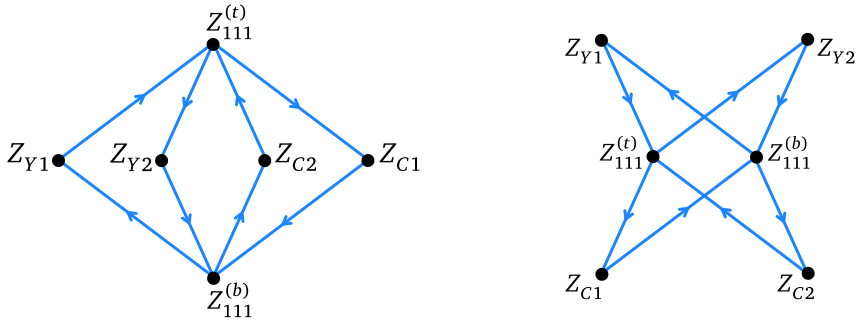

Figure 3.19: The reduced quiver in two equivalent shapes. On the left, the diamond obtained erasing the vertices Z_{Y3} and Z_{C3} directly in Figure 3.17. On the right, a rearranged star allowing for a better visualization of the mutation's action in Figure 3.20.

Therefore, the reduced triple $(\overline{C}_I, \overline{Y}_I, \overline{R}_I)$ is obtained via the identifications

$$Z_{C3}^{1/3} \mapsto Z_{C1}^{-1/3}, \quad Z_{Y3}^{1/3} \mapsto Z_{C2}^{-1/3} Z_{111}^{(b)-1/3} Z_{111}^{(t)-1/3},$$

and its entries only involve the six variables $\{Z_{Y1}^{1/3}, Z_{Y2}^{1/3}, Z_{C1}^{1/3}, Z_{C2}^{1/3}, Z_{111}^{(t)1/3}, Z_{111}^{(b)1/3}\}$ generating $\mathcal{X}_{\mathcal{Q}_1}$.

It turns out that $\overline{C}_I$ is free from fractional powers and thus a genuine element in $\mathsf{SL}_3(\mathcal{X}_{\mathcal{Q}_1})$:

$$\overline{C}_I = \begin{pmatrix} 1 & -1 - q^{-1/3} Z^{(t)}_{111} - q^{-1/3} Z_{C2} Z^{(t)}_{111} (q^{-1} + Z^{(b)}_{111}) & q + q^{1/3} Z_{C1} (q^{1/3} + q^2 Z^{(t)}_{111} + q Z_{C2} Z^{(t)}_{111}) \\ 0 & 1 & -q - q^{2/3} Z_{C1} \\ 0 & 0 & 1 \end{pmatrix}. \tag{3.3.6}$$

Notice that, by the very definition of the ideal I, all the diagonal elements are turned into unities matching the diagonal part of U.

To push the match further, we need to take advantage of the cluster structure on the $\mathcal{X}$-space [15]. Indeed, to connect the quantum (cluster) torus $\mathcal{X}_{\mathcal{Q}_1}$ to the $\mathcal{X}_{\mathcal{Q}_2}$ one of the triple $(U, \widehat{L}, \widehat{\Pi})$, we need the quantum mutation (3.3.5). In quiver terms, mutating at vertex α translates to a 3-step recipe [16]:

1. For each oriented two-arrow path $i \to \alpha \to j$, add a new arrow $i \to j$;

2. Flip all arrows incident with α;

3. Remove all pairwise disjoint 2-cycles.

Therefore, mutating at vertex $Z^{(b)}_{111}$, we turn the reduced quiver in Figure 3.19 from star-shaped to box-shaped as in Figure 3.20.

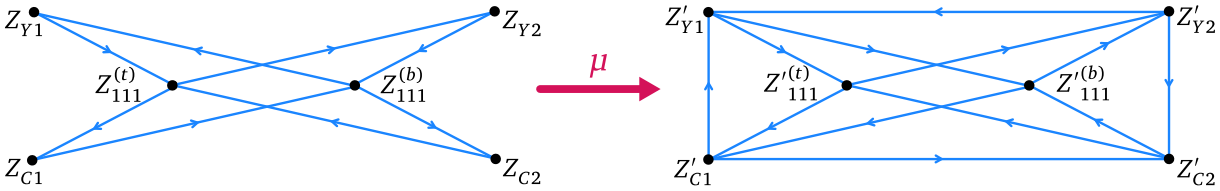

Figure 3.20: Reduced quiver, before and after quantum cluster mutation.

As expected, this mutated quiver encodes the q-commutations in $\mathcal{X}'_{\mathcal{Q}_1}$. On the corresponding quantum tori, μ acts as a quantum analogue of a pullback sending $\mathcal{X}'_{\mathcal{Q}_1}$ to $\mathcal{X}_{\mathcal{Q}_1}$.

The gain in using μ is made manifest by the algebra isomorphism (3.3.4). Indeed, ι reveals that the mutated quiver is equivalent to the triangular one in the right hand side of Figure 3.15, provided all arrows are reversed. This is visually displayed in Figure 3.21.

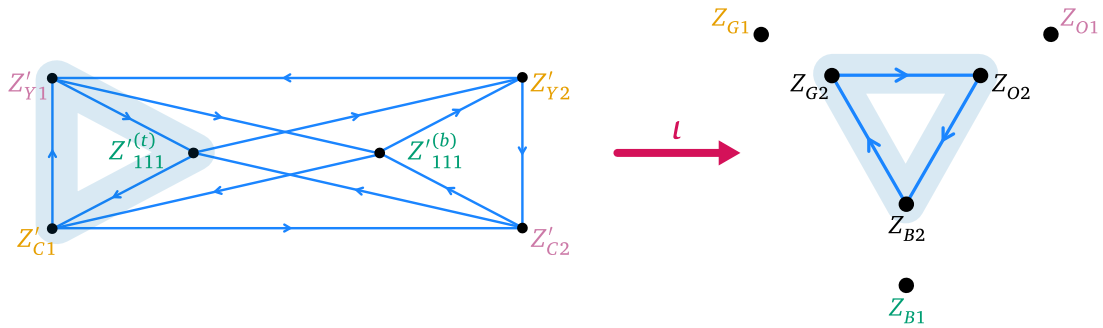

Figure 3.21: The quiver counterpart of the isomorphism ι. Highlighted are the 3-cycles identified by the map, while we color-coded each isolated vertex on the right with the corresponding pair of vertices on the left: e.g., $Z_{B1} \propto Z'^{(t)}_{111} Z'^{(b)-1}_{111}$.

The quantum $\mathcal{X}$-torus counterpart of this arrow reversal is the τ map (3.3.3).

Now that quantum algebras agree, direct computations prove that the entry-wise action of the composition $\mu\iota\tau$ on $(U, \widehat{L}, \widehat{\Pi})$ matches the reduced triple $(\overline{C}_I, \overline{Y}_I, \overline{R}_I)$.

Before we detail these computations, let us illustrate the phenomena allowing them to run successfully. On the one hand, only Z_{O1}, Z_{B1}, Z_{G1} make a fractional appearance in $(U, \widehat{L}, \widehat{\Pi})$ and their image under $\mu\iota$ does not involve the formal inverse of $1 + qZ_{111}^{(b)-1}$:

$$\mu\iota(Z_{O1}^{-1}) = q^{-2/3} Z_{C2} Z_{Y1}^{-1}, \quad \mu\iota(Z_{B1}^{-1}) = q^{-2/3} Z_{111}^{(b)} Z_{111}^{(t)-1}, \quad \mu\iota(Z_{G1}^{-1}) = q^{-2/3} Z_{Y2} Z_{C1}^{-1}. \tag{3.3.7}$$

Therefore, no fractional powers of a formal inverse appear. On the other hand, $\left(1+qZ_{111}^{(b)-1}\right)^{-1}$ does appear through $\mu\iota(Z_{G2}^{-1})$ but its algebra relations are easily figured out: indeed, for a formal power series $f(x)$,

$$Z_\beta Z_\alpha = q^w Z_\alpha Z_\beta \implies f(Z_\beta) Z_\alpha = Z_\alpha f(q^w Z_\beta). \tag{3.3.8}$$

As a result, despite resorting to the fraction field for the mutation to act, the entry-wise action of μ delivers genuine elements in $\mathsf{SL}_3(\mathcal{X}_{\mathcal{Q}_1}^{1/3})$: using (3.3.8), each formal inverse simplifies. Further theoretical evidence is given by the fact that, in the *restricted* quiver, $Z_{111}^{(b)}$ is a 4-valent node with alternating incoming and outgoing arrows: as proved in [38], mutations at these special vertices preserve the transport matrix calculus.

We conclude the proof detailing the computations behind the correspondence $U \mapsto \overline{C}_I$. Once U is given the Fock-Goncharov coordinatization via (3.2.9), it is easy to check that

$$\begin{aligned}
\mu\iota\tau U_{12} &= \mu\big(-1 - q^{-1/3} Z'^{(t)}_{111} + q^{-4/3} Z'_{C2} Z'^{(t)}_{111}\big) = -1 - q^{-1/3} Z_{111}^{(t)} + q^{-4/3} Z_{C2}(1 + qZ_{111}^{(b)}) Z_{111}^{(t)} \\
&= -1 - q^{-1/3} Z_{111}^{(t)} - q^{-1/3} Z_{C2} Z_{111}^{(t)} (q^{-1} + Z_{111}^{(b)}) \\
&= (\overline{C}_I)_{12};
\end{aligned}$$

$$
\begin{aligned}
\mu\iota\tau U_{13} &= \mu\iota\big(q + q^{-1}Z_{G2}^{-1} + q^{-1}(1 + Z_{B1}^{-1} + Z_{B1}^{-1}Z_{B2}^{-1} + Z_{O1}^{-1}Z_{B1}^{-1}Z_{O2}^{-1}Z_{B2}^{-1})Z_{B2}^{-1}Z_{G2}^{-1}\big) \\
&= \mu\big(q + q^{2/3}Z'_{C1} + q^{1/3}(1 + q^{-2/3}Z'^{(b)}_{111}Z'^{(t)-1}_{111} + q^{-1}Z'^{(b)}_{111} + q^{-2}Z'_{C2}Z'^{(b)}_{111})Z'^{(t)}_{111}Z'_{C1}\big) \\
&= \mu\big(q + (q^{2/3} + q^{1/3}Z'^{(t)}_{111} + q^{-1/3}Z'^{(b)}_{111} + q^{-2/3}Z'^{(b)}_{111}Z'^{(t)}_{111} + q^{-5/3}Z'_{C2}Z'^{(b)}_{111}Z'^{(t)}_{111})Z'_{C1}\big) \\
&= q + q^{1/3}\big(q^{1/3} + Z^{(t)}_{111} + q^{-1}Z_{C2}Z^{(t)}_{111}\big)(1 + q^{-1}Z^{(b)-1}_{111})Z_{C1}(1 + qZ^{(b)-1}_{111})^{-1} \\
&\overset{(3.3.8)}{=\!=} q + q^{1/3}\big(q^{1/3} + Z^{(t)}_{111} + q^{-1}Z_{C2}Z^{(t)}_{111}\big)Z_{C1}(1 + qZ^{(b)-1}_{111})(1 + qZ^{(b)-1}_{111})^{-1} \\
&= q + q^{1/3}Z_{C1}(q^{1/3} + q^2Z^{(t)}_{111} + qZ_{C2}Z^{(t)}_{111}) \\
&= (\overline{C}_I)_{13};
\end{aligned}
$$

$$
\begin{aligned}
\mu\iota\tau U_{23} &= \mu\iota(-q - q^{-1}Z_{G2}^{-1} - q^{-1}Z_{B1}^{-1}Z_{B2}^{-1}Z_{G2}^{-1}) = \mu(-q - q^{2/3}Z'_{C1} - q^{-1/3}Z'^{(b)}_{111}Z'_{C1}) \\
&= -q - q^{2/3}Z_{C1}\left(1 + qZ^{(b)-1}_{111}\right)^{-1} - q^{-1/3}Z^{(b)-1}_{111}Z_{C1}\left(1 + qZ^{(b)-1}_{111}\right)^{-1} \\
&= -q - q^{2/3}Z_{C1}\left(1 + qZ^{(b)-1}_{111}\right)^{-1} - q^{5/3}Z_{C1}Z^{(b)-1}_{111}\left(1 + qZ^{(b)-1}_{111}\right)^{-1} \\
&= -q - q^{2/3}Z_{C1} \\
&= (\overline{C}_I)_{23}.
\end{aligned}
$$

Analogous operations prove that $\widehat{L}$ matches $\overline{Y}_I$ and $\widehat{\Pi}$ matches $\overline{R}_I$. □

Remark 3.3.4 *The process of reducing to the quantum cluster torus $\mathcal{X}_{\mathcal{Q}_1}$ can be seen as colliding holes in the sense of [5]: we are breaking an edge in the fat graph and treating the two open edges as marked points on the boundary. The resulting fat graph corresponds to $\Sigma_{0,2,2}$ which, according to the theory developed in [4], is precisely the surface of the connection behind our irregular system* (I.3).

Remark 3.3.5 *We give further insight into the seizures making Theorem 3.3.3 happen. The one at Z_{C3} has the natural central monomial of a rhombus, given by multiplying its two vertices not incident with the rest of the quiver—whose product is always central. The other monomial has two further factors instead, corresponding to the other two vertices of its rhombus: indeed, the product $Z^{(t)}_{111}Z^{(b)}_{111}$ is central in the quantum $\mathcal{X}$-torus encoded by the quiver in Figure 3.17. The*

reason why exactly these two monomials appear must be found in the need of setting $\mathrm{diag}(\overline{C}) = (1,1,1)$ *for the match* (3.3.2) *to happen: the very way the transport matrix factorization forms this diagonal implies that the relations one must impose are those defining the ideal* I*, as one can check in* (3.2.12) *by collecting variables with the same power. Figure* 3.22 *offers a visual interpretation of this phenomenon.*

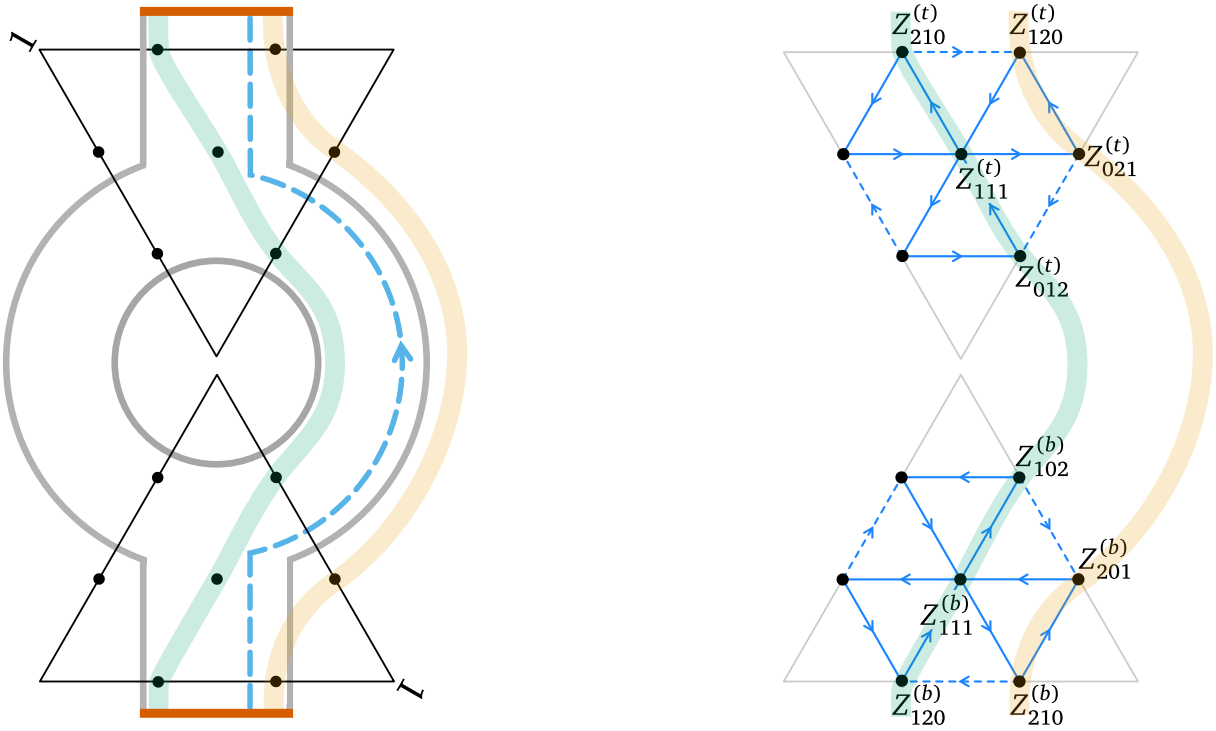

Figure 3.22: On the left, the $n = 3$ fat graph with the cyan loop represented by $\overline{C}$ (the red segments are identified). On the right, the only Fock-Goncharov variables involved by this loop. The transparent closed ribbons highlight the way the central monomials of the two seizures in Theorem 3.3.3 are formed as cycles, with the amalgamations bridging the gaps between the quivers of the two triangles. E.g., the monomial $Z_{C1}Z_{C3} = (Z^{(t)}_{021}Z^{(b)}_{201})(Z^{(b)}_{210}Z^{(t)}_{120})$ corresponds to the outer ribbon while the inner one, passing via the centers of the triangles, triggers the appearance of both $Z^{(t)}_{111}$ and $Z^{(b)}_{111}$ in the monomial $Z^{(t)}_{111}Z^{(b)}_{111}Z_{C2}Z_{Y3}$.

Appendix A

The differential facet

This appendix complements the monodromic investigation of the thesis by detailing the many differential aspects it entails. We only deal with the classical setting, as the quantum one is mostly open (see Figure I.2 and related discussion).

We start by detailing the connection between the Painlevé theory and our pair of systems. Using the middle convolution counterpart for systems, we then give an explicit computation of the correspondence between Fuchsian and irregular systems given by Theorem I.1.

A.1 Painlevé equations and isomonodromic deformations

The Painlevé equations were first encountered by Paul Painlevé in his search for new special functions [35]. By then, it was known that many classical special functions were singled out as solution to linear (e.g., hypergeometric functions) or nonlinear (e.g., elliptic functions) ODEs with polynomial or rational coefficients. Unlike linear ODEs, whose singularities can only come from the equation itself, nonlinear ones can spawn movable singularities.

Inspired by the elliptic framework, Painlevé's search focused on the classification of 'nice' nonlinear ODEs in the form

$$y_{tt} = R(t, y, y_t), \tag{A.1.1}$$

with R rational, in the sense that movable singularities are only allowed to be poles. This

restriction goes by the Painlevé property, despite being first introduced by Sofia Kovalevskaya in her own classification of integrable rigid bodies [30]. Most of Painlevé's findings boiled down to known elliptic functions, however six of them birthed new special functions now known as the Painlevé transcendents. It took many contributions and almost a century to prove these six nonlinear ODEs, labelled PI to PVI, indeed possessed the Painlevé property and couldn't be subsumed to known special functions.

Nowadays, solutions to an extraordinarily broad array of scientific problems, from neutron scattering theory, fibre optics, transportation problems, combinatorics, random matrices, quantum gravity to number theory, can be expressed in terms of the Painlevé transcendents.

Actually, the full form of PVI was discovered by Richard Fuchs [18] studying monodromy preserving deformations of special systems of ODEs

$$\frac{\mathrm{d}}{\mathrm{d}\lambda}\Phi = \left(\sum_{i=1}^{m} \frac{A_i}{\lambda - u_i}\right)\Phi, \tag{A.1.2}$$

now known as Fuchsian. Since there are generically many Fuchsian systems sharing the same monodromy data, Fuchs studied isomonodromic deformations, i.e., deformations of the system preserving prescribed monodromy data. These deformations are characterized by the Schlesinger equations: the matrices $A_i(u)$, now depending on the poles' positions, must satisfy

$$\frac{\partial A_i}{\partial u_j} = \frac{[A_i, A_j]}{u_i - u_j}, \quad i \neq j; \qquad \sum_j \frac{\partial A_i}{\partial u_j} = 0. \tag{A.1.3}$$

As mentioned in the Introduction, for our Fuchsian system (I.1) with $(u_1, u_2, u_3) = (0, t, 1)$, these equations are equivalent to PVI.

The Schlesinger equations were then generalized by Jimbo, Miwa, Mori and Sato [25] to include irregular singularities. For the Poincaré rank 1 case (order 2 pole) allowing an

extra term $\mathfrak{D} = \mathrm{diag}(v_1, \dots, v_n)$, they read as

$$\mathrm{d}A_i = -\sum_{j\neq i}[A_i, A_j]\,\mathrm{d}\log(u_i - u_j) - [A_i, \mathrm{d}(u_i\mathfrak{D}) + \Xi], \quad i = 1, \dots, m, \tag{A.1.4}$$

for $A_i \in \mathsf{Mat}_n(u, v)$ and the matrix-valued one form

$$\Xi_{rs} = (1 - \delta_{rs})\left(\sum_{i=1}^{m} A_i\right)_{rs} \mathrm{d}\log(v_r - v_s),$$

and control the isomonodromic deformations of the differential operator

$$\frac{\mathrm{d}}{\mathrm{d}\lambda} - \left(\mathfrak{D} + \sum_{i=1}^{m}\frac{A_i}{\lambda - u_i}\right). \tag{A.1.5}$$

Remark A.1.1 *Equation* (A.1.4) *manifestly generalizes the Schlesinger ones, which are easily recovered by setting* $\mathfrak{D} = 0 = \Xi$.

Using moment maps on loop algebras, Harnad showed [20] that the two systems (I.1) and (I.3) are dual to each other, in the sense that both isomonodromic deformations are governed by the same equation (A.1.4), itself equivalent to PVI. For $F, G \in \mathsf{Mat}_{m\times n}(u, v)$ of maximal rank, this isomonodromic duality reads as a map of differential operators, sending the rational one

$$\frac{\mathrm{d}}{\mathrm{d}\lambda} - \left(\mathfrak{D} + G^t(\lambda - D)^{-1}F\right) \tag{A.1.6}$$

to its dual

$$\frac{\mathrm{d}}{\mathrm{d}\lambda} - \left(D + F(\lambda - \mathfrak{D})^{-1}G^t\right). \tag{A.1.7}$$

The case of PVI is given by setting $n = 2$, $m = 3$, $\mathfrak{D} = 0$ and $D = \mathrm{diag}(0, 1, t)$: indeed, the swap $(G^t, F) \mapsto (F, G^t)$ entailed by the duality allows the dual operators to live on different rank bundles—2 and 3, respectively for the Fuchsian and irregular case.

Another interpretation of this duality is given by the *inverse* Laplace transform, which is known to send d_λ to $\lambda\cdot$ and vice versa. Indeed, one can rewrite local solutions to (A.1.6) as the system

$$\begin{cases} \frac{\mathrm{d}}{\mathrm{d}\lambda} S = \mathfrak{D} S + G^t \widehat{S}, \\ (\lambda - D)\widehat{S} = FS, \end{cases} \tag{A.1.8}$$

whose exchanges $\frac{\mathrm{d}}{\mathrm{d}\lambda} \mapsto \lambda\cdot, \lambda \mapsto \frac{\mathrm{d}}{\mathrm{d}\lambda}$ give

$$\begin{cases} \lambda S = \mathfrak{D} S + G^t \widehat{S}, \\ \frac{\mathrm{d}}{\mathrm{d}\lambda}\widehat{S} - D\widehat{S} = FS, \end{cases} \tag{A.1.9}$$

i.e., $\widehat{S}$ solves the Harnad dual operator (A.1.7).

A.2 Additive middle convolution

The middle convolution functor exhibits a dual version for Fuchsian systems [10], the two connected by a fundamental Riemann-Hilbert correspondence.

Let $\mathrm{Fu}_{\mathbf{A}}$ denote the n-dimensional Fuchsian system (A.1.2) defined by the m-tuple of matrices $\mathbf{A} = (A_1, \dots, A_m) \in (\mathbb{C}^{n\times n})^m$. The construction of the additive functor is similar: for $i = 1, \dots, m$, build the block matrices

$$B_i := \begin{pmatrix} \mathbb{0} & & & \dots & & \mathbb{0} \\ & \ddots & & & & \\ A_1 & \dots & A_{i-1} & A_i + \mu\mathbb{1} & A_{i+1} & \dots & A_m \\ & & & & \ddots & & \\ \mathbb{0} & & & \dots & & \mathbb{0} \end{pmatrix} \in \mathbb{C}^{nm\times nm},$$

each one zero outside the corresponding i-th block row.

Then, take the quotient over two $\langle B_1, \ldots, B_m \rangle$-invariant subspaces of the vector space[1] $\mathbb{C}^{nm}$:

$$\mathfrak{K} = \bigoplus_{i=1}^{m} \mathfrak{K}_i,$$

for

$$\mathfrak{K}_i = \begin{pmatrix} \mathbb{0} \\ \vdots \\ \mathbb{0} \\ \ker(A_i) \\ \mathbb{0} \\ \vdots \\ \mathbb{0} \end{pmatrix} \quad (i\text{-th entry}),$$

and

$$\mathfrak{L} = \bigcap_{i=1}^{m} \ker(B_i) = \ker(B_1 + \ldots + B_m).$$

Definition A.2.1 *The tuple* $\mathscr{C}_\mu^+(\mathbf{A}) := (B_1, \ldots, B_m)$ *is the* additive convolution *of* $\mathbf{A}$ *with* μ. *The tuple* $\mathscr{M}_\mu^+ := \left(\tilde{B}_1, \ldots, \tilde{B}_m\right) \in \mathbb{C}^{l \times l}$ *is the* additive middle convolution *of* $\mathbf{A}$ *with* μ, *where each* $\tilde{B}_i$ *is induced by the action of the corresponding element of* $\mathscr{C}_\mu^+(\mathbf{A})$ *on* $\mathbb{C}^l \simeq \mathbb{C}^{nm}/(\mathfrak{K} + \mathfrak{L})$.

Remark A.2.2 *In general,* $l \neq nm$, *allowing to map between Fuchsian systems of different dimensions. Moreover, for* $\mu \neq 0$,

$$\mathfrak{L} = \left\langle \begin{pmatrix} v \\ \vdots \\ v \end{pmatrix} \;\middle|\; v \in \ker(A_1 + \cdots + A_m + \mu \mathbb{1}) \right\rangle \qquad \textit{and} \qquad \mathfrak{K} + \mathfrak{L} = \mathfrak{K} \oplus \mathfrak{L}.$$

Finally, the Riemann-Hilbert correspondence relating the middle convolution with its

[1] Meant as a column vector space, for the natural action of $B_1, \ldots, B_m$.

additive version can be stated as follows:

Theorem A.2.3 ([10], Theorem 1.1) *Let* $\mathbf{M} = \mathrm{Mon}(\mathrm{Fu}_{\mathbf{A}}) = (M_1, \dots, M_m) \in \mathsf{GL}_n(\mathbb{C})^m$ *be the tuple of independent monodromy generators for* $\mathrm{Fu}_{\mathbf{A}}$, $\mathbf{A} = (A_1, \dots, A_m) \in (\mathbb{C}^{n\times n})^m$, $\mu \in \mathbb{C}\backslash\mathbb{Z}$ *and* $\lambda = e^{2\pi i\mu}$. *If* $\mathbf{M}$ *satisfies the condition of Theorem 1.2.3 and*

$$\begin{aligned} \mathrm{rank}(A_i) &= \mathrm{rank}(M_i - \mathbb{1}), \\ \mathrm{rank}(A_1 + \ldots + A_m + \mu\mathbb{1}) &= \mathrm{rank}(\lambda M_m \cdots M_1 - \mathbb{1}), \end{aligned} \tag{A.2.1}$$

then

$$\mathrm{Mon}\left(\mathrm{Fu}_{\mathscr{M}^+_{\mu-1}(\mathbf{A})}\right) = \mathscr{M}_\lambda(\mathbf{M}). \tag{A.2.2}$$

In other words, $\mathscr{M}_{e^{2\pi i\mu}}$ is *the* map between the monodromy data of the corresponding Fuchsian systems mapped by $\mathscr{M}^+_\mu$. The commutation of the left square in diagram (I.15) follows as a direct consequence; playing such a foundational role in the thesis, this correspondence is thoroughly inspected in Appendix B.

A.3 Application: explicit Harnad duality

In this section, we explicitly prove Theorem I.1 using the additive middle convolution, giving an alternative realization of the Harnad's duality (A.1.6-A.1.7) in diagram (I.15). First, our 2-dimensional system (I.1) is mapped to the 3-dimensional Fuchsian

$$\frac{\mathrm{d}}{\mathrm{d}\lambda}X = \left(\sum_{k=1}^{3}\frac{\tilde{B}_k}{\lambda - u_k}\right)X, \tag{A.3.1}$$

where

$$\tilde{B}_k = -E_k\Theta, \qquad \text{i.e.,} \quad (\tilde{B}_k)_{ij} = -\Theta_{ij}\delta_{ik}, \tag{A.3.2}$$

and $\tilde{B}_\infty = -\sum_{k=1}^{3}\tilde{B}_k = \Theta$. Notice that all four singularities are unaffected.

Now that dimensions agree, such Fuchsian system is mapped to the irregular one via the

(inverse) Laplace transform

$$\Psi(z) = \oint X(\lambda) e^{z\lambda} \mathrm{d}\lambda, \tag{A.3.3}$$

convergent for a loop in the λ-plane avoiding branch cuts. To see this, remember that $D = \mathrm{diag}(u_1, u_2, u_3)$ and rewrite (A.3.1) as

$$(\lambda - D)\frac{\mathrm{d}}{\mathrm{d}\lambda} X = -\tilde{B}_\infty X. \tag{A.3.4}$$

Then, multiplying by $e^{z\lambda}$ both sides and integrating in λ,

$$\oint \lambda X' e^{z\lambda} \mathrm{d}\lambda - \oint D X' e^{z\lambda} \mathrm{d}\lambda = \oint -\tilde{B}_\infty X e^{z\lambda} \mathrm{d}\lambda = -\tilde{B}_\infty \Psi, \tag{A.3.5}$$

and after two integration by parts[2]

$$-\Psi - z\frac{\mathrm{d}}{\mathrm{d}z}\Psi + zD\Psi = -\tilde{B}_\infty \Psi \implies \frac{\mathrm{d}}{\mathrm{d}z}\Psi = \left(D + \frac{\tilde{B}_\infty - \mathbb{1}}{z}\right)\Psi. \tag{A.3.6}$$

As for the explicit computations, we start from the 2-dimensional Fuchsian system

$$\frac{\mathrm{d}}{\mathrm{d}\lambda}\Phi = \left(\frac{A_1}{\lambda - u_1} + \frac{A_2}{\lambda - u_2} + \frac{A_3}{\lambda - u_3}\right)\Phi, \tag{A.3.7}$$

having matrices A_k in form (I.5) with

$$A_\infty = -(A_1 + A_2 + A_3) = \frac{1}{2}\begin{pmatrix} -a_1 b_1 - a_2 b_2 - a_3 b_3 & a_1^2 + a_2^2 + a_3^2 \\ \left(\frac{\theta_1^2}{a_1^2} - b_1^2\right) + \left(\frac{\theta_2^2}{a_2^2} - b_2^2\right) + \left(\frac{\theta_3^2}{a_3^2} - b_3^2\right) & a_1 b_1 + a_2 b_2 + a_3 b_3 \end{pmatrix} \tag{A.3.8}$$

matching form (I.2) under conditions (I.7).

We want the additive middle convolution to send the 3-tuple (A_1, A_2, A_3) of 2×2 matrices to the $(\tilde{B}_1, \tilde{B}_2, \tilde{B}_3)$ one of 3×3 matrices. This is achieved by suitably tailoring the dimensions

[2] $\lambda X' e^{z\lambda} = -X e^{z\lambda} - z\lambda X e^{z\lambda}$ and $DX' e^{z\lambda} = -zDX e^{z\lambda}$ when integrating along a suitable loop.

of the subspaces $\mathfrak{K}$ and $\mathfrak{L}$.

On the one hand, we fix $\dim(\mathfrak{K}) = 3$ using an elementary shifting (functorial) operation: the *addition functor*

$$\mathrm{add}_\delta : (A_1, \ldots, A_m) \mapsto (A_1 + \delta_1 \mathbb{1}, \ldots, A_m + \delta_m \mathbb{1}), \tag{A.3.9}$$

dependent on a vector parameter $\delta = (\delta_1, \ldots, \delta_m)$. By choosing $\delta_\theta = \left(\frac{\theta_1}{2}, \frac{\theta_2}{2}, \frac{\theta_3}{2}\right)$, each shifted matrix becomes rank 1 in that

$$\mathrm{eigen}\left(A_k + \frac{\theta_k}{2}\mathbb{1}\right) = \{0, \theta_k\}\,. \tag{A.3.10}$$

Remark A.3.1 *The addition functor admits a monodromic analogue via the Riemann-Hilbert correspondence*

$$\mathrm{add}_\delta \longleftrightarrow \mathrm{mult}_\omega,$$

for

$$\begin{array}{rccc} \mathrm{mult}_\omega : & \mathsf{GL}(V)^m & \longrightarrow & \mathsf{GL}(V)^m \\ & (M_1, \ldots, M_m) & \mapsto & (\omega_1 M_1, \ldots, \omega_m M_m) \end{array} \tag{A.3.11}$$

where the vector parameter $\omega = e^{2\pi i \delta} := \{e^{2\pi i \delta_1}, \ldots, e^{2\pi i \delta_m}\}$. *Thus, the functor* $\mathscr{M}_\mu^+ \circ \mathrm{add}_\delta$ *delivers a map between Fuchsian systems of prescribed dimensions, and the Riemann-Hilbert correspondences ensure* $\mathscr{M}_{e^{2\pi i \mu}} \circ \mathrm{mult}_{e^{2\pi i \delta}}$ *is* the *map between the corresponding Fuchsian monodromy data.*

On the other hand, for $\mu \neq 0$ the characterization of Remark A.2.2 ensures that as long as $\mu \notin \mathrm{eigen}\left(A_\infty - \frac{1}{2}(\theta_1 + \theta_2 + \theta_3)\right)$, $\dim(\mathfrak{L}) = 0$ and $\mathfrak{K} + \mathfrak{L} = \mathfrak{K} \oplus \mathfrak{L}$.

Summing up, precomposing $\mathrm{add}_{\delta_\theta}$ to $\mathscr{M}_\mu^+$ provided $\mu \notin \left\{0, \mathrm{eigen}\left(A_\infty - \frac{1}{2}\sum_i \theta_i\right)\right\}$, the quotient is exactly of dimension $3 = \dim\left(\mathbb{C}^{2\cdot 3}\right) - \dim(\mathfrak{K} \oplus \mathfrak{L}) = 6 - 3$ as wished. Clearly,

these are not the only values to craft a 3-dimensional subspace out of $\mathfrak{K}+\mathfrak{L}$; we're going to show such special choice recovers our target matrix Θ (I.6).

For an easy realization of the quotient, we build a basis out of the kernels

$$\ker\left(A_i+\frac{\theta_i}{2}\mathbb{1}\right)=\left\langle\left(\frac{a_i^2}{a_ib_i+\theta_i},1\right)\right\rangle,$$

suitably completed to match the exact form of Θ. This change of coordinates turns out to be

$$C=\begin{pmatrix}\frac{a_1^2}{a_1b_1+\theta_1} & 0 & 0 & 0 & 0 & 0\\ 1 & 0 & 0 & 1 & 0 & 0\\ 0 & \frac{a_2^2}{a_2b_2+\theta_2} & 0 & 0 & 0 & 0\\ 0 & 1 & 0 & 0 & \frac{a_1}{a_2} & 0\\ 0 & 0 & \frac{a_3^2}{a_3b_3+\theta_3} & 0 & 0 & 0\\ 0 & 0 & 1 & 0 & 0 & \frac{a_1}{a_3}\end{pmatrix},$$

with the first three columns being indeed a basis of $\mathfrak{K}$. We can thus perform the quotient by just restricting to the 3×3 lowest diagonal blocks of the 3-tuple $\left(C^{-1}B_1C,C^{-1}B_2C,C^{-1}B_3C\right)$, where $(B_1,B_2,B_3)=\mathscr{C}_\mu^+\left(\mathrm{add}_{\delta_\theta}(A_1,A_2,A_3)\right)$.

The output reads

$$\tilde{B}_1:=\begin{pmatrix}\theta_1+\mu & \frac{1}{2}\left(a_2b_1-a_1b_2+\theta_1\frac{a_2}{a_1}+\theta_2\frac{a_1}{a_2}\right) & \frac{1}{2}\left(a_3b_1-a_1b_3-\theta_1\frac{a_3}{a_1}+\theta_3\frac{a_1}{a_3}\right)\\ 0 & 0 & 0\\ 0 & 0 & 0\end{pmatrix},$$

$$\tilde{B}_2:=\begin{pmatrix}0 & 0 & 0\\ \frac{1}{2}\left(a_1b_2-a_2b_1+\theta_1\frac{a_2}{a_1}+\theta_2\frac{a_1}{a_2}\right) & \theta_2+\mu & \frac{1}{2}\left(a_3b_2-a_2b_3+\theta_2\frac{a_3}{a_2}+\theta_3\frac{a_2}{a_3}\right)\\ 0 & 0 & 0\end{pmatrix},$$

$$\tilde{B}_3 := \begin{pmatrix} 0 & 0 & 0 \\ 0 & 0 & 0 \\ \frac{1}{2}\left(a_1b_3 - a_3b_1 + \theta_1\frac{a_3}{a_1} + \theta_3\frac{a_1}{a_3}\right) & \frac{1}{2}\left(a_2b_3 - a_3b_2 + \theta_2\frac{a_3}{a_2} + \theta_3\frac{a_2}{a_3}\right) & \theta_3 + \mu \end{pmatrix}.$$

The resulting Fuchsian system

$$\frac{\mathrm{d}}{\mathrm{d}\lambda}X = \left(\frac{\tilde{B}_1}{\lambda - u_1} + \frac{\tilde{B}_2}{\lambda - u_2} + \frac{\tilde{B}_3}{\lambda - u_3}\right)X \tag{A.3.12}$$

is in the anticipated form (A.3.1) with

$$\tilde{B}_\infty = -(\tilde{B}_1 + \tilde{B}_2 + \tilde{B}_3) = \Theta - \mu\mathbb{1}. \tag{A.3.13}$$

This means the Laplace transform maps it to the irregular system

$$\frac{\mathrm{d}}{\mathrm{d}z}\Psi = \left(D + \frac{\Theta - \mu\mathbb{1} - \mathbb{1}}{z}\right)\Psi. \tag{A.3.14}$$

Notice there is a μ-shift with respect to our target system (I.3), that can be readily absorbed by the following Gauge transform:

$$\Psi \mapsto \tilde{\Psi} = z^\mu\Psi. \tag{A.3.15}$$

Indeed,

$$\frac{\mathrm{d}}{\mathrm{d}z}\tilde{\Psi} = \frac{\mu\mathbb{1}}{z}z^\mu\Psi + z^\mu\left(D + \frac{\Theta - \mu\mathbb{1} - \mathbb{1}}{z}\right)\Psi = \left(D + \frac{\Theta - \mathbb{1}}{z}\right)\tilde{\Psi}. \tag{A.3.16}$$

We have thus explicitly confirmed the additive middle convolution functor lies behind the correspondence in Theorem I.1.

Remark A.3.2 *One might try to avoid the Gauge performing a middle convolution with $\mu = 0$.*

However, as already pointed out by Filipuk [13], this degenerate case leads to a 3*-tuple of* 2×2 *matrices.*

Supported by the Riemann-Hilbert correspondences, one could push these computations to monodromy and send the Fuchsian data (1.1.12) to the irregular ones:

$$\begin{array}{ccccc} (M_1,M_2,M_3) & \xrightarrow{\text{mult}_{e^{2\pi i\delta_\theta}}} & \left(-e^{\frac{p_1}{2}}M_1,-e^{\frac{p_2}{2}}M_2,-e^{\frac{p_3}{2}}M_3\right) & \xrightarrow{\mathscr{M}_{e^{2\pi i\mu}}} & \left(\tilde{R}_1,\tilde{R}_2,\tilde{R}_3\right) \\ & & & & \Big\downarrow{\scriptstyle \tilde{R}_1\tilde{R}_2\tilde{R}_3=S_1S_2} \\ & & & & \left(M_0^L,S_1,S_2\right)(\mu) \\ & & & & \Big\downarrow{\scriptstyle \mu=0} \\ & & & & \left(M_0^L,S_1,S_2\right) \end{array} \tag{A.3.17}$$

Nevertheless, all these triples can be obtained by taking the classical limit of the components of the GDAHA functor. As such, their explicit matrices are omitted.

Appendix B

Middle convolution's Riemann-Hilbert correspondence

This appendix studies in detail the correspondence (A.2.2) between the middle convolution functor and its additive counterpart. To fully understand the proof of Theorem A.2.3, we first need a detour on both the Pochhammer double loop contour and the Euler transform.

B.1 Pochhammer contours and Euler transform

The Pochhammer double loop contour was originally devised [36] as an ingenious path of integration allowing for an extended definition of the beta function on the whole of $\mathbb{C}^2$. We recall that such special function was originally introduced in the integral form

$$B(x,y)=\int_0^1 t^{x-1}(1-t)^{y-1}\mathrm{d}t, \qquad x,y\in\mathbb{C}, \tag{B.1.1}$$

for $\mathrm{Re}\,(x),\mathrm{Re}\,(y)>0$, and made meromorphic on $\mathbb{C}^2\setminus\mathbb{Z}^2_{\leqslant 0}$ via analytic continuation by the Γ function:

$$B(x,y)=\frac{\Gamma(x)\Gamma(y)}{\Gamma(x+y)}. \tag{B.1.2}$$

In fact, it can be made analytic on the whole of $\mathbb{C}^2$ by tweaking the above integral formulation as

$$\int_{\gamma_{Ph}} t^{x-1}(1-t)^{y-1}\mathrm{d}t, \tag{B.1.3}$$

where γ_{Ph} is the Pochhammer double loop encircling 0 and 1 in the following figure:

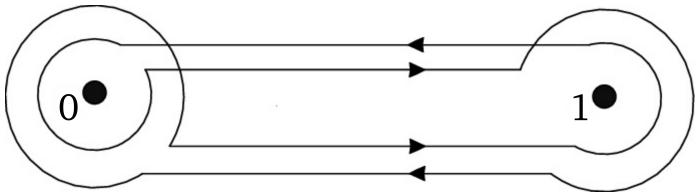

Figure B.1: The Pochhammer double loop contour

The integrand's multi-valuedness manifests through monodromy phenomena when we compute the integral along γ_{Ph}: a counterclockwise loop around 1 induces a factor $e^{2\pi iy}$ while a counterclockwise one around 0 induces a factor $e^{2\pi ix}$. Using Cauchy's theorem and these monodromy data, we can freely collapse γ_{Ph} to a line from ε to $1-\varepsilon$ and small circles $C(0,\varepsilon), C(1,\varepsilon)$ of radius ε to get that

$$\begin{aligned}\int_{\gamma_{Ph}} t^{x-1}(1-t)^{y-1}\mathrm{d}t = \\ \int_{\varepsilon}^{1-\varepsilon} t^{x-1}(1-t)^{y-1}\mathrm{d}t + \oint_{C(1,\varepsilon)} t^{x-1}(1-t)^{y-1}\mathrm{d}t + e^{2\pi iy}\int_{1-\varepsilon}^{\varepsilon} t^{x-1}(1-t)^{y-1}\mathrm{d}t \\ + e^{2\pi iy}\oint_{C(0,\varepsilon)} t^{x-1}(1-t)^{y-1}\mathrm{d}t + e^{2\pi i(x+y)}\int_{\varepsilon}^{1-\varepsilon} t^{x-1}(1-t)^{y-1}\mathrm{d}t \\ + e^{2\pi i(x+y)}\oint_{C(1,\varepsilon)} t^{x-1}(1-t)^{y-1}\mathrm{d}t + e^{2\pi ix}\int_{1-\varepsilon}^{\varepsilon} t^{x-1}(1-t)^{y-1}\mathrm{d}t \\ + e^{2\pi ix}\oint_{C(0,\varepsilon)} t^{x-1}(1-t)^{y-1}\mathrm{d}t.\end{aligned} \tag{B.1.4}$$

Since for $\mathrm{Re}(x), \mathrm{Re}(y) > 0$ we have that

$$|t^{x-1}(1-t)^{y-1}| = e^{(\mathrm{Re}(x)-1)\log|t|}e^{(\mathrm{Re}(y)-1)\log|t-1|} \xrightarrow{t\to 0,1} 0, \tag{B.1.5}$$

taking the limit $\varepsilon \to 0$ the circles' contributions vanish, and we prove the integral (B.1.3) extends the original beta definition:

$$\begin{aligned}\lim_{\varepsilon\to 0}\int_{\gamma_{Ph}} t^{x-1}(1-t)^{y-1}\mathrm{d}t &= \int_0^1 t^{x-1}(1-t)^{y-1}\mathrm{d}t + e^{2\pi i y}\int_1^0 t^{x-1}(1-t)^{y-1}\mathrm{d}t \\ &\quad + e^{2\pi i(x+y)}\int_0^1 t^{x-1}(1-t)^{y-1}\mathrm{d}t + e^{2\pi i x}\int_1^0 t^{x-1}(1-t)^{y-1}\mathrm{d}t \\ &= \left(1-e^{2\pi i x}\right)\left(1-e^{2\pi i y}\right)B(x,y).\end{aligned} \tag{B.1.6}$$

Since the integral (B.1.3) converges for all $x, y \in \mathbb{C}$, such extension is indeed the analytic continuation of the beta function on all $\mathbb{C}^2$.

Remark B.1.1 *Notice that, even if the integrand is multi-valued, its scalar nature and the double loop topology together leave its value unchanged after* γ_{Ph}.

We now move to the Euler transform: a solving method for special linear ODEs $L_x(y) = 0$ of order n, in which the coefficient of each derivative $y^{(r)}$ is a degree r polynomial. Over the complex plane, those boundary contributions that are usually neglected when integrating by parts deserve much more care due to monodromy phenomena. However, we anticipate these very obstructions can be used to build a basis in the solution space.

Following [23], for a constant parameter μ the method constructs solutions of $L_x(y) = 0$ in the form

$$y(x) = \int_a^b (x-t)^{n+\mu-1} v(t)\mathrm{d}t, \tag{B.1.7}$$

v a function integrated against the so-called Euler kernel $(x-t)^{n+\mu-1}$ and a, b to be suitably determined. The action of the differential operator L_x on the kernel can be written, for some $p \leqslant n$, as

$$L_x\left[(x-t)^{n+\mu-1}\right] = \mu(\mu+1)\cdots(n+\mu-1)\sum_{r=0}^{p}(-1)^r \frac{(x-t)^{\mu-r+1}}{\mu(\mu+1)...(\mu+r-1)}G_r(t), \tag{B.1.8}$$

for each G_r a polynomial of degree $n-r$. This is achieved with a special decomposition of the operator, that recursively defines the polynomials G_i. E.g., for $n=2$,

$$\begin{aligned} L_x[y] &= P_2(x)y'' + P_1(x)y' + P_0(x)y \\ &= G_0(x)y'' - \big(G_1(x) + \mu G_0'(x)\big)y' + \left(G_2(x) + (\mu+1)G_1'(x) + \frac{1}{2}\mu(\mu+1)G_0''(x)\right)y. \end{aligned} \tag{B.1.9}$$

Out of these polynomials, we define the t-differential operator

$$M_t = G_0(t)\frac{\mathrm{d}^p}{\mathrm{d}t^p} + G_1(t)\frac{\mathrm{d}^{p-1}}{\mathrm{d}t^{p-1}} + \ldots + G_p(t) \tag{B.1.10}$$

whose crucial property, for a suitable constant c, reads as

$$L_x\left[(x-t)^{n+\mu-1}\right] = cM_t\left[(x-t)^{p+\mu-1}\right]. \tag{B.1.11}$$

The outcome of this machinery is the potential reduction in the operator complexity due to the swap from n to p.

Acting on the integral form (B.1.7), we get that

$$L_x[y] = \int_a^b L_x\left[(x-t)^{n+\mu-1}\right]v(t)\mathrm{d}t = c\int_a^b M_t\left[(x-t)^{p+\mu-1}\right]v(t)\mathrm{d}t, \tag{B.1.12}$$

which vanishes if v is an integrating factor[1] for M_t, provided the endpoints are accordingly fixed. This involves the solution of a simpler equation known as the Euler transform of $L_x[y]=0$, formally defined as the adjoint equation of (B.1.10):

$$\overline{M}_t[v] := (-1)^p\frac{\mathrm{d}^p}{\mathrm{d}t^p}(G_0v) + (-1)^{p-1}\frac{\mathrm{d}^{p-1}}{\mathrm{d}t^{p-1}}(G_1v) + \ldots + G_pv = 0. \tag{B.1.13}$$

[1] I.e., it makes the whole integrand an exact differential

Indeed, for any function u, the Lagrange identity

$$M_t[u]v - u\overline{M}_t[v] = \frac{\mathrm{d}}{\mathrm{d}t}Z(u,v) \tag{B.1.14}$$

holds, for a (suitable) bilinear concomitant Z, showing that a function v solving the Euler equation annihilates (B.1.12).

Remark B.1.2 *The differential operator $\overline{M}_t$ is called the* adjoint *of M_t: rewriting the left-hand side of* (B.1.14) *as*

$$\langle M_t[u], v\rangle - \langle u, \overline{M}_t[v]\rangle, \quad \langle f, g\rangle := f\,g, \tag{B.1.15}$$

the Lagrange identity can be seen as an adjoint property 'up to an exact differential'.

When $p = 1$, the transform is just a first order ODE: one can explicitly solve for $v(t)$ and obtain a solution for the original differential equation.

Example B.1.3 (Legendre equation) *For a parameter α, the Legendre equation reads*

$$\left(1-x^2\right)y'' - 2xy' + \alpha(\alpha+1)y = 0, \tag{B.1.16}$$

i.e.,

$$L_x = \left(1-x^2\right)\frac{\mathrm{d}^2}{\mathrm{d}x^2} - 2x\frac{\mathrm{d}}{\mathrm{d}x} + \alpha(\alpha+1). \tag{B.1.17}$$

One can easily solve the operator decomposition imposing $p = 1 < 2 = n$ as

$$G_0(x) = 1-x^2, \quad G_1(x) = 2(\mu+1)x, \quad G_2(x) = 0, \tag{B.1.18}$$

for $\mu \in \{-\alpha-2, \alpha-1\}$. Thus,

$$M_t[u] = \left(1-t^2\right)\frac{\mathrm{d}}{\mathrm{d}t}u + 2(\mu+1)tu, \tag{B.1.19}$$

and the first order Euler equation reads

$$\overline{M}_t[v] = -\frac{\mathrm{d}}{\mathrm{d}t}\left[\left(1-t^2\right)v\right] + 2(\mu+1)tv = 0, \tag{B.1.20}$$

which is indeed easily solved as $v(t) = \left(1-t^2\right)^{-\mu-2}$. *The bilinear concomitant is found by explicit computation:*

$$M_t[u]v - \overline{M}_t[v]u = (1-t^2)(u'v+uv') - 2tuv = \frac{\mathrm{d}}{\mathrm{d}t}\left((1-t^2)uv\right). \tag{B.1.21}$$

Therefore,

$$\begin{aligned} L_x[y] &= c\int_a^b M_t\left[(x-t)^\mu\right]\left(1-t^2\right)^{-\mu-2}\mathrm{d}t = c\int_a^b \frac{\mathrm{d}}{\mathrm{d}t}\left((x-t)^\mu\left(1-t^2\right)^{-\mu-1}\right)\mathrm{d}t \\ &= c\left[(x-t)^\mu\left(1-t^2\right)^{-\mu-1}\right]_a^b, \end{aligned} \tag{B.1.22}$$

which vanishes setting $a=-1, b=1$ *provided that* $\mu = -\alpha-2,\ \alpha+1>0,\ |x|>1$. *We have thus found the solution*

$$y(x) = \int_{-1}^{1}(x-t)^{-\alpha-1}\left(1-t^2\right)^\alpha \mathrm{d}t, \tag{B.1.23}$$

known as the Legendre function of the second kind.

Let us now expand on the previous example to the general theory of the $p=1$ case, highlighting the crucial role played by Pochhammer contours.

Rewriting the differential operator for this special case as

$$\begin{aligned} L_x[y] = Q(x)y^{(n)} - \mu Q'(x)y^{(n-1)} + \frac{1}{2}\mu(\mu-1)y^{(n-2)} - \dots \\ - R(x)y^{(n-1)} + (\mu+1)R'(z)y^{(n-2)} - \dots \end{aligned} \tag{B.1.24}$$

the Euler transform assumes the compact form

$$(Q(t)v)' = R(t)v, \tag{B.1.25}$$

formally solved by $v(t) = \frac{1}{Q} e^{\int \frac{R}{Q} \mathrm{d}t}$. Using (B.1.11), for any n we have that

$$\begin{aligned} L_x[y] &= c \int_\gamma M_t \left[(x-t)^\mu\right] v(t) \mathrm{d}t = c \int_\gamma \left(Q(t) \frac{\mathrm{d}}{\mathrm{d}t} (x-t)^\mu + R(t)(x-t)^\mu \right) v(t) \mathrm{d}t \\ &= c \int_\gamma \frac{\mathrm{d}}{\mathrm{d}t} \underbrace{\left((x-t)^\mu e^{\int \frac{R}{Q} \mathrm{d}t} \right)}_{Z} \mathrm{d}t. \end{aligned} \tag{B.1.26}$$

For the latter expression to vanish and make (B.1.7) a solution, we need to focus on the path of integration, resorting to complex variables to take full advantage of monodromy phenomena.

Now that we let it be a full-fledged path on the complex plane, γ can either be chosen as a closed contour, provided that the initial and final values of Z coincide, or as a curvilinear arc such that Z vanishes at its end-points. As a rule of thumb, when Q is a polynomial with n distinct zeroes, there are n corresponding loops of the first kind generating n distinct contour integral solutions. If $Q(z)$ has repeated zeroes or its degree is less than n, the deficit in the number of possible distinct loops is filled by paths of the second type.

Denoting $u_1, \ldots, u_m$ the $m \leqslant n$ distinct zeroes of $Q(z)$,

$$\frac{R(t)}{Q(t)} = \sum_{i=1}^{m} \frac{\sigma_i}{t - u_i} + S(t), \tag{B.1.27}$$

for a polynomial S. Consequently,

$$Z(t) \propto e^{\int S \mathrm{d}t} (x-t)^\mu \prod_{i=1}^{m} (t-u_i)^{\sigma_i} \tag{B.1.28}$$

and its monodromy for each (counterclockwise) loop $\gamma^{(i)}$ encircling a single pole u_i is non-

trivial and given by the scalar $e^{2\pi i\sigma_i}$. Therefore, the Pochhammer contour topology suffice to ensure the net monodromy contribution after a double loop encircling any two different u_is is trivial. Thus, we get a solution

$$W_{ij}(x) := \int_{\gamma_{Ph}^{(ij)}} (x-t)^{n+\mu-1} \frac{e^{\int S\mathrm{d}t} \prod_{i=1}^{m} (t-u_i)^{\sigma_i}}{Q} \mathrm{d}t \tag{B.1.29}$$

for any Pochhammer double loop $\gamma_{Ph}^{(ij)}$ encircling u_i and u_j. With similar operations as in (B.1.4), we get that

$$W_{ij} = \left(1-e^{2\pi i\sigma_i}\right) W_j - \left(1-e^{2\pi i\sigma_j}\right) W_i, \quad W_k := \int_{\gamma^{(k)}} (x-t)^{n+\mu-1} \frac{1}{Q} e^{\int \frac{R}{Q}\mathrm{d}t} \mathrm{d}t, \tag{B.1.30}$$

and consequently

$$\left(1-e^{2\pi i\sigma_k}\right) W_{ij} = \left(1-e^{2\pi i\sigma_i}\right) W_{jk} - \left(1-e^{2\pi i\sigma_j}\right) W_{ik}. \tag{B.1.31}$$

For W_{ix} the solution corresponding to the Pochhammer contour encircling u_i and x, the last equation reads

$$\left(1-e^{2\pi i\mu}\right) W_{ij} = \left(1-e^{2\pi i\sigma_i}\right) W_{ix} - \left(1-e^{2\pi i\sigma_j}\right) W_{jx} \tag{B.1.32}$$

and shows that any W_{ij} integral can be expressed linearly in terms of these special integrals $W_{(-)x}$, proving no more than m independent solutions of Pochhammer type can exist.

For n distinct zeroes with $\sigma_i \notin \mathbb{Z}$[2], the method successfully provides a basis in the space of solutions, completely solving (B.1.24).

[2]If $\sigma_i \in \mathbb{Z}$, W_i vanishes (its integrand is now analytic along $\gamma^{(i)}$) and $W_{ix} = 0$, so that the special integrals fail to provide a basis and a complementary technique is needed.

B.2 Proof of Theorem A.2.3

We are now ready to study the crucial steps of the proof in detail. In particular, Pochhammer contours will be used to build a fundamental solution to the Fuchsian system $\mathrm{Fu}_{\mathscr{C}^+_{\mu-1}(\mathbf{A})}$ in the same spirit of the $p = 1$ Euler transform method. The topological setting is given by the α and β paths in Figure B.2.

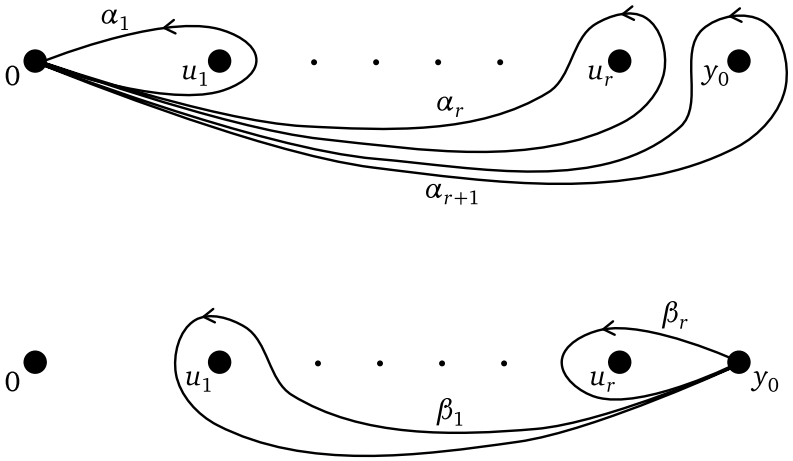

Figure B.2: All possible paths α_i and β_i

We start defining a Euler transform tailored to our needs:

Definition B.2.1 *Let $g := (g_{ij})$ be a matrix whose entries are (multi-valued) functions holomorphic on the punctured sphere $X := \mathbb{C} \setminus \{u_1, \dots, u_r\}$. The path α_{r+1} encircles an open neighbourhood U of y_0. The matrix valued function*

$$I^{\mu}_{[\alpha_{r+1},\alpha_i]}(g)(y) := \int_{[\alpha_{r+1},\alpha_i]} g(x)(y-x)^{\mu-1}dx,\ y \in U,$$

is the Euler transform *of g with respect to the Pochhammer contour $[\alpha_{r+1}, \alpha_i] := \alpha^{-1}_{r+1}\alpha^{-1}_i\alpha_{r+1}\alpha_i$ encircling u_{r+1} and u_i, and the parameter $\mu \in \mathbb{C}$.*

Such operation is compatible with the additive convolution functor:

Lemma B.2.2 *Let $g(x)$ be a solution to $\mathrm{Fu}_{\mathscr{C}^+_{\mu_1}(\mathbf{A})}$. Then, $I^{\mu_2}_{[\alpha_{r+1},\alpha_i]}(g)(y)$ is a solution to $\mathrm{Fu}_{\mathscr{C}^+_{\mu_1+\mu_2}(\mathbf{A})}$, where y is contained in the open neighbourhood U of y_0 that is encircled by α_{r+1}.*

Proof. In the following, we omit the subscript $[\alpha_{r+1},\alpha_i]$ in the integral sign and use that $\mathrm{Fu}_{\mathscr{C}^+_\mu(\mathbf{A})}$ is equivalent, for $\mathscr{C}^+_\mu(\mathbf{A})=(B_1,\dots,B_r)$, to the Okubo normal form

$$(y-D)\frac{\mathrm{d}}{\mathrm{d}y}Z(y)=\sum_{k=1}^{r}B_kZ(y), \tag{B.2.1}$$

where $D=\mathrm{diag}(\underbrace{u_1,\dots,u_1}_{\text{n times}},\underbrace{u_2,\dots,u_2}_{\text{n times}},\dots,\underbrace{u_r,\dots,u_r}_{\text{n times}})$ and $Z(y)=(z_1(y),\dots,z_{nr}(y))$. For $y\in U$,

$$\begin{aligned}(y-D)\frac{\mathrm{d}}{\mathrm{d}y}I^{\mu_2}_{[\alpha_{r+1},\alpha_i]}(g) &= (y-D)\int\frac{d}{dy}g(x)(y-x)^{\mu_2-1}dx\\ &= \int((y-x)+(x-D))(\frac{d}{dy}g(x)(y-x)^{\mu_2-1})dx\\ &= (\mu_2-1)I^{\mu_2}_{[\alpha_{r+1},\alpha_i]}(g)(y)+(\mu_2-1)\int(x-D)g(x)(y-x)^{\mu_2-2}dx,\end{aligned}$$

where one is allowed to differentiate under the integration sign as $[\alpha_{r+1},\alpha_i]$ is compact. Since the monodromy of $(x-D)g(x)(y-x)^{\mu_2-1}$ due to α_{r+1} is just a multiple of the identity, the net monodromy after $[\alpha_{r+1},\alpha_i]$ is trivial[3]. Therefore,

$$\begin{aligned}0=\int\frac{d}{dx}\left((x-D)g(x)(y-x)^{\mu_2-1}\right)dx=\int g(x)(y-x)^{\mu_2-1}dx+\int(x-D)g'(x)(y-x)^{\mu_2-1}dx\\ -(\mu_2-1)\int(x-D)g(x)(y-x)^{\mu_2-2}dx,\end{aligned} \tag{B.2.2}$$

and

$$(\mu_2-1)\int(x-D)g(x)(y-x)^{\mu_2-2}dx=\int g(x)(y-x)^{\mu_2-1}dx+\int(x-D)g'(x)(y-x)^{\mu_2-1}dx. \tag{B.2.3}$$

[3]The Pochhammer contour plays here its essential role: in this special case of *commuting* monodromy matrices, its topology suffice to ensure the integrand returns to its initial value.

Given that g is a solution of $\mathrm{Fu}_{\mathscr{C}^+_{\mu_1}(\mathbf{A})}$, we conclude that

$$(y-D)\frac{\mathrm{d}}{\mathrm{d}y}I^{\mu_2}_{[\alpha_{r+1},\alpha_i]}(g) = (\mu_2-1)I^{\mu_2}_{[\alpha_{r+1},\alpha_i]}(g) + I^{\mu_2}_{[\alpha_{r+1},\alpha_i]}(g) + \int (x-D)g'(x)(y-x)^{\mu_2-1}dx$$
$$= \sum_{k=1}^{r} B_k I^{\mu_2}_{[\alpha_{r+1},\alpha_i]}(g)(y), \tag{B.2.4}$$

for $(B_1,\ldots,B_r) = \mathscr{C}^+_{\mu_1+\mu_2}(\mathbf{A})$. □

For F a fundamental solution of $\mathrm{Fu}_{\mathbf{A}}$, there exists a special solution for the (additive) convolved system given by

$$G(x) := \begin{pmatrix} F(x)(x-u_1)^{-1} \\ \vdots \\ F(x)(x-u_r)^{-1} \end{pmatrix}.$$

Indeed, the following holds:

Lemma B.2.3 *The columns of G give a solution to $\mathrm{Fu}_{\mathscr{C}^+_{-1}(\mathbf{A})}$ and*

$$I^{\mu}_{[\alpha_{r+1},\alpha_i]}(G) = I^{\mu}_{\alpha_i}(G)(1-e^{2\pi i\mu}) - I^{\mu}_{\alpha_{r+1}}(G)(1-M_i),$$

where M_i is the monodromy of G due to α_i.

Proof. The first assertion is a straightforward check, while the second follows from computations analogous to those in (B.1.30). □

Corollary B.2.4 *If μ is a positive integer, then $I^{\mu}_{[\alpha_{r+1},\alpha_i]}(G) = 0$. If $\mu = 0$ or a negative integer,*

$$I^{\mu}_{[\alpha_{r+1},\alpha_i]}(G) = \frac{2\pi i}{-\mu!}G^{(-\mu)}(y)(-1+M_i).$$

Proof. It follows from the above lemma and Cauchy's integral formula. □

Analogously to the Euler method, we build a fundamental solution out of a special set of Pochhammer contours[4]:

Definition B.2.5 *Let $\mu \in \mathbb{C}$. The matrix*

$$I^{\mu} = I^{\mu}(y) := \left(I^{\mu}_{[\alpha_{r+1},\alpha_1]}(G)(y), \ldots, I^{\mu}_{[\alpha_{r+1},\alpha_r]}(G)(y)\right)$$

is called the period matrix.

The full-rank condition of the period matrix is part of the following result, which reformulates Theorem A.2.3 in the language just introduced:

Theorem B.2.6 ([10], Theorem 4.7) *Let $\mathbf{M} := \mathrm{Mon}(\mathrm{Fu}_{\mathbf{A}}) = (M_1, \ldots, M_r) \in \mathsf{GL}_n(\mathbb{C})^r$ be the tuple of monodromy generators for $\mathrm{Fu}_{\mathbf{A}}$, for $\mathbf{A} = (A_1, \ldots, A_r) \in (\mathbb{C}^{n\times n})^r$, $\mu \in \mathbb{C}\backslash\mathbb{Z}$ and $\lambda = e^{2\pi i\mu}$. If $\langle M_1, \ldots, M_r\rangle$ generates an irreducible subgroup of $\mathsf{GL}_n(C)$ for at least two M_i's different from the identity, then*

1. *The columns of the period matrix $I^{\mu}(y)$ are solutions of $\mathrm{Fu}_{\mathscr{C}^{+}_{\mu-1}(\mathbf{A})}$, where y is contained in a small open neighbourhood U of y_0*

2. *For $v_i \in \ker(M_i - 1)$, $i = 1, \ldots, r$, ($v \in \ker(\lambda M_1 \cdots M_r - \mathbb{1})$) assume that the residue of $G(x)v_i$ at u_i (the residue of $x^{\mu-1}G(x)v$ at ∞) is not identically zero. Then, the period matrix $I^{\mu}(y)$, $y \in U$, is full-rank and the tuple of monodromy generators of $\mathrm{Fu}_{\mathscr{C}^{+}_{\mu-1}(\mathbf{A})}$ with respect to $I^{\mu}(y)$ and the paths $\beta_1, \ldots, \beta_r$ is $\mathscr{C}_{\lambda}(\mathbf{M})$, i.e.,*

$$\mathrm{Mon}\left(\mathrm{Fu}_{\mathscr{C}^{+}_{\mu-1}(\mathbf{A})}\right) = \mathscr{C}_{\lambda}(\mathbf{M})$$

3. *Assuming that*

$$\mathrm{rank}(A_i) = \mathrm{rank}(M_i - \mathbb{1}) \qquad \textit{and} \qquad \mathrm{rank}(A_1 + \ldots + A_r + \mu\mathbb{1}) = \mathrm{rank}(\lambda \mathrm{M}_1 \cdots \mathrm{M}_r - \mathbb{1}),$$

[4]Notice that y_0 plays here the role that x did for the Euler machinery.

$I^\mu(y)$ gives rise to a fundamental solution $\tilde{I}^\mu(y)$, $y \in U$, of the system $\mathrm{Fu}_{\mathscr{M}^+_{\mu-1}(\mathbf{A})}$. *The tuple of monodromy generators of* $\mathrm{Fu}_{\mathscr{M}^+_{\mu-1}(\mathbf{A})}$ *with respect to* $\tilde{I}^\mu(y)$ *and the paths* $\beta_1, \ldots, \beta_r$ *is* $\mathscr{M}_\lambda(\mathbf{M})$, *i.e.,*

$$\mathrm{Mon}\left(\mathrm{Fu}_{\mathscr{M}^+_{\mu-1}(\mathbf{A})}\right) = \mathscr{M}_\lambda(\mathbf{M}).$$

Proof. Point *1* follows from Lemma B.2.3 and Lemma B.2.2.

By definition of $I^\mu_{[\alpha_{r+1},\alpha_i]}$, analytic continuation of the period matrix $I^\mu(y)$ along the path β_k transforms $I^\mu_{[\alpha_{r+1},\alpha_i]}(G)$ into $I^\mu_{[\beta_k \triangleright \alpha_{r+1}, \beta_k \triangleright \alpha_i]}(G)$, where the action $\beta_k \triangleright \alpha_i$ is the deformation of the loop α_i due to the movement of y_0 along b_k. These deformations, for all loops α_i, are shown in Figure B.3.

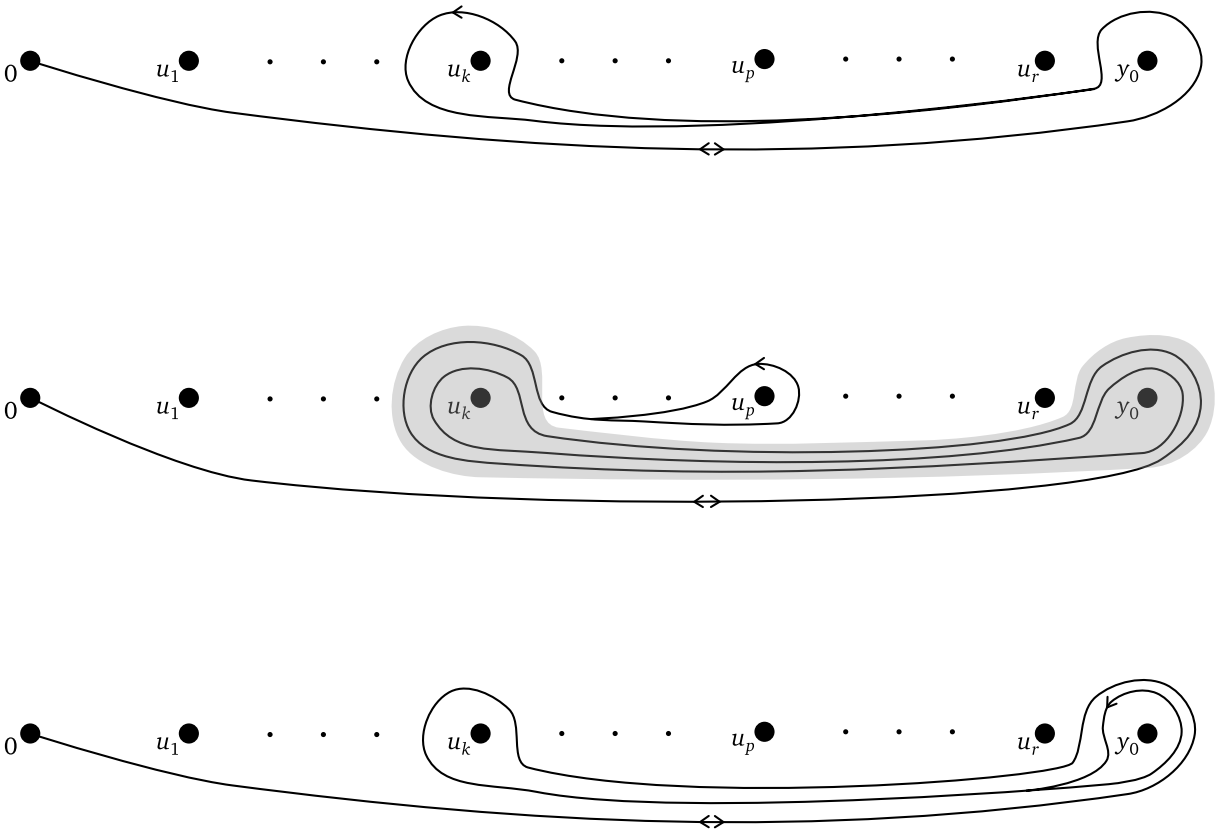

Figure B.3: Deformations due to b_k for, respectively top-down, α_k, α_p, $k < p < r+1$, and α_{r+1}, where the appearing Pochhammer contour is highlighted. Notice that no deformation is imposed on α_i, for $i < k$.

Notice that the topological obstruction to deformations given by the punctures makes Pochham-

mer contours crucially appear once more: for any $k < i < r+1$, $\alpha_i \to [\alpha_k, \alpha_{r+1}]^{-1}\alpha_i[\alpha_k, \alpha_{r+1}]$, where $[\alpha_k, \alpha_{r+1}]$ is a Pochhammer contour encircling u_k and y_0.

Denoting $\tilde{I}(\alpha) := \tilde{I}^{\mu}_{\alpha}(G)$ and recalling that

$$\tilde{I}^{\mu}(\alpha\beta) = \tilde{I}^{\mu}(\alpha)\mathrm{Mon}(\beta) + \tilde{I}^{\mu}(\beta),$$

where $\mathrm{Mon}(\beta)$ is the monodromy of the transform's integrand after a loop β, we get that

$$\begin{aligned}\tilde{I}^{\mu}(\alpha[\alpha_{r+1}, \beta]\varepsilon) &= \left(\tilde{I}^{\mu}(\alpha)\mathrm{Mon}([\alpha_{r+1}, \beta]) + \tilde{I}^{\mu}([\alpha_{r+1}, \beta])\right)\mathrm{Mon}(\varepsilon) + \tilde{I}^{\mu}(\varepsilon) \\ &= \left(\tilde{I}^{\mu}(\alpha)\mathrm{Mon}(\varepsilon) + \tilde{I}^{\mu}(\varepsilon)\right) + \tilde{I}^{\mu}([\alpha_{r+1}, \beta])\mathrm{Mon}(\varepsilon) \\ &= \tilde{I}^{\mu}(\alpha\varepsilon) + \tilde{I}^{\mu}([\alpha_{r+1}, \beta])\mathrm{Mon}(\varepsilon),\end{aligned} \tag{B.2.5}$$

using that $\mathrm{Mon}(\alpha_{r+1}) = e^{2\pi i\mu} = \lambda \implies \mathrm{Mon}([\alpha_{r+1}, \beta]) = \mathbb{1}$. Thus, for $i < k$,

$$\begin{aligned}\tilde{I}([\beta_k \triangleright \alpha_{r+1}, \beta_k \triangleright \alpha_i]) &= \tilde{I}([(\alpha_k\alpha_{r+1})^{-1}\alpha_{r+1}\alpha_k\alpha_{r+1}, \alpha_i]) \\ &= \tilde{I}(\alpha_{r+1}^{-1}[\alpha_k, \alpha_{r+1}]\alpha_i^{-1}[\alpha_{r+1}, \alpha_k]\alpha_{r+1}\alpha_i) \\ &= \tilde{I}([\alpha_{r+1}, \alpha_k])\lambda(M_i - \mathbb{1}) + \tilde{I}([\alpha_{r+1}, \alpha_i]).\end{aligned} \tag{B.2.6}$$

Similarly, for $i = k$

$$\tilde{I}([\beta_k \triangleright \alpha_{r+1}, \beta_k \triangleright \alpha_i]) = \tilde{I}\left((\alpha_k\alpha_{r+1})^{-1}[\alpha_{r+1}, \alpha_k]\alpha_k\alpha_{r+1}\right) = \tilde{I}([\alpha_{r+1}, \alpha_k])\lambda M_k,$$

and for $i > k$

$$\tilde{I}([\beta_k \triangleright \alpha_{r+1}, \beta_k \triangleright \alpha_i]) = \tilde{I}([\alpha_{r+1}, \alpha_k])(M_i - \mathbb{1}) + \tilde{I}([\alpha_{r+1}, \alpha_i]).$$

This proves the second statement of point *2* by showing that the matrix describing this transformation is exactly the k-th element of the r-tuple $\mathscr{C}_{\lambda}(\mathbf{M})$. Omitting the tedious and unen-

lightening proof that $I^{\mu}(y)$ is invertible, point *3* follows from dimensional reasons. Indeed, $\tilde{I}^{\mu}(y)$ is obtained cutting out the $p \times p$ lowest diagonal block from $C^{-1}I^{\mu}(y)$, where C is a change of basis whose first $nr-p$ columns form a basis of $\mathfrak{K}+\mathfrak{L}$. This follows since

$$(y-D)(C^{-1}I^{\mu})' = \sum_{k=1}^{r}\left(C^{-1}B_kC\right)(C^{-1}I^{\mu}),$$

and the lowest blocks of $\left(C^{-1}B_1C,\ldots,C^{-1}B_rC\right)$ give exactly $\mathscr{M}^{+}_{\mu-1}(\mathbf{A})$. It is immediate to check that the monodromy group is invariant under this Gauge transformation. Analogously, one can perform the quotient at the monodromy level taking the lowest diagonal block of $I^{\mu}(y)C'$, for C' now a change of basis whose first set of columns form a basis of $\mathcal{K}+\mathcal{L}$. In turn, this transformation leaves the system untouched, and it's enough for the lowest blocks obtained by the two procedures to agree on dimension, which is ensured by the rank conditions. □

Appendix C

Entries of $\overline{R}$

$$\overline{R}_{11} = q^{2/3} Z_{Y1}^{2/3} Z_{Y2}^{1/3} Z_{C1}^{-1/3} Z_{C2}^{-2/3} Z_{111}^{(t)-1/3} Z_{111}^{(b)-1/3},$$

$$\overline{R}_{12} = q^{1/3} Z_{Y1}^{2/3} Z_{Y2}^{1/3} Z_{C1}^{-1/3} Z_{C2}^{1/3} Z_{111}^{(t)2/3} (Z_{111}^{(b)2/3} + q^{1/3} Z_{111}^{(b)-1/3}) + q^{1/3} Z_{Y1}^{2/3} Z_{Y2}^{1/3} Z_{C1}^{-1/3} Z_{C2}^{-2/3} (q^{1/3} Z_{111}^{(t)-1/3} + Z_{111}^{(t)2/3}) Z_{111}^{(b)-1/3},$$

$$\overline{R}_{13} = q^{1/3} Z_{Y1}^{2/3} Z_{Y2}^{1/3} Z_{C1}^{-1/3} (Z_{C2}^{1/3} + q Z_{C2}^{-2/3}) Z_{111}^{(t)2/3} Z_{111}^{(b)-1/3} + q Z_{Y1}^{2/3} Z_{Y2}^{1/3} (q^{1/3} Z_{C1}^{-1/3} Z_{C2}^{1/3} + Z_{C1}^{2/3} Z_{C2}^{1/3}) Z_{111}^{(t)2/3} Z_{111}^{(b)2/3},$$

$$\overline{R}_{21} = -q^{2/3} (Z_{Y1}^{2/3} + q^{1/3} Z_{Y1}^{-1/3}) Z_{Y2}^{1/3} Z_{C1}^{-1/3} Z_{C2}^{-2/3} Z_{111}^{(t)-1/3} Z_{111}^{(b)-1/3},$$

$$\begin{aligned}\overline{R}_{22} = &-q^{1/3} Z_{Y1}^{2/3} Z_{Y2}^{1/3} Z_{C1}^{-1/3} Z_{C2}^{1/3} Z_{111}^{(t)2/3} (Z_{111}^{(b)2/3} - q^{-1} Z_{111}^{(b)-1/3}) - q^{1/3} Z_{Y1}^{2/3} Z_{Y2}^{1/3} Z_{C1}^{-1/3} Z_{C2}^{-2/3} (Z_{111}^{(t)2/3} + q^{1/3} Z_{111}^{(t)-1/3}) Z_{111}^{(b)-1/3} \\ &- q^{2/3} Z_{Y1}^{-1/3} Z_{Y2}^{1/3} (Z_{C1}^{-1/3} Z_{C2}^{-2/3} Z_{111}^{(t)2/3} + q^{1/3} Z_{C1}^{-1/3} Z_{C2}^{-2/3} Z_{111}^{(t)-1/3} + q^{-1} Z_{C1}^{-1/3} Z_{C2}^{1/3} Z_{111}^{(t)2/3}) Z_{111}^{(b)-1/3},\end{aligned}$$

$$\begin{aligned}\overline{R}_{23} = &-q^{1/3} (Z_{Y1}^{2/3} + q^{1/3} Z_{Y1}^{-1/3}) Z_{Y2}^{1/3} Z_{C1}^{-1/3} Z_{C2}^{1/3} Z_{111}^{(t)2/3} Z_{111}^{(b)-1/3} - q Z_{Y1}^{2/3} Z_{Y2}^{1/3} (q^{1/3} Z_{C1}^{-1/3} + Z_{C1}^{2/3}) Z_{C2}^{1/3} Z_{111}^{(t)2/3} Z_{111}^{(b)2/3} \\ &- q^{4/3} (Z_{Y1}^{2/3} + q^{1/3} Z_{Y1}^{-1/3}) Z_{Y2}^{1/3} Z_{C1}^{-1/3} Z_{C2}^{-2/3} Z_{111}^{(t)2/3} Z_{111}^{(b)-1/3},\end{aligned}$$

$$\overline{R}_{31} = q^{-5/3} Z_{Y1}^{-1/3} (Z_{Y2}^{1/3} + q Z_{Y2}^{-2/3}) Z_{C1}^{-1/3} Z_{C2}^{-2/3} Z_{111}^{(t)-4/3} Z_{111}^{(b)-1/3} + (q^{-1/3} Z_{Y1}^{2/3} + Z_{Y1}^{-1/3}) Z_{Y2}^{1/3} Z_{C1}^{-1/3} Z_{C2}^{-2/3} Z_{111}^{(t)-1/3} Z_{111}^{(b)-1/3},$$

$$\begin{aligned}\overline{R}_{32} = &\, q Z_{Y1}^{-1/3} Z_{Y2}^{1/3} Z_{C1}^{-1/3} Z_{C2}^{1/3} (Z_{111}^{(t)-1/3} + q^{-7/3} Z_{111}^{(t)2/3}) Z_{111}^{(b)-1/3} + (1 + q^{-2}) Z_{Y1}^{-1/3} Z_{Y2}^{1/3} Z_{C1}^{-1/3} Z_{C2}^{-2/3} Z_{111}^{(t)-1/3} Z_{111}^{(b)-1/3} \\ &+ q^{-5/3} Z_{Y1}^{2/3} Z_{Y2}^{1/3} Z_{C1}^{-1/3} Z_{C2}^{1/3} Z_{111}^{(t)2/3} (Z_{111}^{(b)-1/3} + q Z_{111}^{(b)2/3}) + q^{-5/3} Z_{Y1}^{-1/3} (Z_{Y2}^{1/3} + q Z_{Y2}^{-2/3}) Z_{C1}^{-1/3} Z_{C2}^{-2/3} Z_{111}^{(t)-4/3} Z_{111}^{(b)-1/3} \\ &+ q^{-1/3} (Z_{Y1}^{-1/3} + Z_{Y1}^{2/3}) Z_{Y2}^{1/3} Z_{C1}^{-1/3} Z_{C2}^{-2/3} Z_{111}^{(t)2/3} Z_{111}^{(b)-1/3} + q^{-1/3} (Z_{Y1}^{2/3} Z_{Y2}^{1/3} + q^{-2/3} Z_{Y1}^{-1/3} Z_{Y2}^{-2/3}) Z_{C1}^{-1/3} Z_{C2}^{-2/3} Z_{111}^{(t)-1/3} Z_{111}^{(b)-1/3},\end{aligned}$$

$$\begin{aligned}\overline{R}_{33} = &\, Z_{Y1}^{-1/3} Z_{Y2}^{1/3} Z_{C1}^{-1/3} (q^{2/3} Z_{C2}^{-2/3} + Z_{C2}^{1/3}) Z_{111}^{(t)2/3} Z_{111}^{(b)-1/3} + q^{-2/3} Z_{Y1}^{2/3} Z_{Y2}^{1/3} Z_{C1}^{-1/3} (Z_{C2}^{1/3} + q Z_{C2}^{-2/3}) Z_{111}^{(t)2/3} Z_{111}^{(b)-1/3} \\ &+ Z_{Y1}^{2/3} Z_{Y2}^{1/3} (q^{1/3} Z_{C1}^{-1/3} + Z_{C1}^{2/3}) Z_{C2}^{1/3} Z_{111}^{(t)2/3} Z_{111}^{(b)2/3} + Z_{Y1}^{-1/3} Z_{Y2}^{1/3} Z_{C1}^{-1/3} (q^{-1} Z_{C2}^{-2/3} + Z_{C2}^{1/3}) Z_{111}^{(t)-1/3} Z_{111}^{(b)-1/3} \\ &+ Z_{Y1}^{-1/3} Z_{Y2}^{-2/3} Z_{C1}^{-1/3} Z_{C2}^{-2/3} Z_{111}^{(t)-1/3} Z_{111}^{(b)-1/3}.\end{aligned}$$

Bibliography

[1] W. Balser, W. B. Jurkat, and D. A. Lutz. Birkhoff invariants and Stokes' multipliers for meromorphic linear differential equations. *Journal of Mathematical Analysis and Applications*, 71, 1979.

[2] Arkady Berenstein and Andrei Zelevinsky. Quantum cluster algebras. *Advances in Mathematics*, 195(2):405–455, 2005.

[3] P. Boalch. From Klein to Painlevé via Fourier, Laplace and Jimbo. *Proceedings of the London Mathematical Society*, 90, 2005.

[4] L. Chekhov and M. Mazzocco. Colliding holes in Riemann surfaces and quantum cluster algebras. *Nonlinearity*, 31, 2017.

[5] L. Chekhov, M. Mazzocco, and V. Rubtsov. Painlevé monodromy manifolds, decorated character varieties, and cluster algebras. *International Mathematics Research Notices*, 2017, 2016.

[6] L. Chekhov and M. Shapiro. Log-canonical coordinates for symplectic groupoid and cluster algebras. *International Mathematics Research Notices*, 2023, 2022.

[7] J. Coleman. Killing and the Coxeter transformation of Kac-Moody algebras. *Inventiones Mathematicae*, 95, 1989.

[8] D. Dal Martello. Mathematica companion. *doi.org/10.6084/m9.figshare.25888318.v1*, 2024.

[9] D. Dal Martello and M. Mazzocco. Generalized double affine Hecke algebras, their representations and higher Teichmüller theory. *arXiv:2307.06803v2*, 2023.

[10] M. Dettweiler and S. Reiter. Middle convolution of Fuchsian systems and the construction of rigid differential systems. *Journal of Algebra*, 318, 2007.

[11] B. Dubrovin. Geometry of 2d topological field theories. *Integrable Systems and Quantum Groups. Lecture Notes in Mathematics*, 1620, 1996.

[12] P. Etingof, A. Oblomkov, and E. Rains. Generalized double affine Hecke algebras of rank 1 and quantized Del Pezzo surfaces. *Advances in Mathematics*, 212, 2007.

[13] G. Filipuk. On the middle convolution and birational symmetries of the sixth Painlevé equation. *Kumamoto Journal of Mathematics*, 19, 2006.

[14] V. Fock and A. Goncharov. Moduli spaces of local systems and higher Teichmüller theory. *Publications Mathématiques de l'IHÉS*, 103, 2006.

[15] V. Fock and A. Goncharov. The quantum dilogarithm and representations of quantum cluster varieties. *Inventiones mathematicae*, 175, 2009.

[16] S. Fomin, L. Williams, and A. Zelevinsky. Introduction to Cluster Algebras. Chapters 1-3. *arXiv:1608.05735*, 2021.

[17] Y. Fu and S. Shelley-Abrahamson. A family of finite-dimensional representations of generalized double affine Hecke algebras of higher rank. *SIGMA*, 12, 2016.

[18] R. Fuchs. Sur quelques équations différentielles linéaires du second ordre. *Comptes Rendus*, 141, 1905.

[19] A. Goncharov and L. Shen. Quantum geometry of moduli spaces of local systems and representation theory. *arXiv:1904.10491*, 2022.

[20] J. Harnad. Dual isomonodromic deformations and moment maps to loop algebras. *Communications in Mathematical Physics*, 166, 1994.

[21] J. W. Helton and M. C. de Oliveira. NCAlgebra - Version 4.0.7, a noncommutative algebra package for Mathematica. *https://github.com/NCAlgebra/NC*, 2002.

[22] M. Gabella I. Coman and J. Teschner. Line operators in theories of class S, quantized moduli space of flat connections, and Toda field theory. *Journal of High Energy Physics*, 2015.

[23] E. L. Ince. *Ordinary Differential Equations*. Dover Publications, 1956.

[24] M. Jimbo and T. Miwa. Monodromy perserving deformation of linear ordinary differential equations with rational coefficients. ii. *Physica D: Nonlinear Phenomena*, 2, 1981.

[25] M. Jimbo, T. Miwa, Y. Mori, and M. Sato. Density matrix of an impenetrable Bose gas and the fifth Painlevé transcendent. *Physica D: Nonlinear Phenomena*, 1, 1980.

[26] N. Katz. *Rigid Local Systems*. Princeton University Press, 1996.

[27] T. Koornwinder. The relationship between Zhedanov's algebra $AW(3)$ and the double affine Hecke algebra in the rank one case. *SIGMA*, 3, 2007.

[28] T. Koornwinder and F. Bouzeffour. Nonsymmetric Askey–Wilson polynomials as vector–valued polynomials. *Applicable Analysis*, 90, 2011.

[29] V. Kostov. The Deligne–Simpson problem—a survey. *Journal of Algebra*, 281, 2004.

[30] S. Kovalevskaya. Sur le problème de la rotation d'un corps solide autour d'un point fixe. *Acta Mathmematica*, 12, 1889.

[31] I. Macdonald. *Affine Hecke Algebras and Orthogonal Polynomials*. Cambridge University Press, 2003.

[32] M. Mazzocco. Painlevé sixth equation as isomonodromic deformations equation of an irregular system. *CRM Proceedings & Lecture Notes*, 32, 2002.

[33] M. Mazzocco. Embedding of the rank 1 DAHA into $\mathsf{Mat}(2, \mathbb{T}_q)$ and its automorphisms. *Advanced Studies in Pure Mathematics*, 76, 2018.

[34] A. Oblomkov and E. Stoica. Finite dimensional representations of the double affine Hecke algebra of rank 1. *Journal of Pure and Applied Algebra*, 213, 2009.

[35] P. Painlevé. Mémoire sur les équations différentielles dont l'intégrale générale est uniforme. *Bulletin de la Société Mathématique de France*, 28, 1900.

[36] L. Pochhammer. Zur Theorie der Euler'schen Integrale. *Mathematische Annalen*, 35, 1890.

[37] N. Reshetikhin. The Knizhnik-Zamolodchikov system as a deformation of the isomonodromy problem. *Letters in Mathematical Physics*, 26, 1992.

[38] G. Schrader and A. Shapiro. Continuous tensor categories from quantum groups I: algebraic aspects. *arXiv:1708.08107*, 2017.

[39] V. Tarasov and A. Varchenko. Duality for Knizhnik–Zamolodchikov and dynamical equations. *Acta Applicandae Mathematicae*, 73, 2002.

[40] V. Toledano-Laredo. A Kohno-Drinfeld theorem for quantum Weyl groups. *Duke Mathematical Journal*, 112, 2002.

[41] V. Toledano Laredo and X. Xu. Stokes phenomena, Poisson–Lie groups and quantum groups. *Advances in Mathematics*, 429, 2023.